NEW ELECTROSPINNING STRATEGIES FOR THE PREPARATION OF SOLID-PHASE MICROEXTRACTION COATINGS

A THESIS SUBMITTED TO
THE GRADUATE SCHOOL OF NATURAL AND APPLIED SCIENCES
OF
MIDDLE EAST TECHNICAL UNIVERSITY

BY

ALPER ŞAHİN

IN PARTIAL FULFILLMENT OF THE REQUIREMENTS
FOR
THE DEGREE OF MASTER OF SCIENCE
IN
CHEMISTRY

JANUARY 2025

Approval of the thesis:

NEW ELECTROSPINNING STRATEGIES FOR THE PREPARATION OF SOLID-PHASE MICROEXTRACTION COATINGS

submitted by **ALPER ŞAHİN** in partial fulfillment of the requirements for the degree of **Master of Science** i**n Chemistry, Middle East Technical University** by,

Prof. Dr. Naci Emre Altun
Dean, **Graduate School of Natural and Applied Sciences** _____

Prof. Dr. Ali Çırpan
Head of the Department, **Chemistry** _____

Assoc. Prof. Dr. Ezel Boyacı
Supervisor, **Chemistry, METU** _____

Examining Committee Members:

Prof. Dr. Gülay Ertaş
Chemistry, METU _____

Assoc. Prof. Dr. Ezel Boyacı
Chemistry, METU _____

Prof. Dr. Caner Durucan
Metallurgical and Materials Eng, METU _____

Assoc. Prof. Dr. Mehmet Gümüştaş
Chemistry, Ankara University _____

Assist. Prof. Dr. Erol Yıldırım
Chemistry, METU _____

Date: 08.01.2025

I hereby declare that all information in this document has been obtained and presented in accordance with academic rules and ethical conduct. I also declare that, as required by these rules and conduct, I have fully cited and referenced all material and results that are not original to this work.

Name Last name : Alper Şahin

Signature :

ABSTRACT

NEW ELECTROSPINNING STRATEGIES FOR THE PREPARATION OF SOLID-PHASE MICROEXTRACTION COATINGS

Şahin, Alper
Master of Science, Chemistry
Supervisor : Assoc. Prof. Dr. Ezel Boyacı

January 2025, 157 pages

Solid phase microextraction (SPME) is a well-known, versatile sample preparation technique with several critical advantages. The versatility of SPME comes from the availability of a large variety of extractive phases and homemade coating preparation methods. However, in SPME, the extractive particles are immobilized in the bulk phase on the surface of support, which decreases the diffusion of analytes within the phase and the kinetic of extraction. This can be eliminated using nanofibrous extractive phases developed directly on the support without needing a bulk polymeric immobilizer, resulting in faster extraction kinetics and fast analysis. Production of nanofibrous extractive phase-coated SPME samplers is possible using an electrospinning process with the advantage of direct deposition of nano- and micro-fibrous polymers on the surface of a support.

In this study, two new electrospinning strategies for the SPME probe preparation were proposed. The first strategy included a novel extractive phase preparation method based on imprinting the analyte during the electrospinning. Templates (trifluralin and carbaryl) were immobilized into a ready-made polymer (polyacrylonitrile) using electrospinning to produce analyte-specific regions, enabling easier production and enhanced analyte-selective extraction. The second

strategy was proposed to overcome the reproducibility issues of electrospinning. Opposing the traditional syringe electrospinning, a high voltage was applied to a sword-shaped blade with one drop of polymer mixture, containing poly(divinylbenzene) and polyacrylonitrile. This method provided more controllable production of SPME samplers with fast extraction kinetics.

Both samplers were evaluated successfully in proof-of-concept studies using pesticides (trifluralin, carbaryl, diazinon, malathion, and parathion) frequently used in agricultural production.

Keywords: Solid Phase Microextraction, Thin Film Microextraction, Molecularly Imprinted Polymer, Electrospinning, Coating Method

ÖZ

KATI FAZ MİKROEKSTRAKSİYON KAPLAMALARI İÇİN YENİ ELEKTROEĞİRME STRATEJİLERİ

Şahin, Alper
Yüksek Lisans, Kimya
Tez Yöneticisi : Doç. Dr. Ezel Boyacı

Ocak 2025, 157 sayfa

Katı faz mikroekstraksiyon (SPME), yaygın olarak kullanılan, çok yönlü bir örnek hazırlama tekniğidir. SPMEnin çok yönlülüğü, çok çeşitli ekstraktif fazların ve özel kullanımlara imkân sağlayan kaplama hazırlama yöntemlerinin bulunmasından kaynaklanmaktadır. SPME örnekleyicileri için hazırlık esnasında ekstraktif partiküller, destek yüzeyindeki yığın halindeki yapıştırıcı fazda sabitlenir, bu da faz içindeki analitlerin difüzyonunu ve ekstraksiyon kinetiğini yavaşlatır. Bu durum, yapıştırıcı faza ihtiyaç duyulmadan doğrudan destek üzerinde geliştirilen nanofiber yapısındaki polimerik ekstraktif fazlar kullanılarak ortadan kaldırılabilir ve böylece daha hızlı ekstraksiyon kinetiği ve hızlı analiz elde edilebilir. Nanofiber yapısındaki ekstraktif polimer kaplı SPME örnekleyicilerinin üretimi, bir desteğin yüzeyinde ekstraktif özelliklere sahip nano ve mikro-fiber yapılı polimerlerin doğrudan biriktirilmesi avantajına sahip elektroeğirme işlemi ile mümkündür.

Bu çalışmada, SPME problarının hazırlanması için iki yeni elektroeğirme stratejisi önerilmiştir. İlk strateji, elektroeğirme sırasında analitin baskılanmasına dayanan yeni bir ekstraktif faz hazırlama yöntemidir. Şablonlar (trifluralin ve karbaril), analite özgü bölgeler üretmek için elektroeğirme tekniği kullanılarak hazır bir

polimere (poliakrilonitril) immobilize edilmiş, böylece daha kolay üretim ve gelişmiş analit seçici ekstraksiyon sağlanmıştır. İkinci strateji, elektroeğirmenin tekrarlanabilirlik sorunlarının üstesinden gelmek için önerilmiştir. Geleneksel elektroeğirmenin aksine, poli(divinilbenzen) partikülleri içeren poliakrilonitril karışımı bir bıçağa damlatılmış ve yüksek voltaj uygulanmıştır. Bu yöntem, hızlı ekstraksiyon kinetiği ile ince kaplamaların daha kontrol edilebilir üretimini sağlamıştır.

İki örnekleyici de tarımsal üretimde sıklıkla kullanılan pestisitlerin (trifluralin, karbaril, diazinon, malathion ve parathion) kullanıldığı kavram kanıtlama çalışmalarında başarıyla değerlendirilmiştir.

Anahtar Kelimeler: Katı Faz Mikroekstraksiyon, İnce Film Mikroekstraksiyon, Moleküler Baskılanmış Polimer, Elektroeğirme, Kaplama Yöntemi

This thesis is dedicated to the Great Old One

Iä! Iä! Cthulhu Fhtagn!

ACKNOWLEDGMENTS

The author wishes to express his deepest gratitude to his supervisor Assoc. Prof. Dr. Ezel Boyacı for her guidance, advice, criticism, encouragement, and insight throughout the research.

The author would also like to thank Prof. Dr. Jale Hacaloğlu for allowing him to utilize the resources in her facility.

The author would also like to thank Prof. Dr. Ayşen Yılmaz for allowing him to utilize the resources in her facility and İpek Yıldırım for her assistance for XRD.

The author thanks Dr. Yeliz Akpınar for her valuable suggestions. Lastly, the author thanks all the members of Boyacı Research Group and C-50 members for having a great environment in the lab.

The author would also like to thank Prof. Dr. Gülay Ertaş, Prof. Dr. Caner Durucan, Assoc. Prof. Mehmet Gümüştaş, and Assist. Prof. Dr. Erol Yıldırım for their valuable time, insightful feedback, and constructive discussions during his thesis defense.

The study in Chapter 3 is funded by the METU Coordinatorship of Scientific Research Projects under grant number GAP-103-2023-11392

TABLE OF CONTENTS

LIST OF TABLES

TABLES

LIST OF FIGURES

FIGURES

LIST OF ABBREVIATIONS

ABBREVIATIONS

AIBN	Azobisisobutyronitrile
BET	Brunauer-Emmett-Teller
BJH	Barrett-Joyner-Halenda
COF	Covalent-organic frameworks
DMF	N, N-Dimethylformamide
DVB	Divinylbenzene
EDMA	Ethylene glycol dimethacrylate
FTIR	Fourier transform infrared spectroscopy
GC-MS	Gas chromatography-mass spectrometry
HLB	Hydrophilic-lipophilic balanced
IL	Ionic liquids
LLE	Liquid-liquid extraction
MIP	Molecularly imprinted polymer
MOF	Metal-organic frameworks
MRL	Maximum Residual Level
NIP	Non-imprinted polymer
PA	Polyacrylate
PAN	Polyacrylonitrile
PDMS	Poly(dimethylsiloxane)

PEG	Polyethylene glycol
PI	Polyimide
PMIP	Pseudo-molecularly imprinted polymers
SE	Soxhlet extraction
SEM	Scanning electron microscope
SPE	Solid phase extraction
SPME	Solid phase microextraction
TFME	Thin film microextraction
TRIM	Trimethylolpropane trimethacrylate
TWA	Time-weighted average
UPW	Ultrapure water
XRD	X-ray diffraction

LIST OF SYMBOLS

SYMBOLS

A_C	Integral area of the crystalline peaks in the XRD patterns
A_T	Total area of diffraction in the XRD patterns
a_e	Activity of the analyte in the extraction phase
a_s	Activity of the analyte in the sample matrix
C_0	İnitial concentration of analyte
C_e	Concentration of an analyte in the extraction phase
C_s	Concentration of an analyte in the sample matrix
IF	Imprinting factor
K_0	Distribution constant
K_{fs}	Distribution coefficient
K_{fw}	Distribution constant for the analyte between fiber and pure water
n	Amount of extracted analyte
R	Gas constant
S_e	Surface area concentration of the analyte adsorbed by the coating
S_{rel}	Relative selectivity
V_e	Volume of the extraction phase
V_s	Volume of sample
°C	Degree Celsius
ΔH	Change in enthalpy

CHAPTER 1

INTRODUCTION

Solid phase microextraction (SPME) is a technique that has gained popularity due to its several advantages. These advantages are the ability to combine sampling and sample preparation, suitability for in-vivo applications, geometric flexibility, and the capacity to determine free and total concentration in the sample. The versatility of SPME is due to the wide range of options available for the components that comprise an SPME sampler, including the extractive phase, sampler geometry, and coating method. Currently, a variety of sampler geometries have been developed (i.e. fiber, thin-film, and in-tube SPME), providing a wide range of applications including areas such as clinical [1], [2], environmental [3], [4], food [5], [6], and agricultural [7], [8] analyses.

Although some commercial SPME samplers are available, due to their limited numbers of varieties that cannot suit extreme applications (i.e. single cell analysis, coupling to analytical instrument, in-vivo samplings), their inadequate affinity for polar analytes, slow extraction kinetics associated with the use of bulk polymer for their production and their high costs, requires the home-made production of new samplers and extractive phases with tuned properties. In this note, various functional materials including inorganic and carbon-based nanoparticles, polymeric particles, metal-organic frameworks (MOF) [9], [10], covalent-organic frameworks (COF) [11], [12], and ionic liquids (IL) [13], [14] have been used as extractive phases. Moreover, homemade advanced materials such as molecularly imprinted polymers (MIPs) are frequently employed as extractive phases with analyte selective nature [15], [16]. However, MIPs also exhibit significant limitations, including insufficient specific extraction, challenging preparation as numerous parameters must be

optimized to obtain the best selectivity, and an inability to be used in aqueous media, which is a common feature of most MIP materials [17].

In this thesis, new strategies based on the electrospinning approach were proposed to prepare new SPME-based extractive phases with a selective nature and samplers with enhanced extraction kinetics that can suit various applications where high sensitivity, selectivity, and reliability are needed.

In the first chapter of the study, a novel selective solid phase microextraction (SPME) sorbent production strategy was proposed which was based on imprinting the polymer with analyte during the production of electrospun nanofibrous mat. Differently from the MIP production technique where the analyte-monomer couple first interacts and then polymerization is conducted, in this approach, the analyte was dissolved in a polymeric solution that was used to create analyte-specific regions. Thus, the technique was named pseudo-molecularly imprinted polymers (PMIPs). With this method, nanofibrous coatings with selectivity towards two pesticides (carbaryl and trifluralin, selected as probe analytes) were prepared, optimized for the best selectivity, and tested successfully for the extraction of the analytes from water.

The second chapter of this thesis was focused on new electrospinning strategies to produce ultra-thin coatings with fast extraction kinetics which at the same time can be made reproducibly. Although the electrospinning process can produce extractive phases with high surface area and, therefore, high extraction capacities, our studies showed that the primary constraint of this technique is that even minor instantaneous alterations in environmental conditions impact the electrospinning process, making it challenging to maintain precise control over coating thickness. To overcome these problems in this chapter a novel approach based on electrospinning of a single-drop polymer solution (made of PAN containing PDVB nanoparticles) under static conditions was proposed for the fabrication of SPME coatings. The prepared probes were optimized for the best coating solution and evaluated for their production reproducibility and extraction kinetics using four frequently used pesticides (trifluralin, malathion, parathion, and diazinon) as model compounds.

1.1 Sample Preparation

In analytical chemistry, sample preparation is a crucial step to be implemented before separation and quantification, which must be applied carefully to obtain meaningful data in most measurements. In addition, sample preparation is as necessary as sampling, which is essential for an accurate analysis. Although it was often overlooked in the past, with the increase in production, technology, and environmental awareness to date, the need for developments in the field of sample preparation has also arisen. As a result, it has become one of the key components of separation-based analytical methods.

The separation-based analytical methods consist of five main steps. Those steps are sampling, sample preparation, separation, quantification, and data analysis. In the past decades, when sample preparation was still not as popular as it is today, it was not as thoroughly developed as other steps. Therefore, it was described as a rather long and laborious step, accounting for up to 80% of the total time involved in creating these methods [18]. Luckily, the invention of solid phase extraction (SPE) technology helped speed up the further development of sample preparation and shorten the time spent on the slowest step of analytical procedures [19]. Figure 1.1 shows the general steps of separation-based analytical studies.

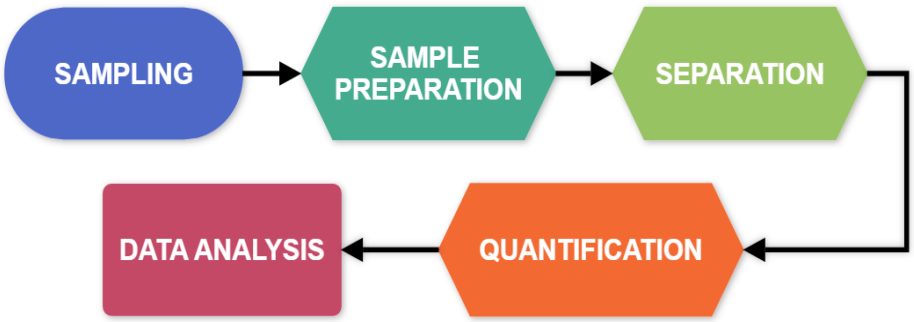

Figure 1.1. General procedural steps of separation-based analysis

The sample preparation step began to be widely used in analytical procedures, certain advantages were achieved, and the quality of the analyses increased. The first of these advantages is that sample preparation increases the compatibility of the analytical device. Since not every analytical instrument can be used directly in all matrices, analytes must be separated from their matrices and made suitable for analysis with the help of sample preparation. In addition, the analytes of samples with very complex matrices can be isolated into simpler matrices using sample preparation methods. In this way, more accessible and reproducible analyses can be carried out by increasing the compatibility of the sample with the instrument to be used.

The second advantage is that the analyte can be extracted and separated from possible interferences with sample preparation methods. This contributes to the selectivity of the total analysis.

The third advantage is related to errors and dysfunctions in some analytical methods and instruments. In cases where the analyte remains below the limit of detection for an instrument due to its low concentration, sample preparation methods solve this problem by preconcentrating the analytes to a detectable concentration.

1.1.1 Applications of Sample Preparation

Thanks to its popularity and critical advantages over the past decades, sample preparation has been utilized in a variety of analytical chemistry applications.

One of the most common application areas is food analysis [20]. As the food industry is developing, sample preparation methods that are cheaper, easier, and consume less reagent than traditional techniques have begun to be used as an integral part of the analysis focused on complex and heterogeneous mixtures. Moreover, the sample preparation step has an important place during the elemental analysis of highly

harmful heavy metals and essential minerals in food products [21] and the analysis of macro- and micro-nutrients such as lipids proteins, and vitamins [22].

Another area that greatly benefits from sample preparation is environmental analysis [23]. Human-induced environmental pollution, which is increasing day by day, has brought attention to ecological sustainability and human health. Therefore, for reliable monitoring of chemicals with anthropogenic sources in environmental samples consisting of very different complex matrices, sample preparation methods are used [24]. In the past decades, many studies have documented the benefits of sample preparation protocols for analyzing pesticides [25], polycyclic aromatic hydrocarbons [26], organotin compounds [27], and other contaminants in environmental samples such as groundwater and sediment. In addition, using greener sample preparation methods is of great importance for a sustainable environment [28].

Like other fields of study, clinical/pharmaceutical analysis involves carefully extracting trace amounts of molecules of interest from highly complex matrices such as blood, plasma, urine, and pharmaceutical excipients [29]. For this reason, sample preparation techniques are frequently used methods to increase the efficiency, sensitivity, cost-effectiveness, and repeatability of analyses for the determination of therapeutics [30], various disease biomarkers [31], illicit drug determination [32].

Apart from these, the benefits of sample preparation are also used in many different fields such as forensic investigations [33], oil and gas analysis [34], DNA sequencing [35] and metabolomics [36]. Sample preparation is the key to extracting relevant insights, making well-informed choices, and increasing scientific knowledge across these varied fields. Methods in each of these application areas may differ based on the nature of the sample and the individual analytical technique being utilized.

1.1.2 Types of Sample Preparation

Sample preparation studies, which have applications in numerous fields, can be traced back to when analytical chemists first began working with complex samples. Many different sample preparation methods are available, from simple grinding of the sample to comprehensive extraction methods. As discussed by Chen et al., there are dozens of sample preparation methods belonging to eleven core principles, such as gravity, phase separation, and sorption/equilibration [18].

Although some of these core principles are well-established and deeply developed, some of them may be more advantageous than others in terms of their speed, selectivity, solvent consumption, and high throughput quantification. For this reason, there are promising techniques that can be considered new trends.

On the other side of the coin, there are non-chemical methods. Among the non-chemical techniques, examples of mechanical processes, such as seizing and grinding or centrifugation using gravity, are relatively simpler and more accessible. Apart from these, the extraction techniques that include the focus of this thesis are widely accepted and have been successfully developed and more advanced in terms of sample preparation over the last few decades. Extraction techniques, which isolate analytes from complicated matrices by non-chemical processing, are among one of the most widely used approaches [37]. Liquid-Liquid Extraction (LLE), Solid-Phase Extraction (SPE), and Solid-Phase Microextraction (SPME) can be given as examples of the most popular and valuable extraction methods.

1.1.3 Sample Preparation by Extraction

The goal of extraction techniques in chemistry is to acquire a pre-concentration of the target compound while separating it from the undesirable matrix components. The primary characteristic shared by extraction-based sample preparation techniques

is the extraction phase's interaction with the sample matrix. In this manner, the analyte can be transferred between phases, such as the extractive phase and the sample matrix.

1.1.3.1 Types of Extraction Techniques

There are many different sample preparation methods based on extraction. The methods vary in their application depending on factors such as different extractive phases and sample matrices, extraction capacity, duration, amount of solvent used, and exhaustive/non-exhaustive extraction. As discussed in Pawliszyn et al.'s Handbook of Sample Preparation book, the classification of these methods can be examined under three main headings [19] (Figure 1.2).

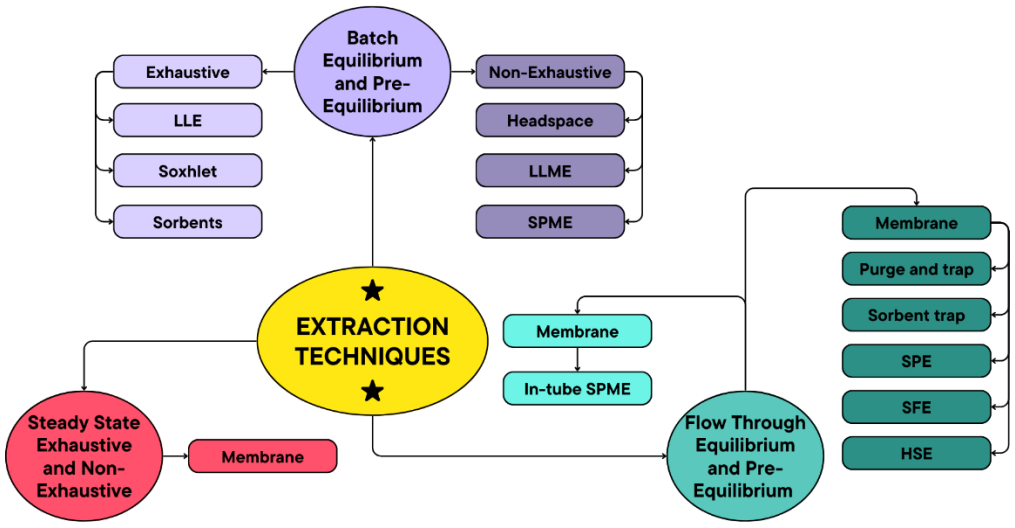

Figure 1.2. Classification of extraction techniques (adapted from Pawliszyn et al.'s Comprehensive Sampling and Sample Preparation [19], with modifications.)

These main topics are flow-through, batch, and steady-state processes, which are related to the working principles of the methods. In batch extraction, the sample and extractive phase are placed in a single container and interact for a certain period. The second process, the flow-through process, occurs by continuously introducing the mobile phase through the stable phase present in a cartridge. Flow-through extraction is more advantageous than the batch mode in terms of using less solvent, higher recovery capacity, or shorter time requirements for exhaustive extractions. Because large volumes of samples can flow through a small extractive phase at once [38]. Additionally, in the sequential extraction analyses, flow-through methods reduce the possibility of analytes returning to the sample matrix [39]. However, batch extraction is used more frequently in laboratory applications because it can be used in small amounts of samples, and time requirements can be reduced by a parallel automation process [40]. Finally, the basis of steady-state extraction relies on the principles of permeation via a semipermeable membrane. When the sample is introduced to one side of the membrane, the analytes of interest pass through it due to the chemical potential difference between the two sides of the membrane material. In Figure 1.3, a schematic diagram of extraction methods is illustrated.

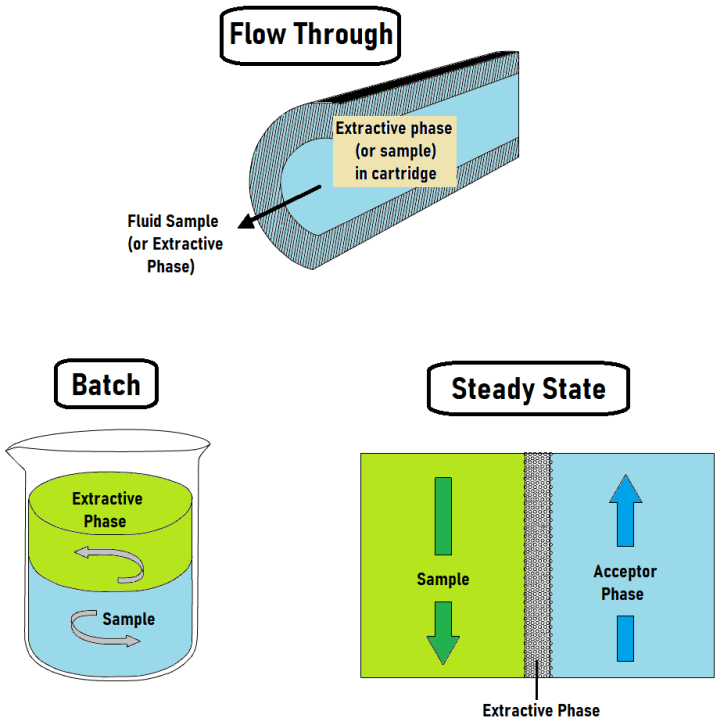

Figure 1.3. Schematic diagram of extraction methods' working principles

The second important element regarding classification is whether extraction is exhaustive or non-exhaustive. Exhaustive methods aim to extract all the analytes in the sample or a non-significant amount of them remain in the sample. In this way, high recovery can be achieved especially in the flow-through model [38]. Moreover, the need for calibration can often be eliminated since the extracted amount can be calculated simply with the equation:

$$n \approx V_s C_0 \qquad \text{Equation 1}$$

Where n is the extracted amount of analyte, V_s is the sample volume, and C_0 is the initial concentration of the analyte in the sample [41].

Contrary to exhaustive extraction, in non-exhaustive extraction small portions of analytes are extracted. Non-exhaustive extraction occurs when the substance transition between the sample and extractive phase reaches equilibrium (analogous to exhaustive equilibrium extraction). Alternatively, it can be a pre-equilibrium process. Non-exhausting approaches can be used with pre-equilibrium extractions for samples that contain a significant amount of analyte, making it easy to obtain higher sensitivity. In this process, the contact time between the extractive phase and the sample is kept short. Equilibrium extraction is performed in both exhaustive and non-exhaustive ways. The main difference between exhaustive and non-exhaustive equilibrium extraction is the capacity of the extractive phase. While the extractive phase in the exhaustive process extracts the analyte completely, the extracting phase in non-exhaustive extraction is not able to do so since it's lower volume or small extractive phase-sample matrix distribution constant.

Permeation extraction mode allows both exhaustive and non-exhaustive extractions. In permeation, it is aimed to reach equilibrium by constant transport of analytes between phases. In addition, it is possible to achieve exhaustive extraction by adjusting the sample and stripping flow, developing appropriate membrane modules, and controlling extraction variables such as sample salinity and temperature [42].

Apart from LLE, different extraction techniques are also subject to these classifications. The first example of one of the most widely used methods is Solid Phase Extraction (SPE), which drew attention to sample preparation technology and pioneered developments in this field [43]. SPE, the majority of which are exhaustive flow-through methods, basically consists of a liquid, fluid, or gas sample passing through an extractive phase packed in a cartridge or a disc. While the sample flows through the extractive phase, analytes are sorbed by the extractive phase. After the retention of analytes, they are eluded using a solvent or thermally desorbed into the gas phase (Figure 1.4). Since the LLE is labor-intensive, difficult to automate, and consumes a higher volume of solvent, SPE is occasionally considered a replacement for LLE [44]. Today, many types of SPEs have been developed in-depth thanks to

their advantages, such as lower solvent consumption, shorter and effortless processing, ease of automation, and a wide range of applications [45].

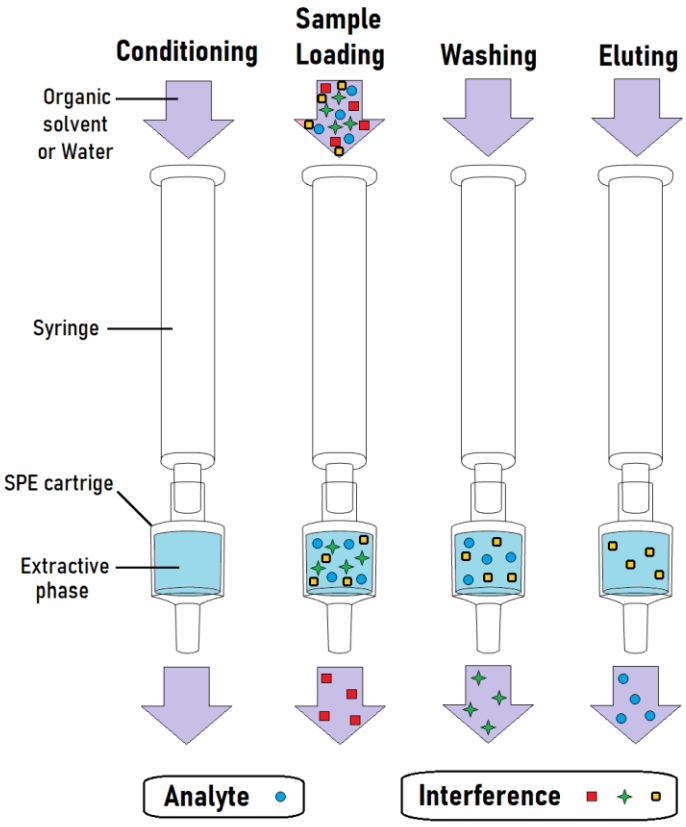

Figure 1.4. Typical steps involved in a SPE

The Soxhlet extraction (SE) method, first used by Franz Ritter von Soxhlet in 1879 to determine fat in milk, is one of the first automated extraction methods [46]. Biologically active substances, such as plant extracts, essential oils, and other components derived from natural sources, are typically extracted from solid samples using this method. SE is an important method that enables automated extraction, especially with effortless equipment. The Soxhlet extractor consists of three main parts, as seen in Figure 1.5.

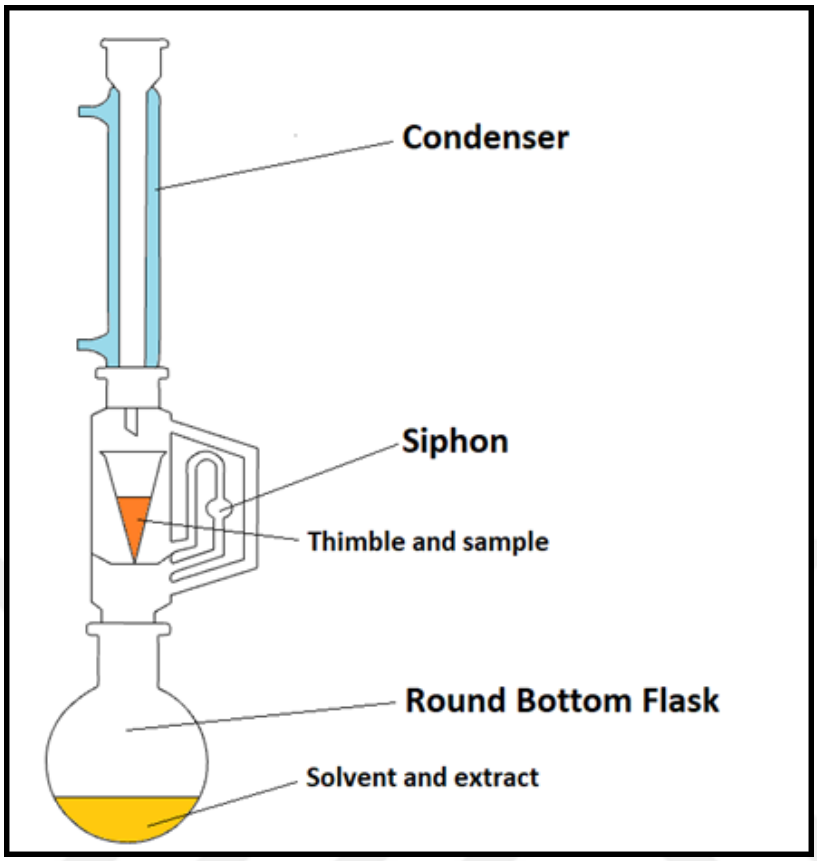

Figure 1.5. Schematic representation of Soxhlet extractor

SE, which has a very simple operating principle, works as follows: the extraction solvent, which constantly evaporates in the round bottom flask, accumulates in the thimble with the help of a condenser. As the accumulation continues, the extraction solvent in the thimble and the siphon tube begin to rise and come into contact with the solid phase inside the thimble. When the accumulated solvent reaches the siphon height, it is unloaded from the thimble to the round bottom flask. This cycle continues as the heating process continues. Thus, the sample is extracted with a fresh solvent that evaporates in each cycle. Thus, the washing or purification process is achieved [47]. However, there are some disadvantages to the method. Firstly, solvent consumption is relatively high, and therefore, the extraction process takes a long time. Also, samples are often extracted for an extended period of time at the boiling

point of the extracting solvent, which has the potential to cause thermal decomposition in the samples [48]. Therefore, SE can be a suitable extraction method for overnight washing, usually using simple equipment.

The general advantages of the technique make the Soxhlet extraction a frequently used method today. In addition, this process has been further developed over the years and has achieved higher performance. To increase the usefulness of this method, Ultrasound Assisted Soxhlet Extractor [49] and Microwave Assisted Soxhlet Extractor [50] can be given as examples of improved SE methods.

Other frequently used techniques are microextraction-based approaches. Microextraction techniques are practical and primarily developed to reduce equipment size and solvent consumption. In this technique, the extractive phase has a relatively smaller volume than classical extraction techniques. These extractive phases, which may have different geometries and physical properties (i.e. solid-phase microextraction and liquid-phase microextraction), extract only a small portion of the analytes from the sample. The amount of analyte to be extracted depends on many essential properties, such as the physicochemical properties of the extractive phase, the volume of the extractive phase, temperature, and interaction time. The technique focused on in this study is Solid-Phase Microextraction (SPME). This method, which is frequently used today, shows its usefulness in many different applications. Low solvent consumption, practical use, ability to work with a wide range of analytical instruments and being suitable for direct sampling are some of the advantages of SPME.

1.2 Solid-Phase Microextraction (SPME)

Solid-phase microextraction was developed in 1990 by Janusz Pawliszyn and has since grown in popularity as one of the chemist's go-to sample preparation method [51].

SPME enables sampling, extraction, preconcentration, and transfer of the analyte to the instrument within easy and less time-consuming steps. Those steps could be as simple as the extraction of analytes from the sample by keeping the sampler for a pre-determined time in the matrix and desorption of the extracted analytes into an analytical instrument (i.e. thermal desorption to GC) or a solvent (solvent desorption prior to instrumental analysis). Before the first step of most SPMEs, a conditioning step is applied to prepare the extractive phase for extraction by wetting the pores (solvent conditioning) or expanding the pores (thermal conditioning) if the extractive phase has a porous structure. If this step is performed with a solvent, the excess solvent is removed with a quick rinsing step just before the extraction. Following the extraction, optionally, any matrix components that remain on the sorbent are cleaned with a wipe followed by a second rinsing step. Finally, the analytes are desorbed. A general representation of the steps of the SPME method is shown in Figure 1.6.

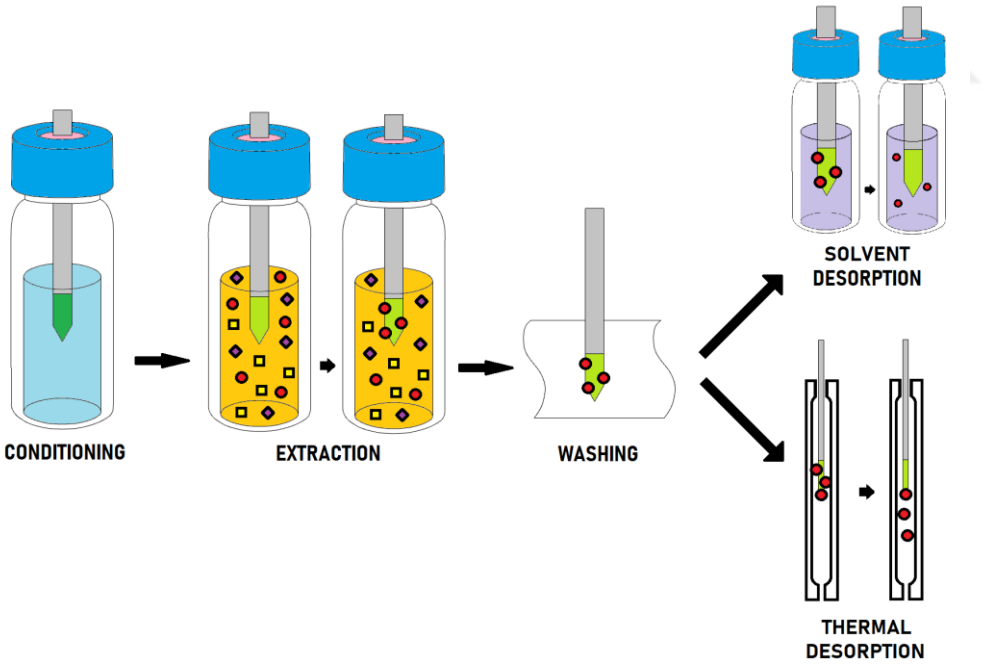

Figure 1.6. Typical steps involved in a SPME

As mentioned before SPME can be integrated with the analytical instrument. In this way, SPME reduces analyte losses, and enables the introduction of all analytes to the instrument, thereby providing high sensitivity despite only a small portion of analytes being extracted from the sample. Other than this, the SPME method has several advantages [52]. Since this method requires no or minimal solvent, it is a greener method than the classical sample preparation methods. In addition, it is a highly versatile extraction technique since, depending on the application area, the size and geometry of the extractive phase can be altered. For example, thin films are suitable for parallel sample preparation processing for 96-well plate enabling high throughput processing of the samples. Furthermore, miniaturized samplers enable low-invasive direct in-vivo applications [53].

1.2.1 Theory of SPME

As mentioned before with SPME the extraction can be done in two different ways: equilibrium and pre-equilibrium. If the extraction time is kept sufficiently long, the partition of the analyte between the extractive phase (coating) and sample matrix is ensured to reach equilibrium. In that case, the maximum extraction and sensitivity level will be reached. As an alternative to equilibrium extraction, pre-equilibrium conditions can be also used with SPME, if a sufficient sensitivity level can be achieved. In that case, the interaction between the extractive phase and the sample matrix can be broken before the extraction process reaches equilibrium [19].

The thermodynamics of the extraction can provide insightful information about the analytical procedure, such as equilibrium time and the concentration of analytes in the extraction phase at equilibrium [54].

Similar to the distribution constant between octanol and water, the distribution constant (K_{fs}) between the extraction phase and sample matrix determines the

process's thermodynamics. K_{fs} is derived from the chemical composition of the extractive phase and various other parameters that will be discussed later.

If the extractive phase is in liquid form, the equilibrium conditions can be explained as follows:

$$K_{fs} = \frac{a_e}{a_s} = \frac{C_e}{C_s} \qquad \text{Equation 2}$$

Where K_{fs} is the distribution constant, a_e and a_s are the activities of the analytes in the extraction phase and the sample matrix, respectively. C_e and C_s are the concentrations of the analytes in the extraction phase and the sample matrix, respectively. If the extractive phase is in a solid (made of porous particles), as this thesis emphasizes, then adsorption also becomes relevant. With the new formula in which the adsorptive surface area is added, the equilibrium conditions can be explained as follows:

$$K_{fs} = \frac{S_e}{C_s} \qquad \text{Equation 3}$$

Where S_e is the surface concentration of the analyte adsorbed by the coating and C_s is the concentration of the analytes in the sample matrix.

As mentioned before, the amount of extracted analytes at equilibrium is related to the coating material, thus the distribution constant. Therefore, in a two-phase system consisting of a sample matrix and the extraction phase, the number of moles of analytes extracted at equilibrium can be determined as follows:

$$n_e = \frac{K_{fs}V_eV_sC_0}{K_{fs}V_e+V_s}$$ Equation 4

Where, V_e and V_s are the volume of extraction phase and sample, respectively. C_o is the initial concentration of the analyte in the sample matrix. If the volume of the sample is very large compared to the extractive phase volume ($V_s >> V_e$) and K_{fs} is significantly small compared to the affinity toward the sample matrix, $K_{fs}V_e$ in the denominator can be omitted. As a result, the above equation can be simplified as follows:

$$n = K_{fs}V_eC_0$$ Equation 5

This equation is handy when the sample volume is unknown (i.e. in-vivo and on-site samplings). Since the amount of extracted analyte will directly correlate to its concentration in the sample without relying on the sample volume, the extractive phase can be exposed to flowing blood, ambient air, lake, or river directly [55].

Several factors affect the equilibrium distribution constant (K_{fs}) between the analyte extracted into the SPME coating and in the sample matrix, which in turn affects the thermodynamics of SPME. Those parameters affecting K_{fs} are temperature, pH, salting, and polarity of the sample matrix and coating material.

1.2.1.1 Factors Affecting K_{fs}

The first factor affecting the K_{fs} value is temperature. The effect of temperature on extraction should be considered in outdoor sampling or extractions that need heating

applications (e.g. headspace extraction). When the temperature of sample and extractive phase change from T_0 to T, K_{fs} changes as shown in the equation below:

$$K_{fs} = K_0 \exp\left[-\frac{\Delta H}{R}\left(\frac{1}{T} - \frac{1}{T_0}\right)\right] \qquad \text{Equation 6}$$

Where K_0 is the distribution constant at initial temperature, R is the gas constant, and ΔH is the molar change in enthalpy of the analyte as it passes from the sample to the fiber coating. Higher extraction temperatures cause the analytes to diffuse more quickly, which increases the extraction kinetics. On the other hand, the partitioning coefficient falls and, thus, the amount of extracted analyte decreases as at equilibrium albeit the volatility of analytes rises at high temperatures. As a result, temperature has a critical impact on SPME performance. Therefore, strict temperature control is required to achieve an accurate SPME process.

Sample pH has also a critical effect on the affinity of the analyte for the extractive phase. Therefore, it is one of the parameters that should be optimized when an SPME procedure is developed. The thermodynamics of SPME can be influenced by the sample pH, especially in the case of analytes that bear acidic and basic moieties. pH changes can impact analyte ionization and, thus, its partitioning behavior (if the coating is extracting a neutral form of the analyte). For example, at acidic pHs acids are present in their neutral forms, which increases partition into the coating and increases the sensitivity of the final method. Similarly, high pH values increase the extraction of basic compounds. If the analyte contains both acidic and basic functional groups, an optimization study is needed for the sample pH [56]. Contrary to ionic molecules, compounds that do not have acidic or basic moieties are unaffected by the sample pH. It should be noted that this discussion is limited to extractive phases that extract analytes via their neutral forms. For ion exchange sorbents, sample pH should be adjusted to increase the charge difference between the sorbent and analyte.

Salting can also alter the extracted amount of analyte depending on the analyte and salt content. When salts are added to an aqueous sample, they increase the ionic strength of the solution. This leads to a decrease in the solubility of polar analytes (salting out), increasing their extraction [57]. Conversely, the salting-in effect can be seen for nonpolar analytes since their solubility increases in the aqueous media when salt is added to the sample. The impact of salting on SPME has only been determined by experimentation thus far, as it has yet to be theoretically investigated [58]. For this reason, many authors have put forward different ideas to attribute the salting effect [59], [60].

The last parameter affecting K_{fs} is the presence of organic solvent in the sample. The following equation can be applied to predict the change in K_{fs} under different sample polarities:

$$K_{fs} = 2.303 K_{fw} exp\left(\frac{P_1 - P_2}{2}\right) \quad \text{Equation 7}$$

where K_{fw} is the distribution constant for the analyte between fiber and pure water, c is the concentration of solvent, and;

$$P_2 = cP_s + (1 - c)P_1 \quad \text{Equation 8}$$

where P_1=10.2 is the polarity index for water, P_2 is the polarity index for water/solvent mixture, and P_s is the polarity index for solvent. It should be noted that this relationship indicates that, to avoid significantly affecting the characteristics and distribution constant of water, the solvent concentration should be maintained below 1% [61].

1.2.1.2 Calibration of SPME

In contrast to conventional sample preparation techniques, SPME, a non-exhaustive extraction, only removes a small amount of the target analyte from the sample matrix. Consequently, it is crucial to calibrate SPME for quantitative analysis. The calibration procedure that is used depends on several variables. The specific analytical application, the accessibility of isotopically labeled standards, the type of sample matrix, and the level of precision and accuracy necessary for the analysis are those factors. Apart from the traditional calibration methods (external standard, internal standard, and standard addition), equilibrium extraction, exhaustive extraction, and diffusion-based calibration methods are also used. According to Ouyang and Pawliszyn's study, the mentioned calibration methods and their advantages and disadvantages are summarized in Table 1.1 [62].

Table 1.1 SPME Calibration Methods and Their Advantages and Disadvantages

Calibration Method		**Advantages**	**Disadvantages**
Traditional	External standard	Do not require extensive sample preparation	Blank sample matrixes for calibration should be available. In the sampling procedure, chromatographic conditions must remain constant.
	Standard addition	Appropriate for the sample compositions unknown and complex (correct sample matrix effects)	Extensive sample preparation and analysis for a large number of samples
	Internal standard	Compensates matrix effects, losses of analytes during sample preparation, and irreproducibility	Suitable internal standards for complex samples are not easy to find. Isotope-labeled standards are expensive and not available for all analytes interested.

Table 1.1. (cont'd) SPME Calibration Methods and Their Advantages and Disadvantages

Equilibrium extraction		The concentration of the analytes can be calculated by the amount of the analytes extracted by the fiber. When the sample volume is vast, e.g., field sampling, the amount of extracted analytes is independent of the sample volume.	The distribution coefficients of the analytes between the fiber coating and the sample matrix (K) should be known or determined.
Exhaustive extraction		The concentration of the target analyte can be easily calculated by calculating the amount of analyte extracted by the fiber coating and the volume of the sample.	Only suitable for small sample volumes and very large distribution coefficients or requires special devices or methods to achieve
Diffusion-based	Fick's first law of diffusion	Suitable for time-weighted average (TWA) sampling. The sampling rate is independent of the face velocity.	The sorbent should be zero sinks for target analytes. The sample rate for water sampling is very low.
	Interface model and cross-flow model	The high sampling rate and short sampling time minimized the competitive effect of the solid coating. Suitable for on-site sampling where the construction of calibration curve and addition of standard are difficult	The flow velocity of the sampling matrix should be controlled or determined. Limited to the linear sampling regime

Table 1.1. (cont'd) SPME Calibration Methods and Their Advantages and Disadvantages

	Kinetic calibration with standard	Suitable for TWA sampling, significantly where the convection and concentrations of analytes always change	Standard loading and *K* value should be known or determined.
	Standard-free kinetic calibration	Does not need standard loading. The concentrations of all extracted analytes in the sample can be calculated.	Need sampling two times and the conditions for sampling should be kept constant. Unsuitable for long-term monitoring. *K* value should be known or determined

1.2.2 Geometries of SPME

In the SMPE, the extractive phase may consist of different geometries with different types of extractive particles (frequently referred to as a coating). Three types of SPME modes can be utilized according to the usage needs and the nature of the target analyte, namely, direct extraction, headspace extraction, and membrane-protected direct extraction modes. The analytes are transferred straight from the sample matrix to the extractive phase when the coated fiber is introduced into the sample in the direct extraction mode. This method is more suitable for non and semi-volatile analytes. Volatile or semi-volatile analytes can be extracted using headspace SPME, which also removes the fiber's contact with the sample matrix. This way, harsh sample conditions (if it is the case) such as strongly acidic or basic samples and non-volatile interferences present in the sample matrix are prevented from reaching the fiber and damaging the fiber. However, because concentrations of the semi-volatile compounds in the gaseous phase at room temperature are usually low, total mass transfer rates are significantly lower, leading to extended extraction times. In the third mode, the membrane is used to protect fibers during the direct mode extraction

from complex sample matrices, similar to the headspace, from damage. Schematic diagrams of the headspace and direct immersion modes of the SPME can be seen in Figure 1.7.

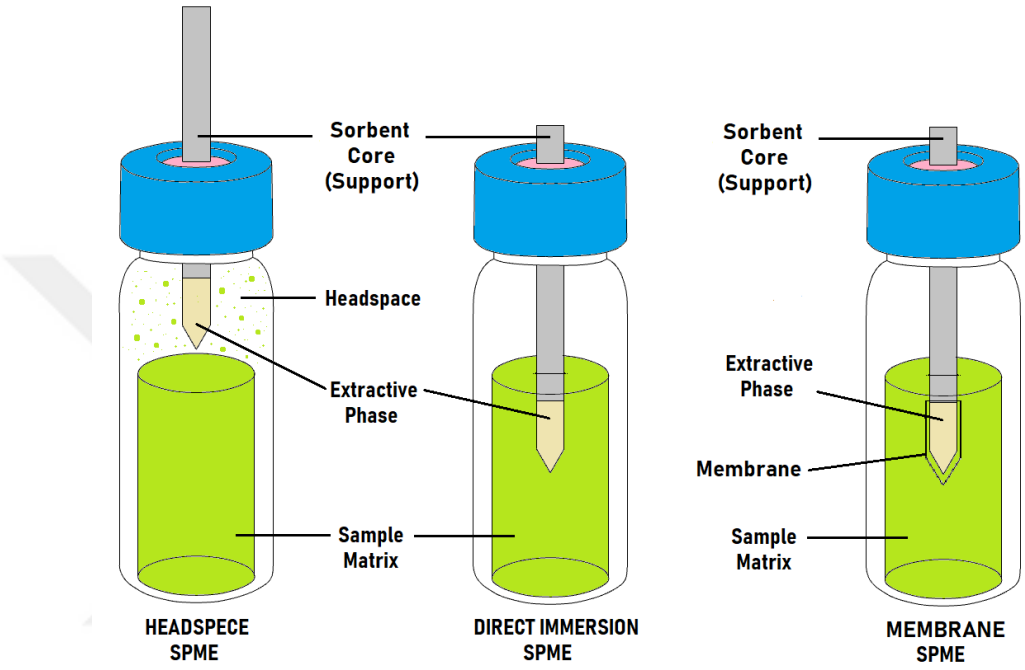

Figure 1.7. Schematic diagram of headspace, direct immersion, and membrane SPME

SPME is a very versatile technique in terms of extraction phase geometry. Different geometries are available to meet the challenges of direct injection to the instrument, suitability for different sampling methods, agitation needs, and automation and on-site applications [63]. Although most popular SPME methods use the batch approach, some flow-through SPMEs also exist [64]. In batch SPME, the sampler is placed directly into a container with the sample to be analyzed, which is particularly useful for sampling from sealed or closed containers. Additionally, flow-through SPME can be used as an alternative to traditional batch SPME. The flow-through method uses a continuous flow of a sample over an SPME material to extract

analytes. This approach enables the use of minimal sample volume and simplifies sample handling, making it easier for continuous monitoring of analytes in a flowing stream.

Numerous SPME sampler geometries are included in batch and flow-through configurations. Batch configurations include fibers, which are one of the most used sampler types. Moreover, large surface area samplers such as thin films and stainless steel wire mesh geometries are included in the batch configuration together with the stir bar, which combines mixing and extraction. Moreover, the flow-through configuration includes in-tube (coating, fiber-packing, sorbent-packing), syringe, and in-tip SPME geometries. Figure 1.8 shows SPME geometries under batch SPME and flow-through SPME categories.

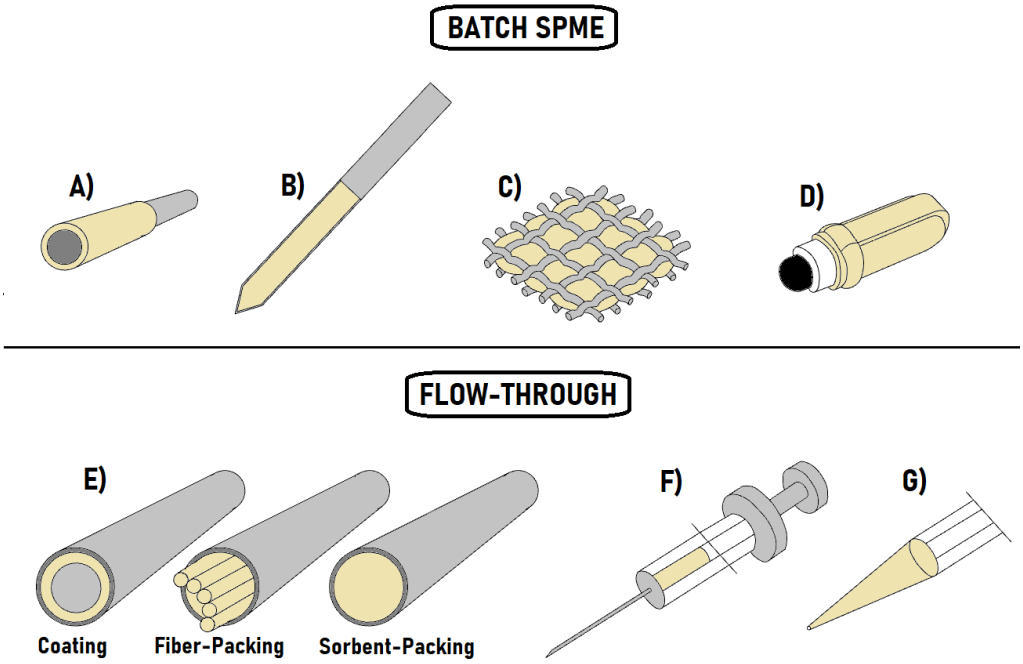

Figure 1.8. Geometries of SPME samplers a) fiber, b) thin-film, c) wire mesh, d) stir bar, e) in-tube, f) in-syringe, and g) in-tip SPME

Fiber is one of the most common SPME geometries. Fiber SPME used for thermal desorption to GC has a modified syringe-like structure and is the first SPME configuration that popularized fiber SPME technology [65]. In this design, the fiber coated with the extractive phase is placed in a stainless steel microtubing. With the help of a plunge, the tip of the fiber can be taken out from the microtubing (exposed to the sample) and pulled back in (retracted into the tubing). The microtubing keeps the coating from wearing out especially when the fiber is desorbed to the GC injector port (during septum penetration) or used in-vivo sampling (during tissue penetration).

Another example of batch SPME sampler geometry is the thin film microextraction (TFME). Unlike traditional fiber geometry, TFME contains a higher volume of extractive phase spread on a greater surface area. Due to the larger volume of the extractive phase, TFME has improved sensitivity, and this geometry enables high extractive capacity and rapid extraction kinetics [66]. A variety of support materials are available, including blade [67], paper [68], and carbon mesh [69], each designed for specific purposes and applications. Another example of TFME support material is the wire mesh. Unlike the blade geometry, both sides of the sorbent material are exposed to the sample matrix in wire mesh. Consequently, the equilibrium time can be shortened with a higher number of contact sites for adsorption [70]. The geometry and design of the wire mesh support are critical to the SPME sorbent's functionality. The needs of the analysis should guide the selection of the mesh size, wire diameter, weave pattern, and overall geometry. For example, mesh size affects the surface area available for coating. A finer mesh with smaller openings can provide better rigidity but limits the surface area for analyte interaction.

In-tube geometry coupled with LC (or open tubular trapping if coupled with GC) can be given as an example of flow-through SPME. In the in-tube SPME mode analytes are extracted using a piece of capillary column that has an appropriate coating applied to its interior surface [71]. The analytes can be delivered straight to the LC system after in-tube SPME, allowing the integration of the sample preparation with instrumental analysis. Since the reduction of manual labor in mode, solvent

consumption can be lowered while the precision and the reproducibility of the extraction increases. In addition, higher sorption capacity compared to fiber geometry is also an advantage of this mode [72].

1.2.3 Sorbents for SPME

Another important aspect of the SPME method is the extractive materials that make up the sorbent and their properties. Many features related to the extractive phase determine the performance of the SPME sampler and the area in which it will be used. These features include the type, thickness, morphology of the extractive phase, and the core to which this phase adheres. Thanks to these features, it is possible to choose sorbents suitable for different analyte types/matrices, extraction capacity, and extraction time. While there are commercially available SPME samplers coated with extractive phases known from stationary phases in GC columns, there are also SPME samplers with new extractive phases that are produced homemade when commercial ones are insufficient.

1.2.3.1 Commercial SPME Sorbents

SPME has become a highly effective and adaptable method for sample preparation. As a result, commercial SPME devices and coatings have become essential in satisfying the growing need for sensitive and selective analytical techniques among researchers and analysts in a variety of fields. These types of devices and coatings are favored based on multiple factors like durability, reusability, and reproducibility between the samplers.

The commercial SPME samplers can be examined under two main headings: Fiber cores and coatings. Since all options have their advantages and disadvantages, it is essential to choose a coating, core, or coating method suitable for the study [73].

Fused silica and quartz were the first materials to be utilized as a fiber core [74], [75]. These relatively inert materials were replaced by other materials over time due to their brittleness. Subsequent stableflex cores were obtained by coating fused silica with a "plastic-like" polymer, making it more resistant to breakage and thermal conditions. However, since this core does not have sufficient thermal resistance and durability due to the fused silica center, metal-based cores have become more preferred.

Various characteristics, including coating thickness, type of extractive materials used, and sorption type (absorption or adsorption) can be used to classify SPME coatings. Among the commercial coatings, polar, nonpolar, or bipolar polymer coatings with affinity for both types of analytes are used to provide selectivity. In addition, the coating thickness determines the capacity of the extractive phase to adsorb/absorb the analyte and the time it takes to reach equilibrium. Sorption type affects the extraction mechanism. The first commercial coatings used were classical polymers that worked with the absorption mechanism. These coatings, which are bonded by crosslinking around the fiber core with crosslinking agent and heat/UV, are liquid-like polymers that can be prepared in different thicknesses. The analytes move further within the coating as they penetrate the coating. Examples of the first classical polymers used are poly(dimethylsiloxane) (PDMS), polyimide (PI), polyethylene glycol (PEG), and polyacrylate (PA) [76].

Adsorbents function differently from absorbent coatings as analyte interacts with a solid particle instead of a liquid polymer. In the case of solid coatings, the analytes move into the adsorbent's pores. Adsorbent surfaces interact with analytes through intermolecular forces, including hydrogen bonds, π-π bonds, or van der Waals interactions [77]. The interacted analyte retains in the adsorbent due to several physical properties, including surface area, pore diameter, and porosity of the

adsorbent. Porous adsorbents can be classified according to their different porosities as micro-, meso- and macro-porous adsorbents with pores diameters ranging between 0.2-2, 2-50, and >50 nanometers, respectively. An analyte that is roughly half the diameter of the pore can be retained in a pore. Adsorbents used for commercial SPME samplers include divinylbenzene (DVB) particles, and carboxen 1006 particles immobilized in PDMS [78], [79]. DVB-PDMS adsorbent is primarily used for the extraction of semi-volatile analytes and larger volatile analytes because this material has a uniform and high degree of meso- and microporosity. Carboxen 1006-PDMS is a member of the carbon molecular sieve group, which is characterized by a very narrow micropore size distribution. The purpose of developing SPME fibers with this adsorbent coating is to extract tiny and volatile analytes. Several commercial fibers include DVB and carboxen particles on the same fiber to increase the molecular weight range of extracted analytes because carboxen-PDMS fibers have trouble desorbing analytes with greater molecular weights, and PDMS-DVB has trouble extracting analytes with lower molecular weights. Table 1.3 shows the types of commercially available SPME coatings, data taken from the Handbook of Solid-Phase Microextraction [73].

Table 1.2 Types of Commercially Available SPME Coatings

Type of coating	**Extraction mechanism**	**Polarity**
7 μm PDMS	Absorbent	Non-polar
30 μm PDMS	Absorbent	Non-polar
100 μm PDMS	Absorbent	Non-polar
85 μm PA	Absorbent	Polar
60 μm Polyethylene glycol (Carbowax)	Absorbent	Polar
15 μm Carbopack Z-PDMS	Adsorbent	Bipolar
65 μm PDMS-DVB	Adsorbent	Bipolar
55 μm/30 μm DVB/Carboxen – PDMS	Adsorbent	Bipolar
85 μm Carboxen – PDMS	Adsorbent	Bipolar

Nevertheless, selectivity, solvent and matrix incompatibilities, and required operating temperatures can be potentially problematic for these generic samplers when a very specific analyte/matrix/instrument combination is needed. Additionally, most fibers have poor extraction performance for non-volatile and strongly polar chemicals [80].

1.2.3.2 Homemade SPME Sorbents

The deficiencies of commercial SPME sorbents created the need to produce new and more advantageous sorbent types. Materials such as molecularly imprinted polymers (MIPs), metal oxides, ionic liquids (ILs), and metal-organic frameworks (MOFs) have emerged as promising alternatives for use as coatings.

1.2.3.2.1 Molecularly Imprinted Polymers (MIPs)

Molecularly Imprinted Polymers (MIPs) are polymers produced by creating predetermined interaction sites that target a specific molecule. MIP extraction phases, which first appeared as an adsorbent for propranolol in in-tube SPME in 2001, have become a frequently used product for studies [81]. Those studies include various applications such as the determination of environmental pollution [82], drug removal [83], and extraction of pesticides [84], herbicides [85], and biological samples [86].

To prepare MIPs, it is necessary to perform the following steps: (1) selection of the template and monomer that will create specific interaction sites for the target analyte. (2) Introduce the template to the monomers that will form the polymer and integrate it physically or chemically with the template. (3) Polymerization of interacting monomers around the template in the presence of a cross-linking agent. (4) Washing

the template, leaves binding sites which selectively bind the analyte [87]. Figure 1.9 shows the schematic representation of the production of MIP.

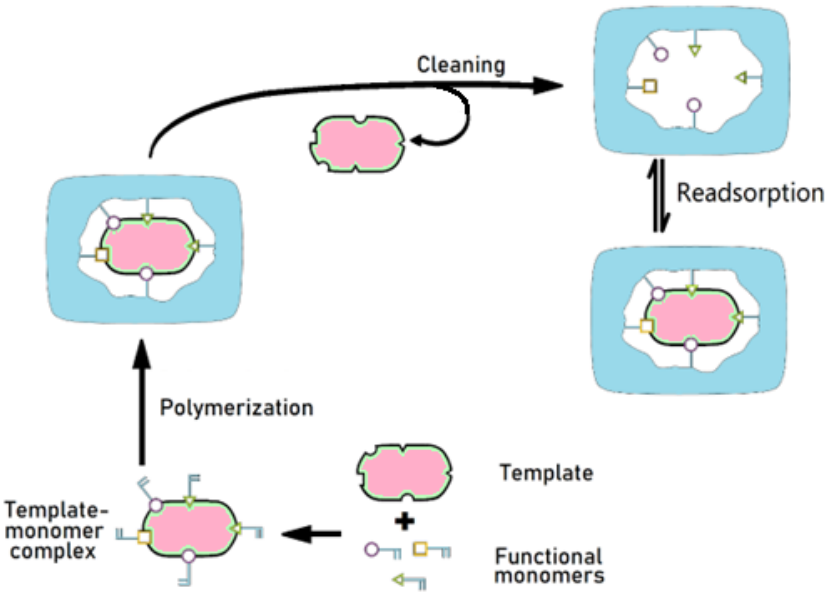

Figure 1.9. Schematic representation of the production of MIP

The selection of an appropriate template-monomer couple is a critical step in the fabrication of MIPs. While most targeted analytes exhibit moderate to high solubility in the polymerization matrix, certain limitations must be taken into account when utilizing them as templates in MIP production [88]. The most fundamental and straightforward of these limitations is that the template must be capable of interacting with functional monomers and maintaining stability during polymerization. However, depending on the degree of interaction between template and monomer, a certain amount of template cannot be removed during washing. Therefore, if the selected template is the same as the analyte to be extracted, the template that has not been completely removed will leach during quantification and cause a certain error. To prevent this, the selected template, if possible, should not be the same as the analyte. At the same time, the template must be a close analog to the analyte so that

the resulting binding sites are also meaningful for the analytes. MIPs must be optimized to decrease the nonspecific binding [89]. Given in Table 1.3, Turiel et al. compiled some important template-analyte selections reported in the literature [90].

Table 1.3 Template-Analyte Selections Reported in the Literature

Template	**Monomers**	**Solvent**	**Initiator**	**Cross linker**	**Analytes**	**Samples**
Prometryn	MAA	Toluene	AIBN	TRIM	Prometryn	Soybean and corn[91]
Prometryn	MAA	Toluene	AIBN	TRIM	Triazines	Soybean, corn, lettuce, and soil [92]
Tetracycline	Acrylamide	Acetone	AIBN	TRIM	Tetracycline	Chicken feed, chicken muscle, and milk [93]
Propanolol	MAA	Acetonitrile	AIBN	TRIM	b-Blockers	Urine and plasma [94]
Ascorbic acid	Chloranil and melamine	DMF	-	-	Ascorbic acid	Human blood serum and pharmaceutical formulations [95]
Propazine	MAA	Toluene	AIBN	EDMA	Triazines	Soil, potatoes, and peas [96]
Diacetylmorphine	MAA	Acetonitrile	AIBN	EDMA	Diacetylmorphine and its analogous	Street heroin [97]
Atrazine	MAA	Acetonitrile	AIBN	EDMA	Triazines	Water, rice, and onion [98]
Ametryn	MAA	Acetonitrile	AIBN	EDMA	Triazines	Tap water, rice, maize, and onion [99]

Table abbreviations: MAA: Methacrylic acid, DMF: N, N-Dimethylformamide, AIBN: Azobisisobutyronitrile, TRIM: Trimethylolpropane trimethacrylate

MIPs have shown to be helpful in many sample preparation applications, but they are not without limitations [100]. First of all, a lot of optimization and effort is required to ensure that polymerization can be carried out correctly. Additionally, various parameters such as percentage of crosslinking, coating thickness, porosity, and aqueous sample compatibility should be optimized [101]. One of the critical limitations is the presence of nonspecific binding sites which are produced by excess monomers that are not included in the template [102]. Because selective cavities can only be accessed after non-specific interaction sites on the surface are occupied, the desired level of selectivity can only be achieved at high concentrations. One of the most important factors that reduce selectivity is cross-reactivity with other molecules via the mentioned nonspecific binding sites. In addition, as mentioned before, removing the template molecules used in MIP production from the extractive phase is a challenging process. Therefore, leakage of the template used potentially interferes with the analyte. To prevent this, dummy templates with minor differences with the analyte can be used [103].

1.2.3.2.2 Ionic Liquids (ILs)

One of the most popular methods that can be offered as an alternative to classical commercial coatings is ionic liquids (ILs), which are chemically bonded or adsorbed to the supporting core [104]. ILs consist of organic salts with melting points below 100°C. An organic (or inorganic) anion and a large organic cation constitute an IL. Commonly used organic anions include bis(trifluoromethyl-sulfonyl)imide, bis(pentafluoroethyl-sulfonyl)imide, trifluoromethane-sulfonate. Inorganic anions include hexafluorophosphate, tetrafluoroborate, and halides. Imidazolium, pyridinium, pyrrolidinium, phosphonium, ammonium, and sulfonium-based cations are also frequently used in ILs [105]. ILs have lower melting temperatures because they are polar ionic compounds with lower cohesive forces than those found in common salts. ILs have several significant advantages over common commercial

alternatives. These advantages include high thermal stability, negligible vapor pressure, and maintaining their liquid state over a wide temperature range. In addition, by changing the substituent group, some important characteristics, such as separation selectivity, hydrophobicity, viscosity, and thermal stability of the ILs, can be altered [106]. Conversely, ILs have some disadvantages that limit their applications. Firstly, these materials significantly limit the use of the resulting coating since they have low durability. Moreover, anion groups such as $[SF_6]^-$ and $[BF_4]^-$ frequently used in hydrophobic ILs, produce dangerous HF when exposed to moisture [107].

1.2.3.2.3 Hydrophilic-Lipophilic Balance (HLB) Particles

Hydrophilic-lipophilic balance (HLB) particles are another frequently used material for the evolution of classic commercial extraction phases. HLB particles have become available for next-generation SPME devices since they were first introduced to the SPME extraction phase polymers such as polyacrylonitrile (PAN) for the quantification of a wide variety of prohibited substances in blood [108]. HLB particles made of poly(divinylbenzene-co-N-vinyl-pyrrolidone) have aromatic rings from divinylbenzene and lactam rings from N-vinylpyrrolidone. Thanks to the groups it contains with different polarities, it provides balanced hydrophilic and hydrophobic interactions [109]. Due to their biocompatibility, suitability for solvent and thermal desorption, and balanced coverage of both polar and nonpolar substances, HLB particles have become increasingly popular in SPME applications [110]. A notable advantage of HLB particles is their complete water-wettability. Consequently, the necessity for a sorbent conditioning phase prior to extraction is eliminated. This property enables the comprehensive recovery of analytes, even in instances where the sorbent becomes dry during the extraction [111].

1.2.4 SPME Coating Approaches

Another critical aspect that contributes to an SPME sampler is the coating approaches utilized to immobilize the extractive phase onto the support material. The coating method determines the surface characteristics of the coating, including coating thickness and surface area to volume ratio. These characteristics significantly affect the extraction performance of the coating. Numerous coating approaches, such as dip coating, spin coating, and electrospinning, have been effectively used to coat the substrate or surfaces.

1.2.4.1 Dip Coating

Dip coating, a simple method, involves immersing the substrate material (i.e., the sampler core) to be coated into a polymer solution, withdrawing it at a constant velocity, and subsequently drying the adhered polymer solution on the core. The critical parameter to consider in this method is that the core should be immersed in the solution without changing the dipping angle and dipping/withdrawing should be performed at a constant speed. Otherwise, undesirable heterogeneity or thickness may be obtained in the coating. Generally, when the withdrawing speed increases, a thicker coating is obtained.

When the core is carefully immersed in the solution and begins to be withdrawn from the solution again, the solvent moves in two different streamlines, as seen in Figure 1.10. One of these streamlines means the solvent returns to the reservoir; the other means it sticks to the core. The point where these two streamlines separate from each other is called stagnation point (S) [112].

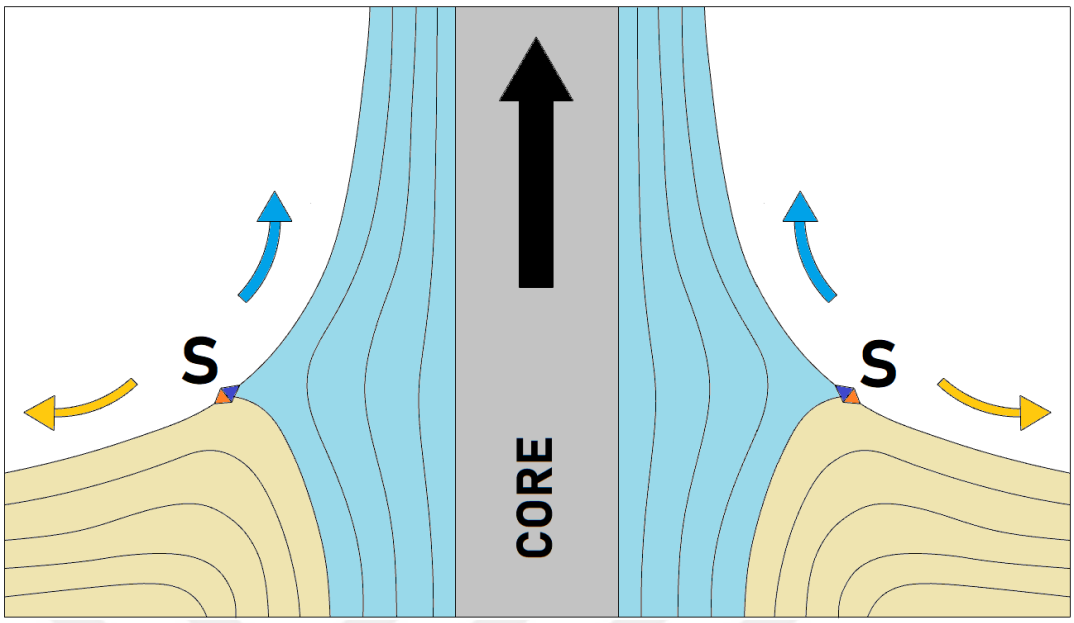

Figure 1.10. Schematic representation of dip coating

Dip coating is a very advantageous method in that it is easy to apply and requires a limited amount of equipment. However, it is necessary to consider the disadvantages of the technique. First, although a uniform coating thickness can be achieved, the coating thickness is extremely sensitive to the withdrawal rate and solution concentration. Obtaining a homogeneous coating is quite challenging due to reasons such as changing concentration with the solvent evaporating during the process and precision errors during withdrawal. In cases where the solvent is not volatile, an extra time-consuming drying step is required. Additionally, a large amount of coating solution is used in this method. For this reason, the technique becomes expensive due to the use of excessive solvents and materials.

1.2.4.2 Spin Coating

Another relatively simple and frequently used coating method is spin coating. In this method, which is based on centrifugal force, the coating mixture dropped on a

rapidly rotating surface is coated. The high-viscosity liquids are coated with a thickness ranging from micrometer to nanometer. Since a volatile solvent is used in viscous liquids, a solid polymer coating is obtained as a result of the coating process [113].

The spin coating consists of four steps: deposition, spin-up, spin-off, and evaporation. In the deposition step, the viscous liquid is dropped onto the surface to be coated. In the spin-up step, the rotation is accelerated in a controlled manner until the desired rotation speed is reached. In the third step, spin-off, rotation is continued at the desired speed to ensure that the deposited liquid is coated on the surface and the coating becomes thinner. In the last step, the coating is dried by evaporation [114].

In spin coating, factors such as spin speed, spin time, acceleration, and fume exhaust are important to obtain the appropriate coated film. For example, since the drying process is more difficult in humid air, a suitable fume exhaust will remove the moisture formed during evaporation, and the drying process will also be shortened [115]. In addition, as the rotation time and speed increase, a thinner coating is obtained as the thinning process continues [116]. The spin coating process is illustrated in Figure 1.11.

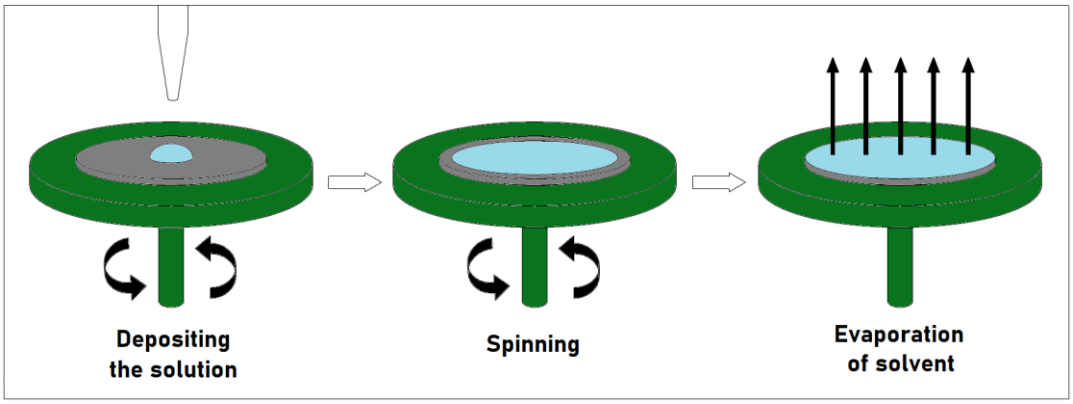

Figure 1.11. Schematic representation of spin coating

Control of thickness is easier in the spin coating method because it is easier to control the parameters on which the thickness depends, such as rotation speed, rotation time, and viscosity. Additionally, since the solution is used in drops, there is much less solution loss. However, this cannot be considered an advantage because most of the deposited material is lost during spinning. This loss goes up to 95-98% [117]. An additional disadvantage of the spin coating technique is that its performance is reduced as the size of the coated particles increases. As the particle size increases, it becomes more challenging to spin at high speed, and thus, it becomes more difficult to obtain the desired thickness [118].

1.2.4.3 Electrospinning

In addition to the commonly used coating methods described above, electrospinning has gained attention for the preparation of nano-micro fibrous coatings. Electrospinning was developed by Anton Formhals in 1934 to produce synthetic filaments [119]. Its popularity has increased over the past few decades, with studies on nanofiber production using various organic polymers [120]. In addition, it has begun to be used to produce nanofiber coatings for SPME extractive phases. Zewe et al. reported the first use of electrospinning technology to prepare an SPME fiber for the extraction of polar and nonpolar substances [121].

Ultra-fine materials, including fibers, mats, membranes, and beads, are created using electrospinning. The shape, diameter, size, and composition of the spinning solutions of molten polymers, carbon materials, silica, and organic compounds can be manipulated by electrically driving them through a spinneret. Nano-micro-fibers produced with this method and whose diameter ranges from 10 nm to 10 μm have certain advantages and limitations compared to other coating methods.

Coatings obtained by electrospinning have significant advantages. The high surface area to volume ratio of electrospun materials is a crucial advantage because their

nano-fibrous network has a higher number of adsorption sites and the total extracted analyte. As a result, lower detection limits and increased sensitivity can be achieved compared to non-electrospun commercial fibers [122]. Another advantage is that the electrospinning method offers a wide range of coating materials such as conductive polymers, nanoparticles, magnetic nanocomposites, and geometries by selection of different sheets or wires as collectors. Also, it is possible to customize electrospun fiber characteristics, including diameter, composition, and shape, using electrospinning [123].

The electrospinning method works with a simple mechanism that requires a low-voltage collector, a high-voltage source, a spinneret (usually a syringe needle) or collector plate, a syringe with a small diameter needle, and a syringe pump. In this setup (Figure 1.12), a circuit is created by connecting a clip to the needle, which is constantly fed with polymer using a syringe pump, and to the collector, which is the surface that will be covered. The liquid's surface tension holds a droplet of the polymer solution at the end of the syringe tip. The molten or dissolved polymer creates a Taylor cone. It travels from the syringe to the collector when a high voltage is applied, producing an electrically charged jet of solution from the small needle. As the solvent evaporates, the polymer solidifies after emerging from the nozzle as a charged jet [124].

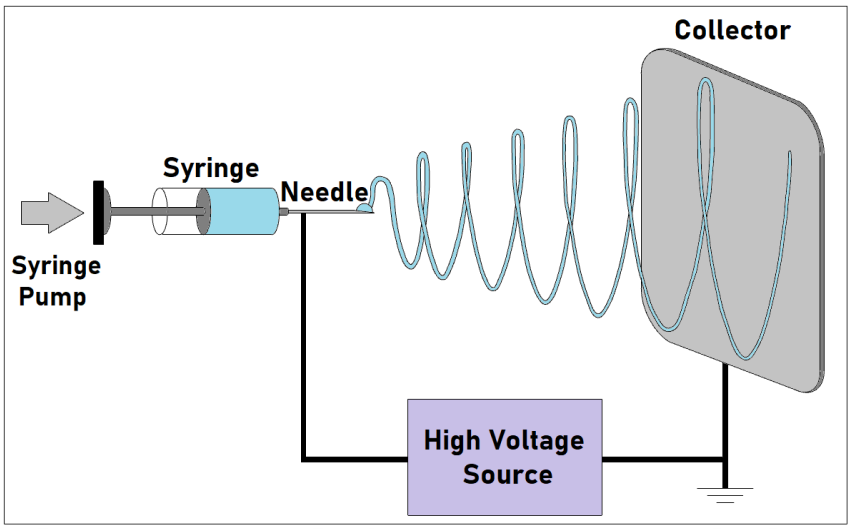

Figure 1.12. Schematic representation of electrospinning

To achieve functional nanofibers with adequate consistency throughout the electrospinning process, certain controlled parameters can be changed to modify the final nanofiber's attributes [125]. Those parameters include the viscosity of the polymer (or polymer-functional particle slurry) in the syringe, applied voltage, flow rate, and the distance between the needle and the collector.

The applied voltage creates an electric field between the needle and the collector. The electric force acting on the charged drop is in opposition to its surface tension. As applied voltage approaches a critical value, surface tension is overcome by surface charge repulsion. Thus, viscosity becomes a crucial element for the electrospinning process as the surface tension rises with the viscosity. Conversely, if the viscosity is excessively high, the solution may dry out or drop at the tip and it will be difficult to pump through the capillary. Factors such as temperature, humidity, solvent, concentration, molecular weight, and polymer type are among the important parameters as they affect viscosity. For example, since the length of the polymer chain influences the entanglements, a higher molecular weight suggests viscous solutions in comparison to a smaller molecular weight. These entanglements prevent the jet from splitting too soon during the procedure.

Another important parameter is the applied voltage. The electrostatic forces that propel fiber generation are controlled by the voltage between the syringe needle and the collector. Due to the polymer jet's more violent discharge, higher voltages usually produce fibers that are finer and have a smaller diameter [126].

The diameter and homogeneity of the nanofibers are also influenced by the flow rate at which the polymer solution is forced through the syringe needle. Thicker fibers are often produced at higher flow rates. Moreover, at high flow rates, polymer builds up at the needle's tip, is unable to reach the collector in sufficient quantity, and spills out in drops. However, the Taylor cone frequently disappears, and the electrospinning process briefly halts because of the needle's slow flow rate. Therefore, to achieve the required diameter, porosity, and form of nanofibers, a continuous and steady flow rate is needed [127].

In addition, the distance between the needle and collector influences fiber morphology. As the gap distance grows, the surface charge density falls because of its negative exponential relationship. Longer distances typically result in thinner fibers because the electric field intensity between the two is reduced. Moreover, the fiber deposition and alignment are influenced by the collector type (spinning drum, flat plate, etc.) and rotation speed [128].

As summarized above, the morphology of electrospun coatings is determined by numerous factors. However, electrospinning is also highly sensitive to environmental factors, which can be a disadvantage of this method. Small changes in factors such as temperature and humidity can significantly alter the structure of the coating obtained at different times [129], [130]. Therefore, achieving the coating requires strict control of these factors, which complicates the optimization of electrospinning parameters. Moreover, when it is used for the preparation of samplers for microextraction purposes, as only a small amount of extractive phases is used, coating the surface in a reproducible manner is the most challenging task.

1.3 Aim of the Study

The aim of this thesis was to develop new electrospinning strategies for the preparation of solid phase microextraction (SPME) probes, thereby enhancing the performance and versatility of SPME samplers. In the first study of the thesis, a new strategy for imprinting polymer during the electrospinning process to produce selective extractive samplers based on the electrospinning approach was proposed. To achieve selectivity, ease of fabrication, and fast extraction kinetics, pseudo-molecularly imprinted polymers were designed. Different from the MIP production technique where the analyte-monomer couple first interacts and then polymerization is conducted, in this approach, analytes (carbaryl and trifluralin) were dissolved in a PAN solution that was used to create analyte-specific regions. In the second study of this thesis, a novel approach based on the electrospinning of a single-drop polymer solution (made of PAN-containing PDVB nanoparticles) under static conditions was proposed for the fabrication of SPME samplers. This alternative electrospinning approach, different from the classical electrospinning approach where a polymeric solution is continuously infused through a needle, is less affected by environmental conditions, requires only a small amount of polymer solution, and can obtain ultrathin coatings in a controlled and reproducible way.

In both studies, the prepared novel probes were successfully optimized and evaluated with model analytes selected from pesticides frequently used in agricultural products in Turkey. The pesticides were selected as model analytes for this thesis because they are one of the critical classes of pollutants albeit their necessity for growing crops in agriculture. Because the uncontrollable excessive use of pesticides has serious effects on nontarget organisms, especially humans, their monitoring of agricultural products and water is crucial. Thus, as proof of the concept, this thesis also showed the possibility of using the new samplers for the determination of pesticides in water samples.

CHAPTER 2

A NEW MOLECULARLY IMPRINTING POLYMER PRODUCTION METHOD FOR USE IN THIN FILM MICROEXTRACTION

2.1 Introductory Summary

In this chapter, a novel selective thin film microextraction (TFME) sampler was proposed which was based on imprinting a water-insoluble polymer with selected probe analytes during the production of electrospun nanofibrous mat. Different from the traditional MIP production technique where the analyte-monomer couple first interacts in a pre-polymerization solution and then polymerization is conducted, in this new approach the analyte was first dissolved in a polymeric solution and then this solution was used to create analyte-specific regions by using electrospinning approach. Thus, the new extractive phase was named pseudo-molecularly imprinted polymer (PMIP). With this method, nanofibrous PAN coatings with selectivity towards two pesticides (trifluralin and carbaryl) were prepared, optimized for the best selectivity, characterized with Fourier Transform Infrared Spectroscopy (FTIR), Scanning Electron Microscopy (SEM) imaging, X-ray Diffraction (XRD), the Brunauer-Emmett-Teller (BET) surface analysis method and then tested successfully for the extraction of the pesticides from water.

2.2 Experimental

2.2.1 Chemicals and Supplies

Polyacrylonitrile (PAN) with an average Mw of 150 KDa (typical) was acquired from Sigma-Aldrich (St. Louis, MO, USA) and used as a polymer for the preparation of electrospun nanofibers. To dissolve PAN for electrospinning, N, N-Dimethylformamide (DMF) which was purchased from Sigma-Aldrich (St. Louis, MO, USA) was used. Technical grade methanol (MeOH) used for template washing was purchased from Tekkim (Mahmutbey, İstanbul, Turkey), and acetic acid (additive in the template removal solvent) was purchased from ISOLAB Chemicals (Eschau, Bavaria, Germany). LC-grade MeOH used for pesticide solution preparation and desorption of analytes (after extraction) was purchased from ISOLAB Chemicals (Eschau, Bavaria, Germany). Helium (high purity, 99.999%), used as the carrier gas in gas chromatography was purchased from Koyuncu (Ümraniye, İstanbul, Turkey). Sodium hydroxide, disodium hydrogen phosphate, potassium dihydrogen phosphate salts, and concentrated (37%) hydrochloric acid were used to prepare buffer solutions with various pHs for evaluation of the effect of sample pH on extraction. From those reagents, sodium hydroxide, disodium hydrogen phosphate, and potassium dihydrogen phosphate were purchased from ISOLAB Chemicals (Eschau, Bavaria, Germany), while hydrochloric acid was purchased from Supelco (Bellefonte, PA, USA).

The pesticides used in the study, namely, trifluralin, carbaryl, malathion, and diazinon (≥98.0% purity), were purchased from Sigma-Aldrich (St. Louis, MO, USA). 1.0 mg/mL stock solution of each pesticide was prepared by dissolving the appropriate amount of the corresponding solid pesticide in LC-grade MeOH. The prepared solutions were stored in the refrigerator at 4°C. Working solutions were prepared before each analysis, and calibration solutions were obtained by diluting this stock solution with LC-grade MeOH.

2.2.2 Instrumentation

To prepare nanofiber coatings, nanoWEB Electro-spin110 coupled with New Era Pump Systems NE-1000 syringe pump (NY, USA) was used. The template molecules were washed from the sorbent using an ELMA LC 30 ultrasonic bath (Bremen, Germany) and Soxhlet extractor. The extraction and desorption were performed using a plate shaker CAT AEK-SH10. The ultrapure water (18.2 MΩ.cm) used in experiments was obtained from Millipore Milli Q Plus (Massachusetts, USA). In the pH studies, the pH of the prepared buffer solutions was measured with a HANNA HI 2002 Edge pH meter (Rhode Island, USA).

An Agilent 6890A gas chromatograph coupled with an Agilent 5973 quadrupole mass selective detector (California, USA) was used to separate and quantify the analytes of the study. In the GC, separation was performed with a 30-meter ultra-inert (5%-phenyl)-methylpolysiloxane column with 0.25 mm inner diameter and 0.25 μm film thickness (Agilent Technologies, HP-5MS), and separation was carried out using helium as carrier gas.

During the extractive phase characterization, a Bruker Alpha Fourier-transform infrared (FTIR) spectrometer (Massachusetts, USA) was used with KBr pellets. A Rigaku Miniflex X-ray Diffractometer (XRD) with Cu Kα radiation, operating at 30 kV and 15 mA (Tokyo, Japan), scanned from 5 to 60° at a rate of 2° per minute, with steps of 1.0 s was used for evaluation the crystal structure of the materials. The surface image of the electrospun mat was acquired using a QUANTA 400F Field Emission Scanning Electron Microscope (SEM) (Oregon, USA). Autosorb-1C/MS pore size analyzer (Florida, USA) was used to obtain the surface characteristics of the samplers by the Brunauer-Emmett-Teller (BET) method. Before BET analysis a 16-hour degassing process at room temperature was applied.

2.2.3 Selection of Analytes and Electrospinning Polymer

In this study, the primary purpose was to develop a new approach for the preparation of selective extractive phases based on the imprinting of analytes in prepolymerized structure using an electrospinning approach, namely, Pseudo-Molecularly Imprinted Polymer (PMIP). To prepare PMIPs, similar to the Molecularly Imprinted Polymer (MIP) technology, the following path was followed. A polymer was selected to prepare a nanofibrous surface. The nanofibrous surface was prepared by adding the selected analytes (as templates) into this polymer solution and electrospinning it. Then, the templates scattered within the nanofibrous structure were washed using a suitable solvent. Thus, analyte-specific sorption sites remained after washing the templates.

For this purpose, as the first step, a polymer was selected. The electrospinnability of the polymer, dissolution of selected analytes in the polymeric solution, analyte-polymer interactions, and polymer insolubility in water (extractive media) and common solvents (desorption media) were considered critical parameters for selection of the polymer. In this study, PAN was preferred as the polymer that will form the coating for several important reasons. These reasons include PAN's mechanical and chemical stability, its relatively affordable price [131], and its electrospinnability when dissolved in DMF. Moreover, PAN nanofibers are insoluble in water and common solvents (i.e. MeOH, acetonitrile) used in sample preparation steps. Most importantly, the extractive properties of PAN are suitable for the study. PAN can form π–π interactions with aromatic ring groups and dipole-dipole interactions with polar compounds because of the cyano group it contains. As a result, it can interact non-specifically with a wide variety of analytes, causing significantly reduced specific bindings [132]. Moreover, when it is used in bulk form as a glue for the immobilization of extractive particles it does not provide significant extraction. The fact that PAN has non-specific interactions allowed the analyte-specific binding sites of the produced PMIP extraction phases to be monitored more easily.

Two commonly used pesticides, namely, trifluralin and carbaryl, were selected as model analytes to study if PMIP will show any selective recognition. Imprinting templates were chosen identically to the analytes to create an analyte-specific binding site. Although both compounds are pesticides, as can be seen from Table 2.1 they have different physicochemical properties (different molecular sizes, functional groups, and lipophilicity); therefore, they may show structure-related selectivity when immobilized in PAN. Thus, it will be possible to see if this proposed imprinting technique can be used for any kind of imprinting purposes or if it is more suitable for imprinting specific compounds. Furthermore, two additional pesticides, namely, diazinon and malathion were used in the evaluation of cross selectivity of PMIP. Structures, molecular weights, solubilities in water, LogP values, of the mentioned analytes, and PAN found in the literature are shown in Table 2.1 [133], [134], [135], [136], [137].

Table 2.1 Structures and the Physicochemical Properties of the PAN, Analytes, and Compounds Used for the Cross-Selectivity

Name	**Structure**	**Molar mass (g/mol)**	**LogP**	**Solubility in water (µg/mL)**	**MRPL Level (ng/mL)**
PAN	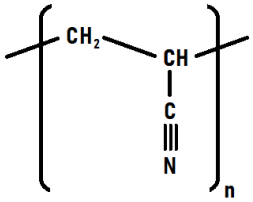	150000 (avg)	NA 0.96	Insoluble	NA
Trifluralin	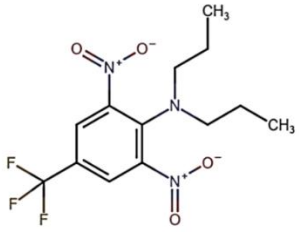	335.28	5.3	0.221	10.0

Table 2.1. (cont'd) Structures and the Physicochemical Properties of the PAN, Analytes, and Compounds Used for the Cross-Selectivity

Carbaryl	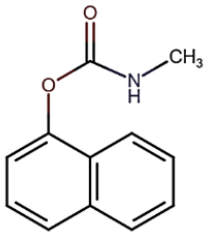	201.22	2.4	110	10.0
Diazinon	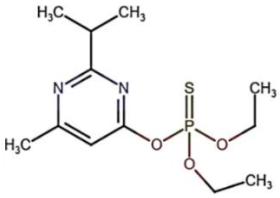	304.34	3.8	40	10.0
Malathion	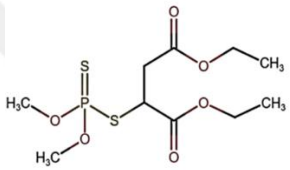	330.36	2.4	143	20.0

2.2.4 Preparation of the SPME Samplers

In this study, novel homemade SPME samplers were produced. Using the electrospinning method, non-imprinted polymer (NIP) extractive phases consisting of fine nanofibers of PAN were also prepared. Template molecules were added to the PAN solution before the electrospinning step to produce PMIP nanofibers. The prepared extractive phases were sandwiched between two stainless steel wire meshes to obtain the SPME samplers used in this study. The details of the preparation of sorbents are explained in the following headings. The schematic representation of the preparation of the PMIP extractive phase is shown in Figure 2.1.

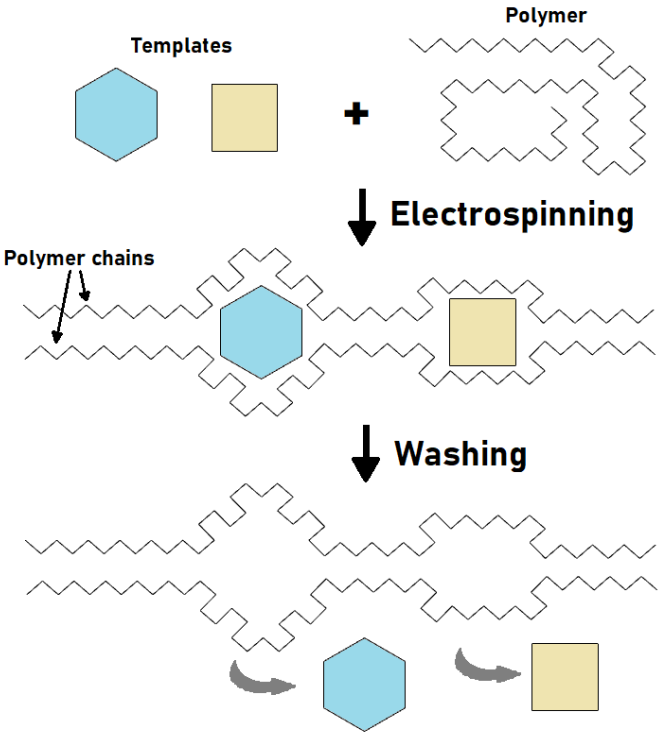

Figure 2.1. Schematic representation of PMIP production

2.2.4.1 Preparation of NIP and PMIP Solutions

Before utilizing the electrospinning, a PAN solution was prepared to obtain the extractive phase. For this purpose, 1.0 g of PAN, which will form the electrospun extractive phase was added into 10.0 mL DMF and stirred at 600 rpm for 24 hours. This prepared solution (NIP solution) was then used to prepare NIP extractive phases and PMIP solutions.

Depending on the experiments in which they will be used, different concentrations of PMIP solutions were obtained by adding different amounts of templates (trifluralin and carbaryl) into the resulting NIP solution. Thus, 0.5, 1.3, 2.5, and 5.0 mg of each template was weighed and dissolved in 1.0 mL of PAN solution. These solutions and the samplers prepared from them were coded as P0.5, P1.3, P2.5, and

P5, respectively. After the template molecules were added, the solutions were stirred at 600 rpm for 15 minutes. Figure 2.2 shows the prepared NIP and P5 solutions.

(a) (b)

Figure 2.2. a) NIP and b) PMIP solutions prepared for electrospinning.

2.2.4.2 Electrospinning

After the solutions were prepared, the electrospinning method was used to obtain electrospun mats. During the electrospinning, the polymer was coated on aluminum foil. The coating was done with a vertical electrospinning setup containing a syringe pump, solution in a syringe, collector, and circuit clips (Figure 2.3).

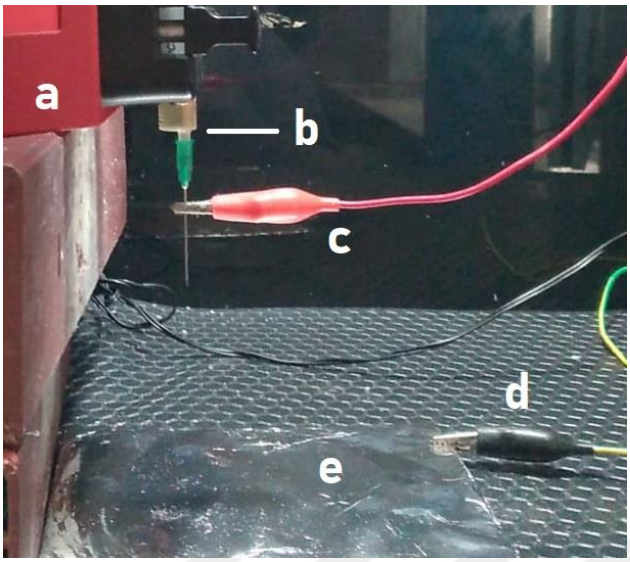

Figure 2.3. Electrospinning set-up used in the study, a) syringe pump, b) polymer solution filled syringe, c) and d) alligator clips connected to the voltage supply, e) collector plate.

Electrospinning parameters were optimized before the coatings were obtained. The optimizations aimed to obtain a homogeneous coating with minimum solution waste during electrospinning. For this, different values of the voltage supply, the flow rate of the polymer fed into the syringe tip, the distance between the syringe needle and collector, and coating time were tried. The used electrospinning parameters are shown in Table 2.2.

Table 2.2 Optimized Electrospinning Parameters

Parameter	**Used value**
Voltage supply	20 kV
Flow rate	1 mL/h
Distance between syringe tip and collector plate	15 cm
Coating time	30 min

After the electrospinning parameters were optimized, coatings were prepared using the NIP and PMIP solutions. Then, the coated polymer was peeled and sandwiched between stainless steel wire mesh, as described in the next heading. Figure 2.4 shows electrospun-coated aluminum foil.

Figure 2.4. NIP polymer-coated aluminum foil

2.2.4.3 Sandwiching Extractive Phase

After the coating was obtained on the aluminum foil, it was sandwiched between two stainless steel wire meshes. This process includes the following steps: Peeling off the electrospun mat from the aluminum foil, cutting a piece of the desired weight from it, placing the mat between two stainless steel meshes with the desired edge lengths, connecting the layers by bending the wires on the edges of the mesh and bending the resulting sorbent to fit into 1.5 mL vial (shaped into cylinders with a diameter of approximately 9.0 mm). The mesh size and wire thickness of the

stainless-steel support were 2.00x2.00 mm and 0.20 mm, respectively. The preparation of samplers is shown in Figure 2.5.

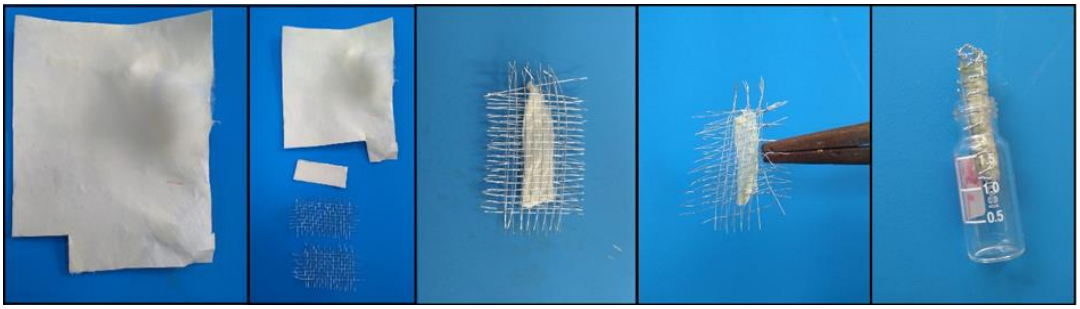

(a) (b) (c) (d) (e)

Figure 2.5. Preparation steps of samplers. (a) electrospun mat on aluminum foil, (b) cutting a piece of the desired weight from the coating and peeling the coating, (c) placing the cut piece between two stainless steel meshes with the desired edge lengths, (d) connecting the layers by bending the wires on the edges of the mesh, (e) bending the resulting sorbent to fit into the vial cap.

2.2.4.4 Washing PMIP Sorbents

The prepared sorbents were washed to remove the template molecules from the electrospun structure and obtain the PMIP samplers. Washing the template molecules from the sorbent was done using an ultrasonic bath and Soxhlet extractor. Each sampler was placed in a 1.5 mL vial filled with 15% (v/v) acetic acid in a technical grade MeOH. After cleaning in an ultrasonic bath for 15 minutes, a fresh washing solution was placed in the vial and sonicated again. This process was repeated ten times. After that, the samplers were washed with Soxhlet extraction. For this purpose, 150.0 mL of technical methanol was placed in a 250 mL flask and connected to a Soxhlet extractor. The flask was placed in an oil bath and washing continued overnight by siphoning of methanol approximately every 75 minutes by

stirring at 650 rpm, 125°C. Afterward, the samplers were desorbed in 500 µL of LC-grade methanol at 1000 rpm for 1 h and analyzed using GC-MS (discussed in Section "2.2.5 GC-MS Method") to test if there is any template leaching from the samplers. If any amount of leaching was encountered, the washing process was repeated.

2.2.4.5 Carryover Test for Desorption of the Analytes

In a typical SPME study, desorption solvent selection can play a critical role in the quantitative desorption of analytes. Therefore, as a first step, the completeness of desorption when MeOH is used to elute the analytes was tested. Before extraction, samplers were kept in 1.5 mL LC-grade methanol for 30 minutes for the conditioning and dried with a tissue before use. Extraction was performed for 1 hour at 1000 rpm from 4.0 mL UPW which was spiked to contain 500.0 ng/mL trifluralin and carbaryl. After extraction, the samplers were dried with a tissue. Then, the samplers were desorbed in 1.50 mL of methanol by shaking at 1000 rpm for 1 hour. Following the first desorption, a second desorption from the samplers was performed utilizing the same parameters. Then, 1.0 µL of each eluate was injected into GC-MS for analysis (the GC-MS method was discussed in Section 2.2.5). NIP and P5 samplers were used in carryover tests.

2.2.5 GC-MS Method

An Agilent 6890A gas chromatograph coupled with an Agilent 5973 quadrupole mass selective detector was used to separate and quantify the analytes. Helium gas (high purity, 99.999%), with a flow rate of 1.2 mL/min, was the carrier. The samples were injected into the injector port with settings including an injection temperature of 250°C, a 1.0 µL injection volume, and a 10:1 split ratio. The GC column used was

an ultra-inert (5%-phenyl)-methylpolysiloxane column, with a length of 30 meters, a film thickness of 0.25 μm, and an inner diameter of 0.25 mm. The temperature gradient used in the analysis is shown in Table 2.3.

Table 2.3 Temperature Gradient of GC-MS Method

Ramp	**ºC/min**	**Next ºC**	**Hold (min)**
Initial		60	5.0
Ramp 1	80	200	2.0
Ramp 2	20	220	1.0
Ramp 3	20	240	0.0

2.2.6 Selection of the Ratio of Template and Polymer

While it is believed that the amount of template used in the preparation of pseudo molecularly imprinted polymers will influence the extraction, the cost of the extractive phase and the labor required to ensure adequate washing also rise with the amount of template utilized. Therefore, tests were carried out to understand the effect of different amounts of template addition on prepared PMIP polymer solutions and their sorbents' extraction performances. Additionally, NIP sorbents were included in these tests to observe the difference between sorbents prepared with non-imprinted polymer and PMIP sorbents. For this purpose, the samplers prepared using NIP, P0.5, P1.3, P2.5, and P5 solutions (0.5, 1.3, 2.5, and 5.0 mg of trifluralin and carbaryl dissolved in 1.0 mL of PAN solution, respectively) were evaluated for their extraction performances. Three samplers (N=3) for each type were used in the experiment.

The TFME conditions were set as follows. In the conditioning step, the samplers were kept in 1.5 mL LC-grade methanol for 30 minutes and then dried with a tissue.

In the extraction, the samplers were placed in 4.0 mL of UPW spiked to contain 200.0 ng/mL trifluralin and 500.0 ng/mL carbaryl. Then, the extraction was performed for 2 hours with an agitation speed of 1000 rpm. Once the extraction was complete, the samplers were dried with a tissue. For desorption, 1.5 mL LC-grade methanol was used as eluent and the samplers were kept for 1 hour at 1000 rpm in this solution.

2.2.7 Selection of the Sampler Size

The effect of the sorbent amount on extraction was tested to find a sampler size that provides a good extraction sensitivity. For this, samplers with different amounts of sorbents and surface areas were prepared, and extractions were performed. For the preparation of PMIP samplers, P5 polymer solutions were used. The dimensions (in mm) and mass of sorbent (in mg coded in the names) of prepared samplers were 3x3 (S1), 7x3 (S2.5), 10x5 (S5), 15x5 (S7) and 20x5 (S10). The prepared samplers are shown in Figure 2.6. The evaluation was conducted under the aforementioned extraction and desorption conditions. Three sorbents for each type were used in the experiment.

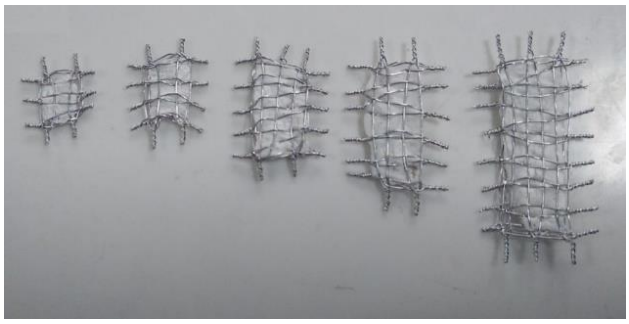

(a)

Figure 2.6. S1, S2.5, S5, S7, and S10 samplers prepared with a) NIP and b) P5 polymer solutions.

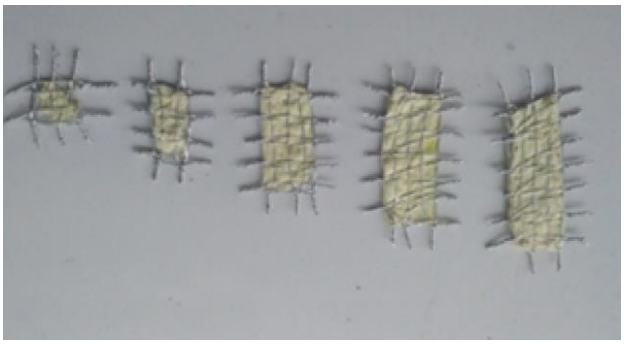

(b)

Figure 2.6. (cont'd) S1, S2.5, S5, S7, and S10 samplers prepared with a) NIP and b) P5 polymer solutions.

2.2.8 Optimization of the SPME Parameters

In this part, with the selected sampler from the previous experiment, several parameters that are critical for a reliable SPME method were investigated. An SPME run consists of the following essential steps: (I) conditioning the sorbents to get them prepared for extraction, then rinsing the sorbent to get rid of any extra conditioning solvent; (II) performing the extraction step, which involves the transfer of analytes from the sample matrix to the extractive phase; (III) rinsing/cleaning, where the loosely attached matrix components are removed with water or a paper towel; and (IV) performing desorption, which involves transferring the analytes from the sorbent to another solvent (usually compatible with analytical instrument) or direct desorption to an analytical instrument. In this study, samplers were kept in 1.5 mL LC-grade methanol for 30 minutes for conditioning and dried using a clean tissue. 4.0 mL UPW spiked to contain 200.0 ng/mL trifluralin and 500.0 ng/mL carbaryl (if not stated otherwise in the related experiment) was used as a sample in the extraction. The excess extraction matrix was removed by drying the sampler with a tissue. After that, 1.5 mL LC-grade methanol was used in the desorption step.

Many parameters can be optimized for an SPME run. In this study, the pH of the samples, extraction time, and desorption time were optimized as described under the following headings.

2.2.8.1 Optimization of pH of the Samples

For analytes and sorbents that have acidic or basic moieties in their structure, one of the most important parameters that can influence the extraction is sample pH. Thus, it can be optimized to enhance the extraction capacity. As mentioned above, for analytes with acidic or basic nature, the partitioning of the analytes between the sample matrix and the sampler changes when analytes bear a charge which may occur at different pH ranges for different analytes. Therefore, a series of tests were conducted to learn the partitioning of the analytes used in this study in samples with different pH values and to find the optimum pH accordingly.

Buffer solutions with pH values of 3.0, 5.0, 7.0, and 10.0 were prepared for this. Trifluralin and carbaryl were spiked in these solutions to have a final concentration of 200.0 ng/mL and 500.0 ng/mL, respectively. Then, the TFME was performed with three P5 samplers for each pH value. In the conditioning step, samplers were kept in 1.5 mL LC-grade methanol for 30 minutes and then dried with a tissue. In the extraction, the samplers were placed in 4.0 mL of prepared samples. Then, the extraction was performed for 2 hours with an agitation speed of 1000 rpm. Subsequently, the samplers were dried with a tissue. For desorption, 1.5 mL LC-grade methanol was used as eluent and the samplers were kept for 1 hour at 1000 rpm in this solution.

2.2.8.2 Optimization of Extraction Time

Extractions were performed at different times to obtain an extraction time profile for trifluralin and carbaryl and to optimize the extraction time. Extraction times of 5 minutes, 15 minutes, 30 minutes, 1 hour, 2 hours, 4 hours, and 6 hours were applied. Three P5 samplers were utilized for each extraction time point to observe the effect of those extraction times on the amount of extracted analytes.

In the conditioning step, the samplers were kept in 1.5 mL LC-grade methanol for 30 minutes and subsequently dried with a tissue. In the extraction, the samplers were placed in 4.0 mL of UPW spiked to contain 200.0 ng/mL trifluralin and 500.0 ng/mL carbaryl. The agitation speed was 1000 rpm. Then, the samplers were dried with a tissue. For desorption, 1.5 mL of LC-grade methanol was utilized as the eluent, and the samplers were kept for 1 hour at 1000 rpm in this solution.

2.2.8.3 Optimization of Desorption Time

Similar to extraction, tests were conducted to obtain desorption time profiles. The times tested were as follows: 5 minutes, 15 minutes, 30 minutes, 1 hour, 2 hours, and 6 hours. Three P5 samplers were used for each desorption time.

The TFME conditions were set as follows. In the conditioning step, the samplers were kept in 1.5 mL LC-grade methanol for 30 minutes and then dried with a tissue. In the extraction, the samplers were immersed in 4.0 mL of UPW spiked to contain 200.0 ng/mL trifluralin and 500.0 ng/mL carbaryl. The extraction was carried out for two hours at a speed of 1000 rpm. The samplers were dried with a tissue when the extraction was finished. 1.5 mL of LC-grade methanol was used as the eluent for the desorptions, and the samplers were agitated at 1000 rpm.

2.2.9 Effect of Nanofibrous Surface of the Sampler

To observe the contribution of having a nanofibrous structure on extraction performance, TFME samplers containing nanofibrous and bulk polymer extractive phases were prepared. Nanofibrous electrospun NIP and P5 samplers were prepared as described in Section 2.2.4.2. For the preparation of bulk polymer extractive phases, the dip coating method was utilized. The preparation of the PAN solution for dip coating was as follows: 5.0 g of PAN was added to 72.5 mL of DMF. It was heated for 1 hour in an oven heated to 90 ^{o}C to dissolve the polymer. The mixture was stirred with the help of a glass rod at 10-minute intervals.

After the preparation of the polymer solution, aluminum foil sheets with the same side lengths as PMIP sorbents (20x5 mm) were prepared as the support material. To remove moisture and any dirt from these prepared cores, they were kept in technical-grade methanol for 5 minutes and dried at 90 ^{o}C in the oven for 1 minute. It was then weighed, and its weight was subtracted from the weight of the coatings to be obtained, allowing the amount of coating to be tracked.

During the dip coating, the aluminum foil supports were completely immersed in the polymer solution, kept for 1 minute, withdrawn at a constant speed of 1.3 mm/s, and dried at 90^{o}C for 1 minute in an oven. The coated sampler was weighted, and the coating process was repeated until the foil sheets had the same amount (10.0 mg) of extractive phase as the NIP and PMIP samplers (Figure 2.7). The produced samplers with non-fibrous bulk polymer surfaces were coded as bulk-NIP samplers. Then, extraction was performed from samples containing UPW spiked with 200.0 ng/mL trifluralin and carbaryl using three bulk-NIP, electrospun-NIP, and electrospun-P5 sorbents. The abovementioned optimized parameters were utilized in the SPME procedure described in Section 2.2.8.3.

Figure 2.7. Bulk-NIP samplers, prepared by the dip-coating method.

2.2.10 Selectivity Investigations

In the last experiment, template (trifluralin and carbaryl) and non-template (diazinon and malathion) analyte-spiked samples were prepared and used in extraction to observe the cross-reactivity of PMIPs for non-imprinted analytes. Extractions were performed from UPW spiked to contain 200.0 ng/mL trifluralin and 500.0 ng/mL of carbaryl, malathion, and diazinon. In the extraction step, electrospun NIP and P5 samplers were used. The aforementioned optimized parameters were employed in the TFME procedure.

2.3 Results and Discussion

2.3.1 Characterization Studies

Electrospun nanofibers were characterized using SEM imaging, FTIR Spectroscopy, XRD, and the Brunauer-Emmett-Teller (BET) surface analysis method. The characterization results are examined in detail in the following headings.

2.3.1.1 Scanning Electron Microscopy

The morphologies of electrospun nanofibers obtained with NIP and P5 polymers were examined with the help of SEM. Figure 2.8 shows that a uniform nanofibrous morphology was obtained with both NIP and P5 polymers. The thickness of NIP and PMIP nanofibers was also measured. ImageJ software was used to measure the diameters of randomly selected nanofibers (N=20). The mean diameter of NIP nanofibers was 343 ± 12 nm, while PMIP nanofibers exhibited a mean diameter of 516 ± 196 nm. This can be attributed to the presence of template molecules in the PMIP solution, which may affect the physicochemical properties of the PAN solution.

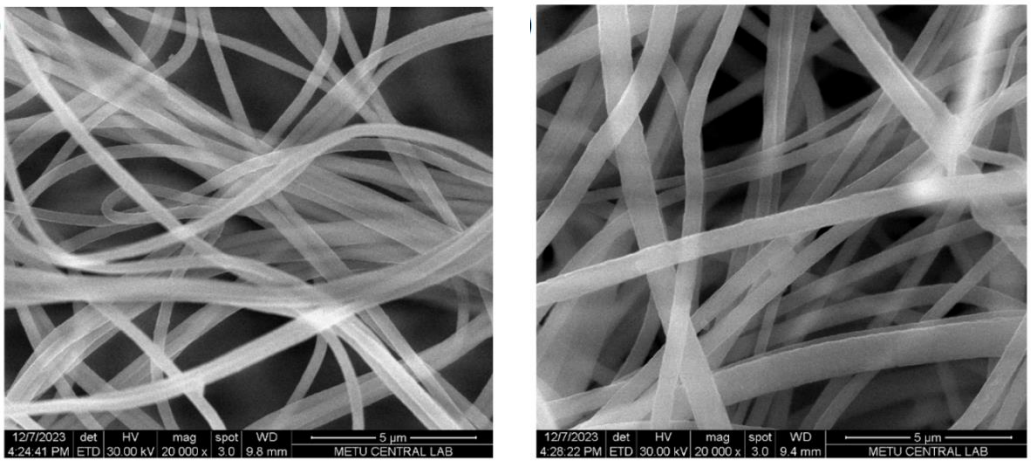

(a) (b)

Figure 2.8. SEM images of a) NIP and b) PMIP (P5) polymers

2.3.1.2 Fourier Transform Infrared Spectroscopy

NIP and unwashed PMIP (P5) mats were further characterized using FTIR Spectroscopy. For this, NIP and PMIP nanofibrous polymer mats were ground using mortar and pestle, mixed with KBr powder, and 10 tons of pressure was applied to produce pellets. Figure 2.9 shows the FTIR spectrum of the NIP extractive phase containing only PAN. The absorption peak observed at 2938 cm^{-1} (C-H stretching) and 1454 cm^{-1} (C-H bending) in the PAN spectrum represent the methylene on the polymer chain, 1665 cm^{-1} represents the alkene (C=C stretching), and 2243 cm^{-1} represents the nitrile group (C≡N stretching) [138], [139].

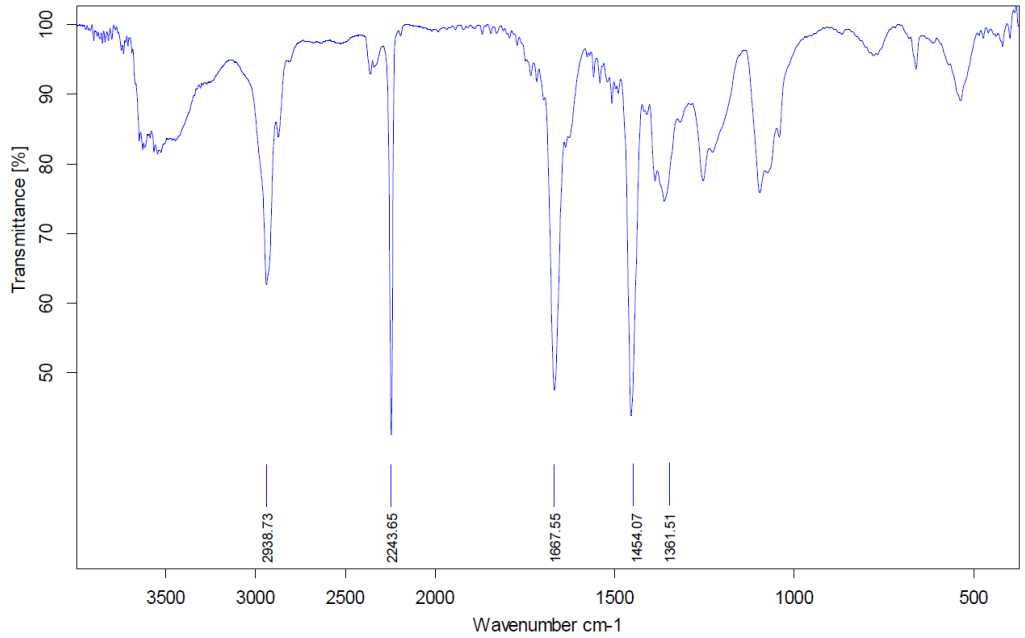

Figure 2.9. FTIR spectrum of NIP extractive phase containing only PAN

In Figure 2.10, NIP and P5 spectra are shown together in red and blue, respectively. As expected, the PAN peaks in the PMIP polymer spectra appear at similar positions as in NIP. The spectrum of the produced PMIP polymer was compared to those of trifluralin and carbaryl found in the literature to analyze the observed peaks. Aromatic group signals in the fingerprint region, the strong carbonyl peak at 1739 cm^{-1}, and N-H bands of the amide at 3420 cm^{-1} correspond to carbaryl [140]. Additionally, trifluralin is identified by symmetric (1115 cm^{-1}) and asymmetric (781 cm^{-1}) CF_3 stretching, as well as asymmetric (1540 cm^{-1}) and symmetric (1312 cm^{-1}) N-O stretching bands [141], [142].

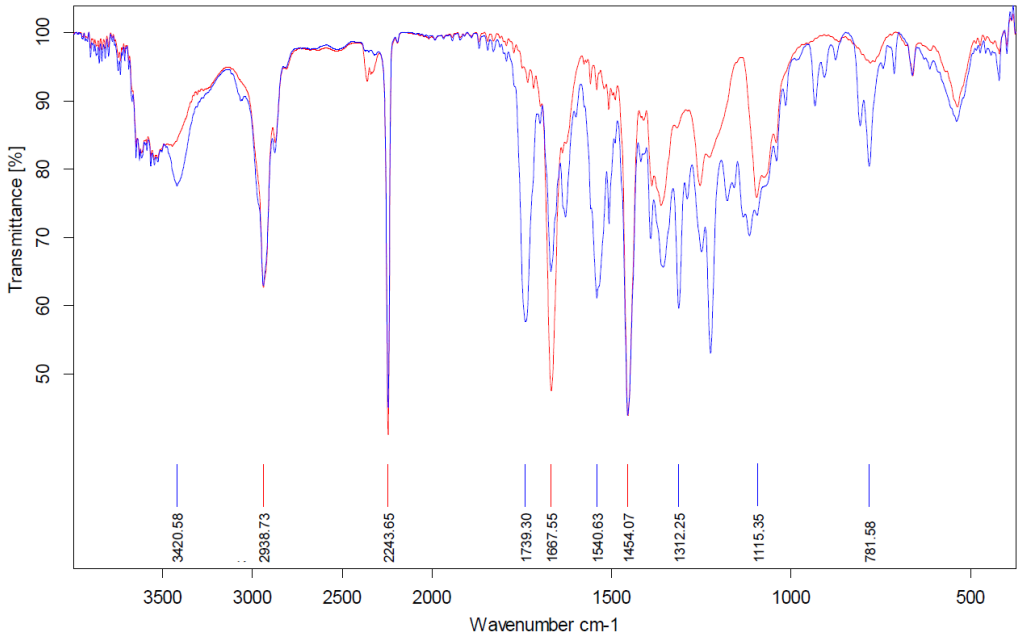

Figure 2.10. FTIR spectra of NIP (red) and P5 (blue) extractive phases

2.3.1.3 X-ray Diffraction

In the next characterization study, XRD spectroscopy was utilized. In this study, PAN powder (pure PAN), NIP nanofibers (electrospun PAN), and PMIP (electrospun P5) nanofibers were investigated. The degree of crystallinity was calculated from the obtained diffraction patterns using the following equation:

$$C(\%) = \frac{A_C}{A_T} x100 \qquad \text{Equation 9}$$

Where A_C is the integral area of the crystalline peaks and A_T is the total area of diffraction in the XRD patterns.

As seen in Figure 2.11, with a crystallinity of 11%, the PAN powder's XRD pattern showed a sharp crystalline peak at 2θ = 17°, which corresponds to the orthorhombic reflection [143], [144]. The electrospun PAN and PMIP nanofibers' XRD patterns similarly displayed a sharp peak at 2θ = 17°. Additionally, as reported in the literature, a weaker peak appeared at 2θ = 25°, along with an unidentified peak at 2θ = 14°, in the XRD pattern of electrospun PAN [145], [146], [147]. The calculated crystallinity of the electrospun NIP nanofibers was 48%, suggesting that electrospinning enhanced PAN's crystallinity. Lastly, the electrospun PMIP nanofibers' XRD pattern was the same as the NIP nanofibers', indicating that the crystallinity was unaffected by the template used during nanofiber fabrication.

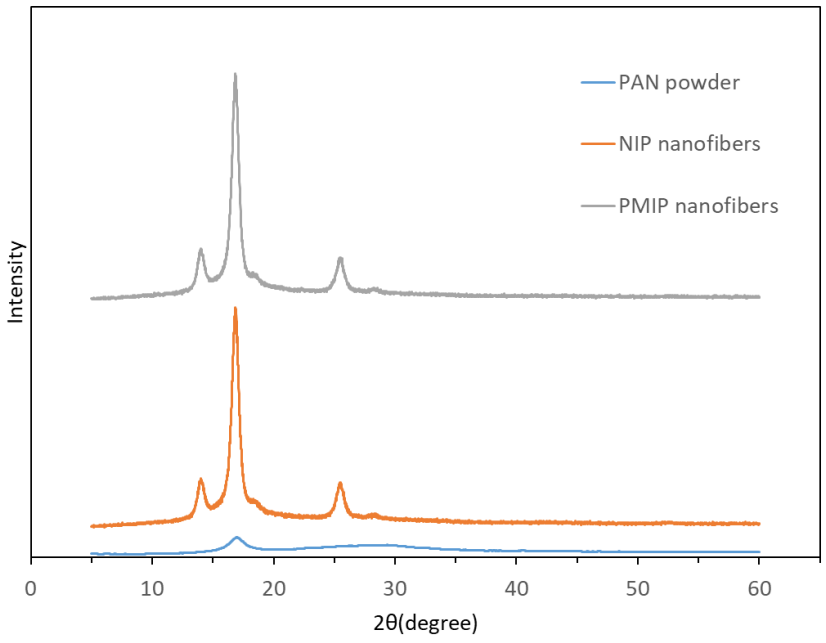

Figure 2.11. XRD patterns of PAN powder (blue), electrospun NIP (PAN) nanofibers (orange), and electrospun PMIP (P5) nanofibers (grey).

2.3.1.4 Brunauer–Emmett–Teller (BET) Studies

In the final study, surface areas, pore volumes, and the pore sizes of the NIP and washed PMIP (P5) extractive phases were determined. In this characterization, firstly, the extractive phases were degassed at room temperature for 16 hours. An Autosorb-1C/MS pore size analyzer was used to obtain the surface characteristics of the extractive phases used in the PMIP and NIP samplers.

The surface area was calculated using the BET method. Pore volume and pore size were calculated with Barrett, Joyner, and Halenda's (BJH) method. The calculated data is given in Table 2.4.

Table 2.4 Textural properties of NIP and PMIP extractive phases (based on BJH method)

Extractive Phase	**Multipoint Surface Area (m^2/g)**	**Pore Volume (cm^3/g)**	**Pore Diameter (nm)**
NIP	51	1.1	1.3
PMIP	42	1.5	4.0

As given in Table 2.4, NIP and PMIP extractive phases have similar surface area values of 51 m^2/g and 42 m^2/g, respectively. This can be attributed to nanofibrous structures of both polymers. In addition, an increase in pore volume was observed from NIP (1.1 cm^3/g) to PMIP (1.5 cm^3/g). Similarly, significant increase occurred in pore size from 1.3 nm to 4.0 nm for NIP and PMIP, respectively. This suggests that the imprinting process resulted in the formation of a mesoporous PMIP morphology. The increase in pore volume and pore diameter can be attributed to the pseudo molecularly imprinting with the template molecules. A review of the literature indicates that MIPs show a similar increase in pore volume and pore size

compared to non-imprinted polymers [148], [149]. Moreover, the surface area for those MIPs have been also reported to increases. However, in our study, since the primary source of the high surface area is nanofibrous structure of electrospun polymer, the contribution of the imprinting to the surface area is negligible.

2.3.2 GC-MS Method

In this study, the pesticides trifluralin, carbaryl, malathion, and diazinon were separated and quantified. Typical chromatograms and mass spectra for the analytes are shown in Appendix Figures A1-A5 and Figures B1-B5, respectively. During the extraction-related evaluations performed in this chapter, analytes were quantified using instrumental calibration. For instrumental calibration, solutions with different analyte concentrations (100.0, 200.0, 400.0, 600.0, 750.0, 1000.0, 2500.0 ng/mL) were prepared in methanol. Typical external calibration curves obtained with the developed GC-MS method are shown in Figure 2.12.

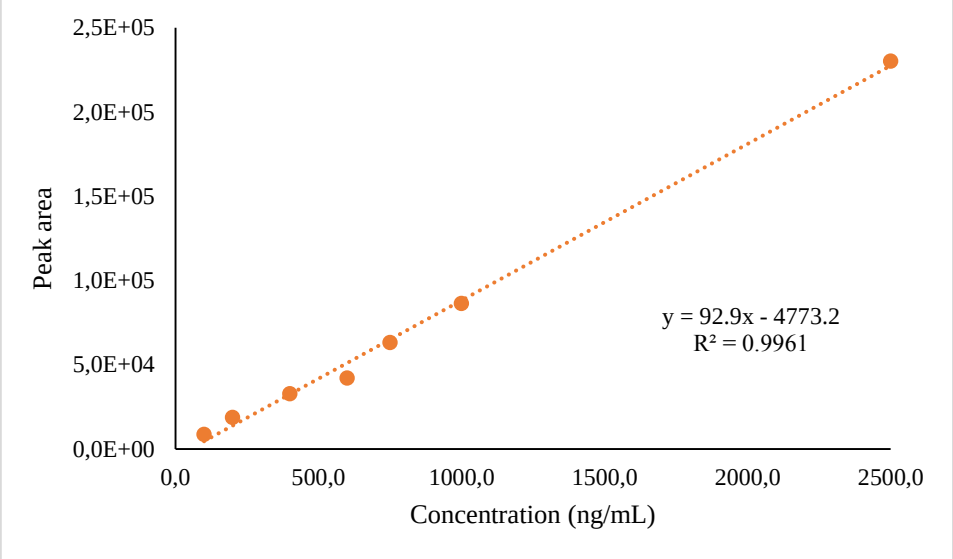

(a)

Figure 2.12. Typical calibration curves of a) trifluralin, b) carbaryl, c) malathion, and d) diazinon obtained in GC-MS

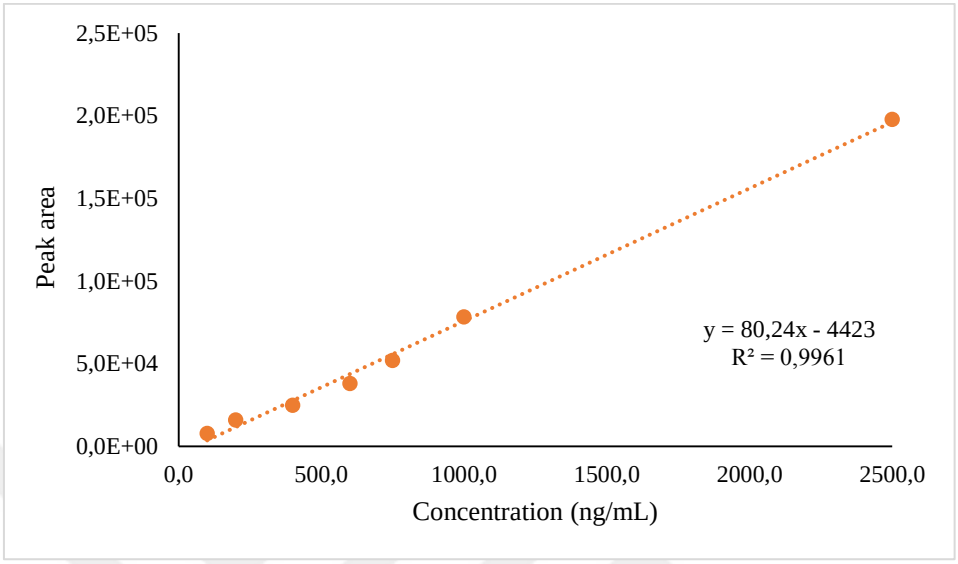

(b)

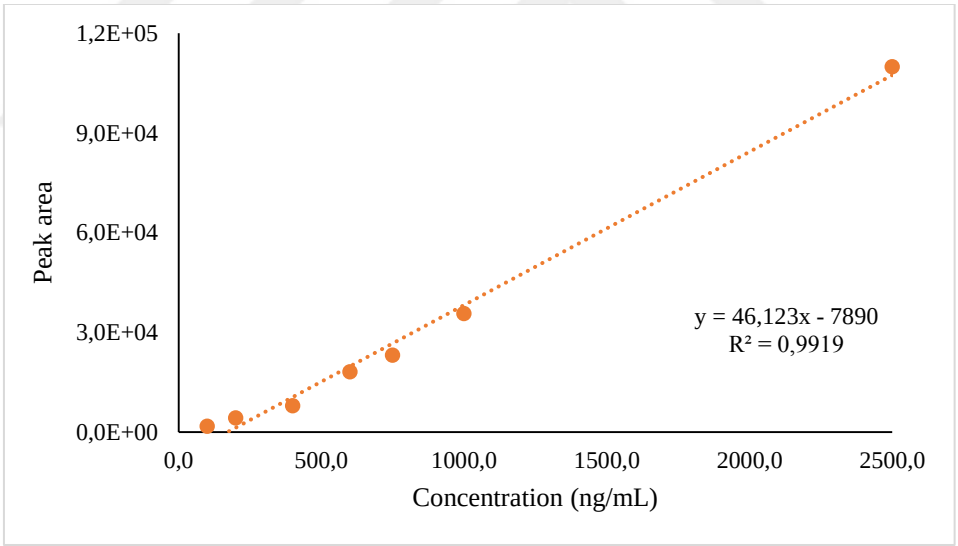

(c)

Figure 2.12. (cont'd) Typical calibration curves of a) trifluralin, b) carbaryl, c) malathion, and d) diazinon obtained in GC-MS

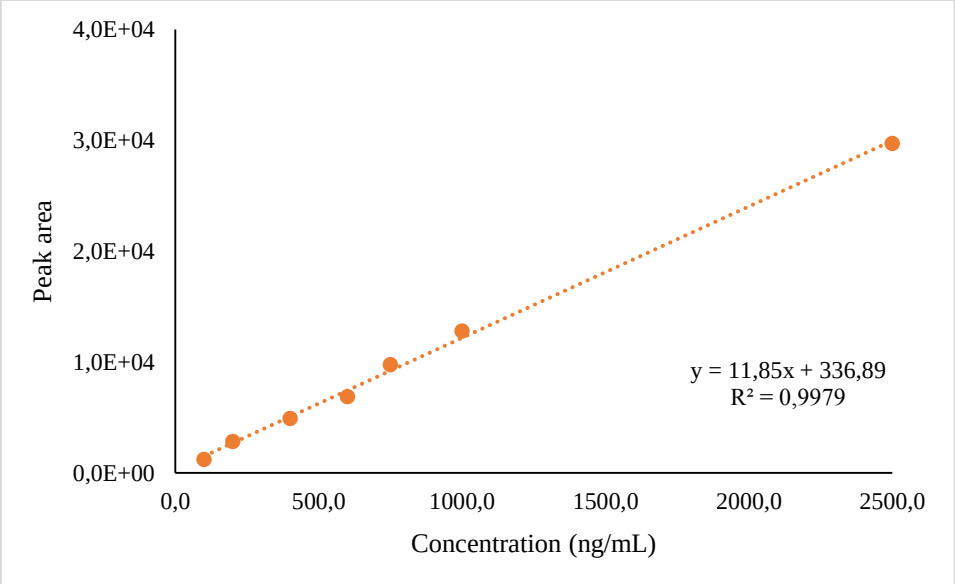

(d)

Figure 2.12. (cont'd) Typical calibration curves of a) trifluralin, b) carbaryl, c) malathion, and d) diazinon obtained in GC-MS

2.3.3 Washing PMIP Sorbents

The washed sorbents were tested to see if they contained any template residuals. For this test, P5 sorbent was washed with a six-day washing cycle (the washing procedure is described under Section "2.2.4.4 Washing PMIP Sorbents"). Unwashed P5 sorbents were also used in the assay to compare the amount of template leached from the unwashed sorbent. The amount of template desorbed into the solvent by washed P5 sorbent and unwashed P5 sorbent is shown in Figure 2.13. The template leakage in unwashed P5 sorbents was eliminated after the washing procedure. Accordingly, the washing procedure was successful, and template leakage was neglected in further studies.

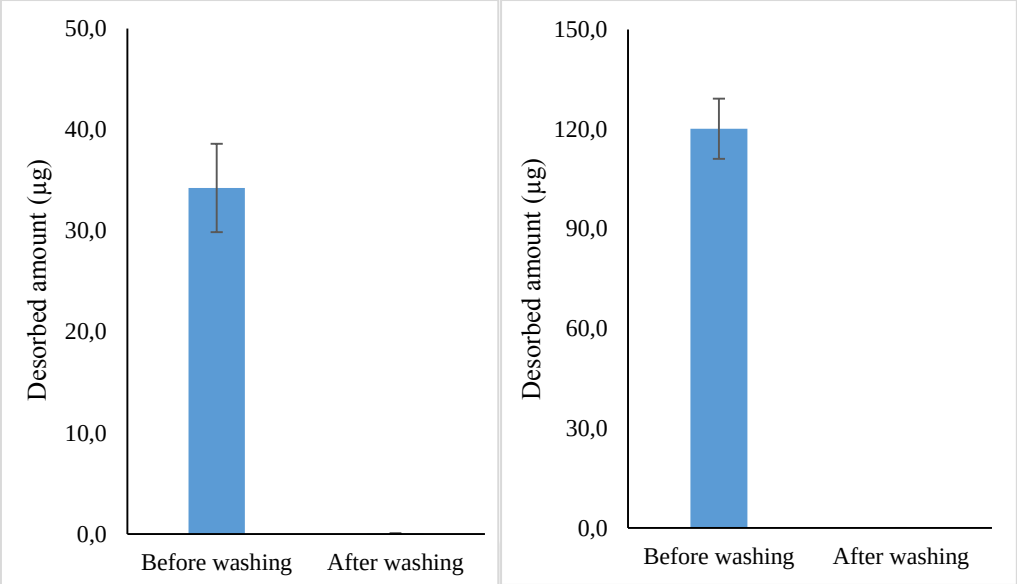

(a) (b)

Figure 2.13. Evaluation of the desorbed amount of a) trifluralin and b) carbaryl before and after washing the PMIP samplers (Desorption parameters: 1.50 mL LC-grade methanol, 1000 rpm agitation speed, 1 hour desorption time)

2.3.4 Carryover of the Analytes

The carryover test was performed as described in Section 2.2.4.5. The test involved extraction with NIP and P5-coated blade samplers followed by two sequential desorptions. The results obtained for this evaluation are shown in Figure 2.14.

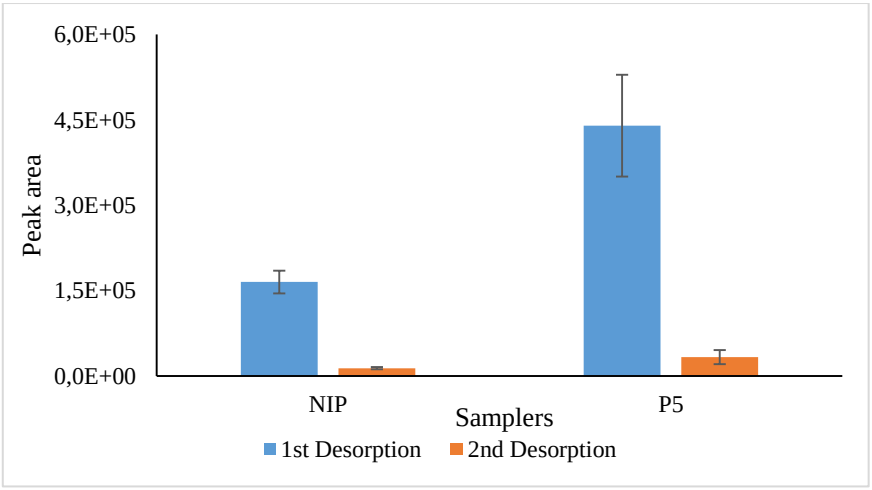

(a)

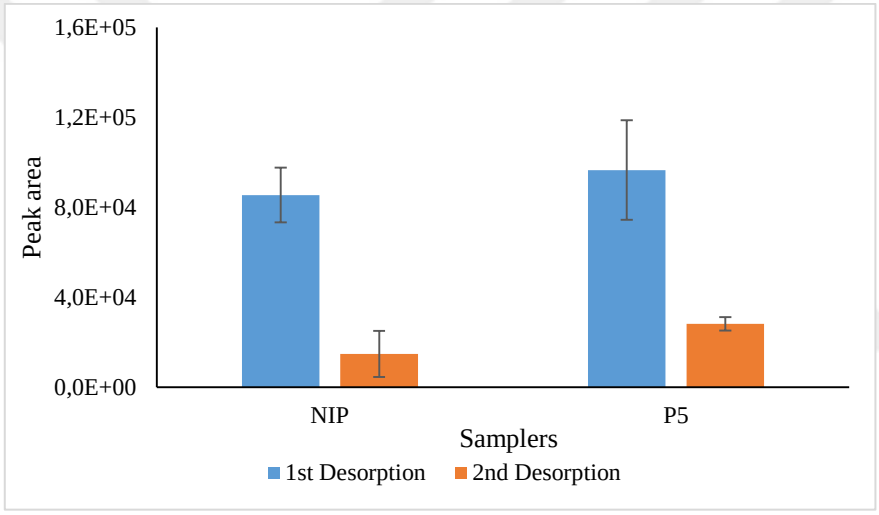

(b)

Figure 2.14. Evaluation of carryover for a) trifluralin and b) carbaryl (Extraction conditions; sample matrix: UPW, analyte concentration: 500.0 ng/mL carbaryl and 200.0 ng/mL trifluralin, sample volume: 4.0 mL, extraction time: 60 min, agitation speed: 1000 rpm, desorption solvent: MeOH, desorption volume: 1.5 mL, desorption time: 60 min, agitation speed: 1000 rpm)

Given in Figure 2.14, it can be said that a less significant amount of analyte was present in the second desorption for trifluralin, as a larger peak area ratio was obtained for the first to second desorption comparison, while a relatively more

significant amount of analyte was observed for carbaryl. Since the carryover amount can be reduced by optimizing SPME parameters such as desorption time, this parameter was optimized in the following studies. This study also showed that the amount of trifluralin extracted is statistically significantly more with P5 samplers than with NIPs (at 95% CL).

2.3.5 Selection of the Ratio of Template and Polymer

The extraction performance evaluation for samplers made with different amounts of templates was carried out using NIP, P0.5, P1.3, P2.5, and P5 samplers (the amount of template in each sampler is given in Section 2.2.6). The results obtained from these evaluations are shown in Figure 2.15. As can be seen from the results for both compounds, increasing the amount of template during the preparation of the samplers increased the extracted amount of analytes.

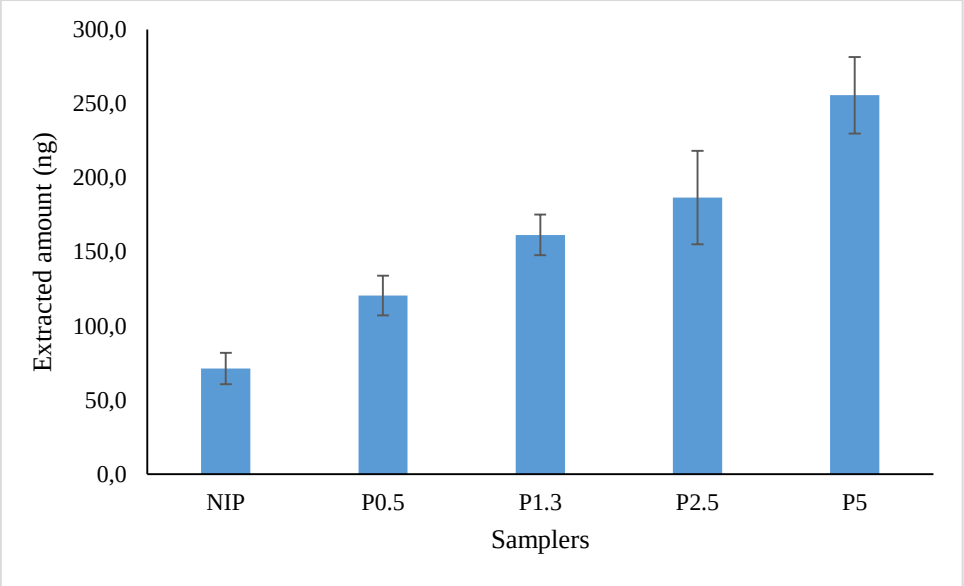

(a)

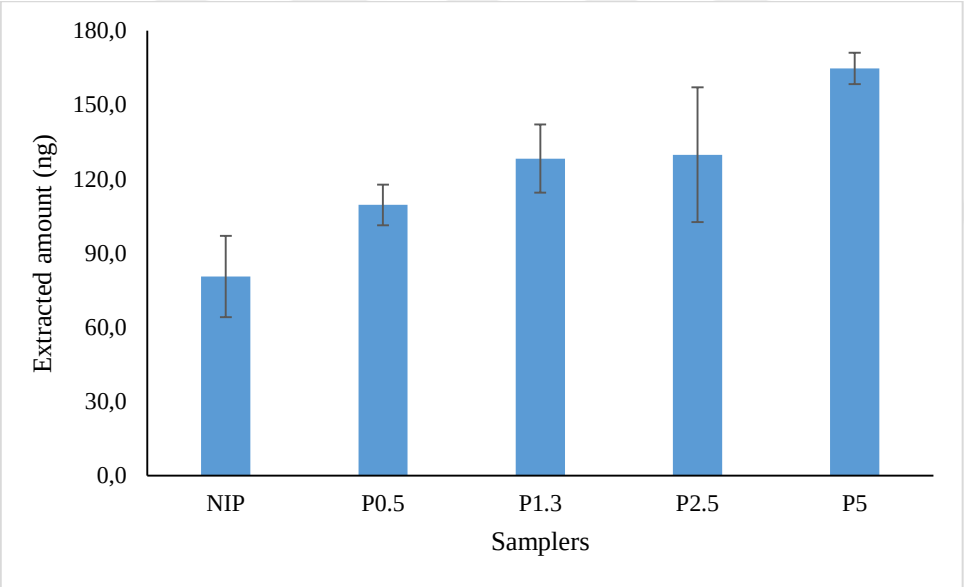

(b)

Figure 2.15. Effect of template-polymer ratio on extracted amount of a) trifluralin and b) carbaryl using samplers prepared with different template amounts (Extraction conditions; sample matrix: UPW, analyte concentration: 500.0 ng/mL carbaryl and 200.0 ng/mL trifluralin, sample volume: 4.0 mL, extraction time: 120 min, agitation speed: 1000 rpm, desorption solvent: MeOH, desorption volume: 1.5 mL, desorption time: 60 min, agitation speed: 1000 rpm)

Moreover, the nitrile group present in PAN's structure interacts non-specifically with various analytes, including dipole-dipole interactions with polar molecules and π–π interactions with aromatic groups. As a result, PAN's non-specific interaction characteristics make it simpler to evaluate analyte-specific binding sites in the PMIP extractive phases. The extracted amount of trifluralin and carbaryl increases as more templates are added during the sorbent production step. This pattern suggests that the number of binding sites increases with the intensity of pseudo-imprinting, improving the extraction performance overall. In addition, comparing the extractions obtained by NIP and P0.5, showed that there is a significant increase in extractions of both analytes (at 95% CL) when P0.5 is used instead of NIP.

It is worth mentioning that even higher extractions can be achieved by using samplers prepared with a larger amount of templates. However, as the template amount increases, the time required for washing the samplers and the amount of solvent use increases. For this reason, using P5 extractive phases as a pseudo-MIP polymer was preferred in further tests.

2.3.6 Selection of the Sampler Size

To examine the extraction performance of the samplers consisting of different sizes and extractive phases, extraction evaluation tests were carried out. The extractions were performed with samplers coded as S1, S2.5, S5, S7, and S10 (samplers with varying sizes in mm; 3x3, 7x3, 10x5, 15x5, and 20x5, respectively) prepared with NIP (only PAN) and P5 (5.0 mg templates dissolved in 1.0 mL PAN) polymers. The obtained results are shown in Figure 2.16.

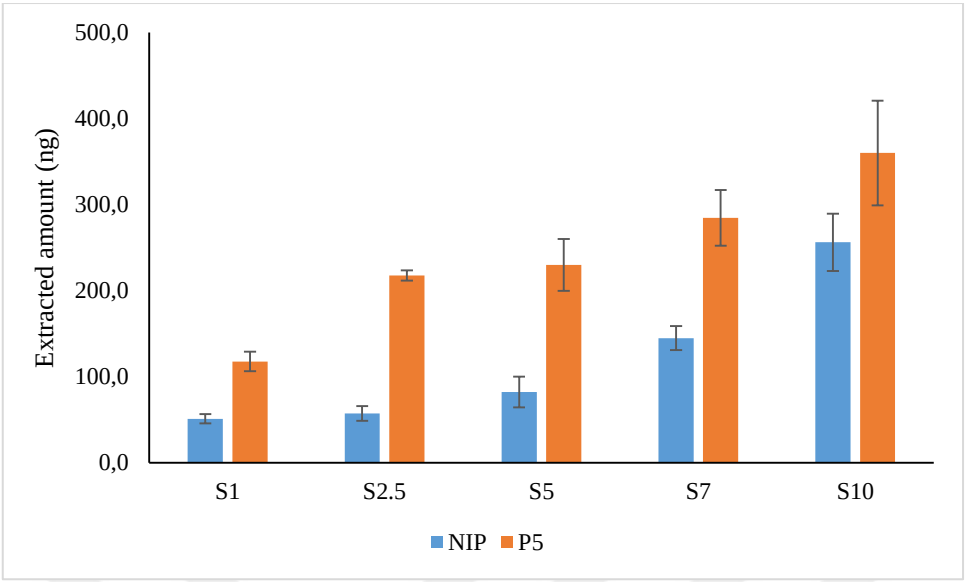

(a)

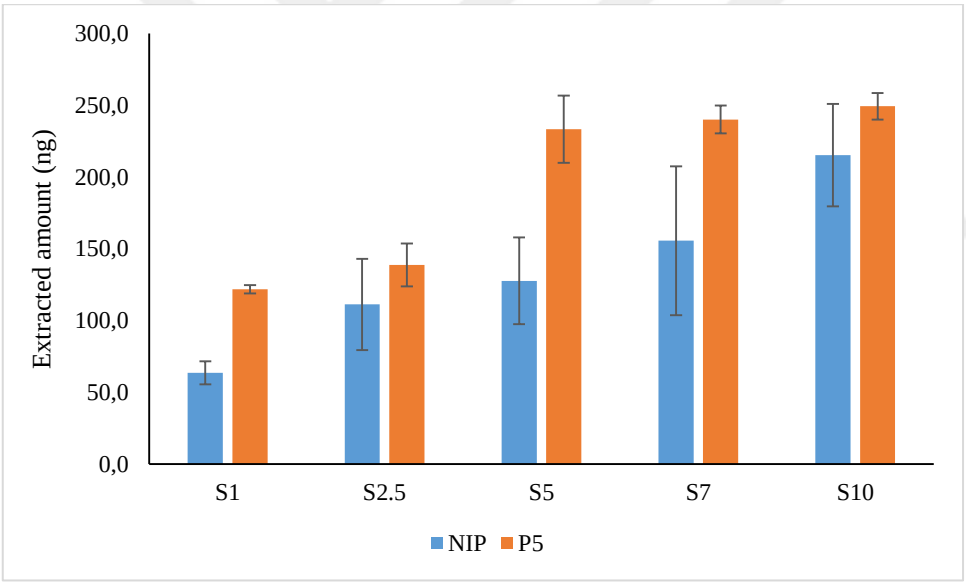

(b)

Figure 2.16. Effect of the sampler size on the extracted amount of a) trifluralin and b) carbaryl (Extraction conditions; sample matrix: UPW, analyte concentration: 500.0 ng/mL carbaryl and 200.0 ng/mL trifluralin, sample volume: 4.0 mL, extraction time: 120 min, agitation speed: 1000 rpm, desorption solvent: MeOH, desorption volume: 1.5 mL, desorption time: 60 min, agitation speed: 1000 rpm)

As given in the figure, trifluralin extraction was statistically significantly higher in all PMIP samplers than in NIP samplers (Student's t-test was performed with 95% CL evaluation criterion). Furthermore, the amount of extracted trifluralin increases in parallel with the amount of sorbent. In the case of carbaryl, the following results were observed: the extracted amount of carbaryl increased as the sorbent amount increased, and extractions of S5 (10x5 mm), S7 (15x5 mm), and S10 (20x5 mm) samplers did not differ significantly (at 95% CL) indicating that the extraction reached a plateau at S5 sampler. In the case of NIPs, carbaryl extraction increased with the increasing amount of NIP sorbents, and under tested conditions, a maximum extraction plateau was not reached. In addition, it can be seen that the difference between NIP and PMIP extraction narrows as the amount of sorbent increases indicating that nonspecific sites present in NIP are effective on extraction. At 95% CL, the difference between these two extractive phases was no longer statistically significant for the S10 samplers. Although S10 samplers did not give the best differentiation between NIP and PMIP recoveries, S10 sorbent-sized samplers were used in subsequent studies due to the ease of preparation by hand.

2.3.7 Optimization of the SPME Parameters

SPME parameters were optimized following sampler selection. The sample pH, the extraction time, and the desorption time were among the optimized parameters. Optimization results and selected experimental conditions are explained in the following headings.

2.3.7.1 Optimization of pH of the Samples

The evaluation of the effect of sample pH on extraction was carried out to examine the extraction performance of the prepared sorbents at different pHs and to find the optimum pH for further evaluation. Extractions were performed from trifluralin and carbaryl-spiked buffers with solution pH values of 3.0, 5.0, 7.0, and 10.0. Three replicate PMIP samplers were used for each pH value in the extractions. Figure 2.17 shows the extracted amounts of each analyte from solutions with different pH values.

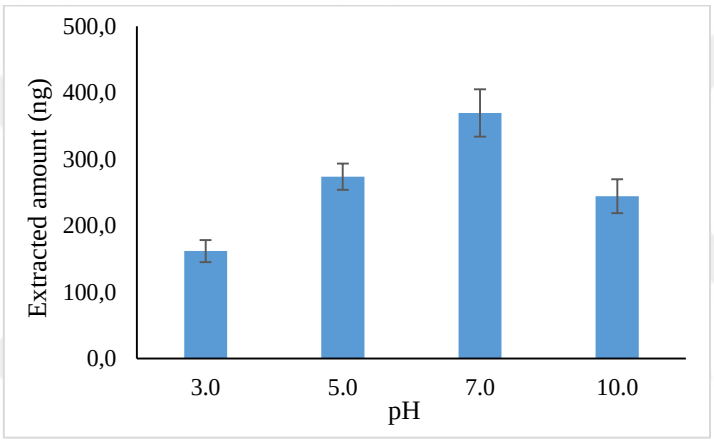

(a)

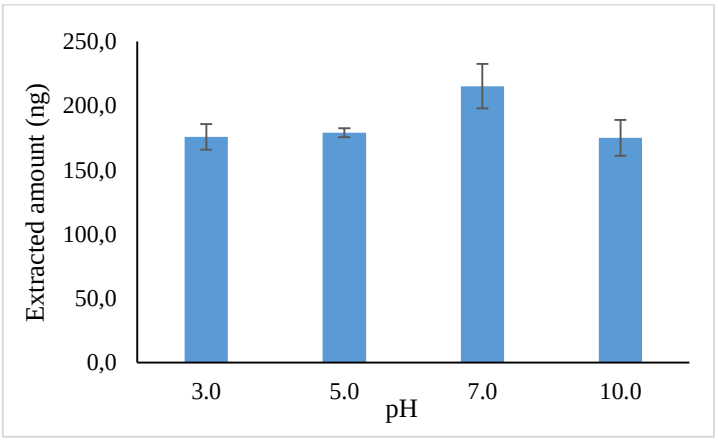

(b)

Figure 2.17. The effect of sample pH on extracted amount of a) trifluralin and b) carbaryl (Extraction conditions; sample matrix: PBS buffer solution, analyte

concentration: 500.0 ng/mL carbaryl and 200.0 ng/mL trifluralin, sample volume: 4.0 mL, extraction time: 120 min, agitation speed: 1000 rpm, desorption solvent: MeOH, desorption volume: 1.5 mL, desorption time: 60 min, agitation speed: 1000 rpm)

As given in Figure 2.17, the highest amount of extraction for both trifluralin and carbaryl was obtained at pH 7.0. Especially for trifluralin, a trend was evident in the form of an increase in extraction from pH 3.0 to 7.0 and a decrease after pH 7.0. This can be explained as follows: PAN fibers have a point of zero charge around 7.2, meaning that at pH 7.2, the net charge on the PAN surface is equal to zero [150]. Above this value, the PAN surface is negatively charged and below it is positively charged. At the tested pH of 7.0 solution, the PAN surface has a slightly positive charge. Given that carbaryl has a pKa value of 10.4, it can be assumed that it is fully positively charged at pH 8.4, two pH units below the pKa. Furthermore, in acidic environments, the protonation of the nitro groups gives trifluralin a positive charge [151]. Although the analyte and sorbent have dipole-dipole and π-π interactions, electrostatic repulsion decreases analyte adsorption in acidic conditions. Additionally, at pH 10.0, the extraction likely decreases because trifluralin and carbaryl are less stable in alkali conditions, making it more susceptible to degradation [152], [153]. Based on these findings, pH 7.0 was chosen for the remaining extractions.

2.3.7.2 Optimization of Extraction Time

In this optimization study, an extraction time profile was developed. The primary goal of this study was to determine the time required for the sorbents to reach the equilibrium extraction conditions. The second objective was to identify the extraction time point that would offer optimal sensitivity in the shortest possible

time. For this, extractions were performed with PMIP samplers for 5 min, 15 min, 30 min, 1 h, 2 h, 4 h, and 6 h. Figure 2.18 shows the resulting extraction time profiles.

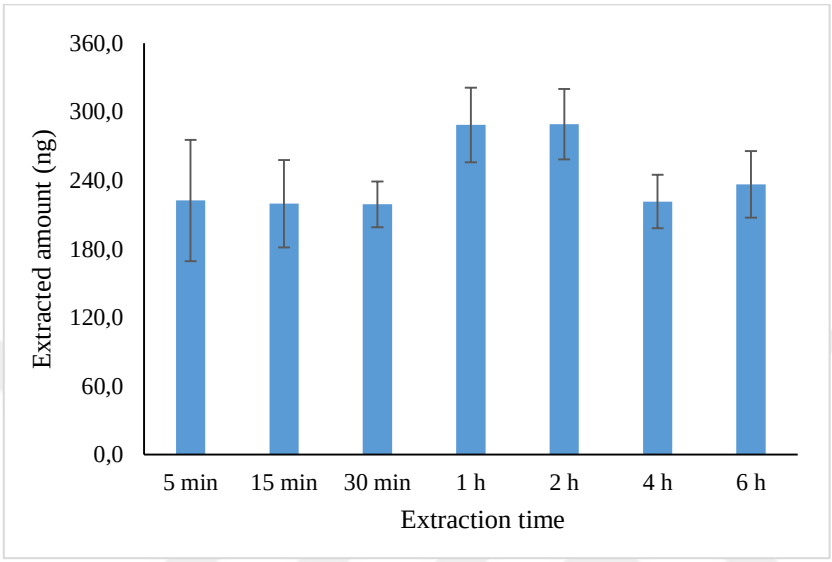

(a)

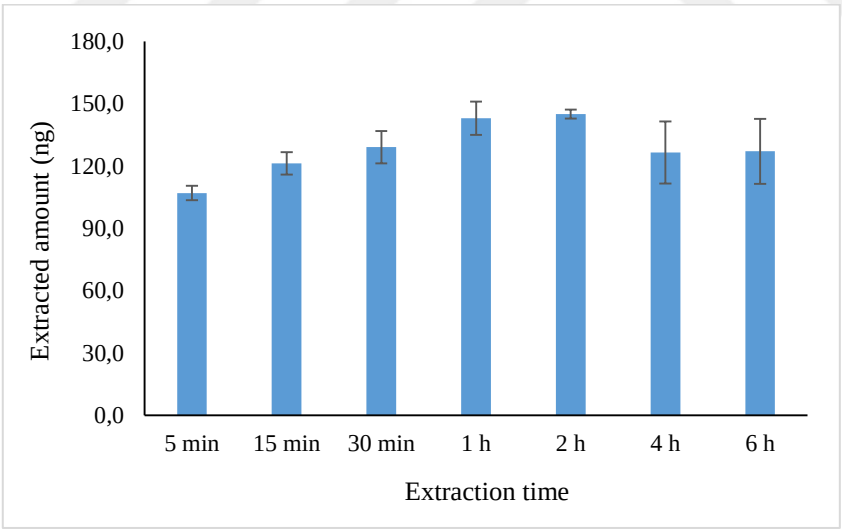

(b)

Figure 2.18. The effect of extraction time on the extracted amount of a) trifluralin and b) carbaryl (Extraction conditions; sample matrix: UPW, analyte concentration: 500.0 ng/mL carbaryl and 200.0 ng/mL trifluralin, sample volume: 4.0 mL, agitation

speed: 1000 rpm, desorption solvent: MeOH, desorption volume: 1.5 mL, desorption time: 60 min, agitation speed: 1000 rpm)

Based on the results, the highest extraction was achieved at 1h of extraction for both compounds. Student's t-test was applied to pairs including 30 minutes and 1 hour, 1 and 2 hours, and 2 and 4 hours to evaluate if there is a significant difference between extracted amounts. The statistical test was only applied to time points that are critical for the decision of optimum extraction time. Based on these evaluations, for trifluralin, a significant difference was found between the extractions at 30 minutes and 1 hour and between 2 and 4 hours, at a 95% confidence level. However, there was no significant difference between 1-hour and 2-hour extractions at the same confidence level. In the case of carbaryl, a significant increase was observed between 30 minutes and 1 hour, but no change was observed between 1 hour and 6 hours (95% CL). The findings indicated that the 1- and 2-hour extractions of trifluralin and carbaryl had the highest extractions. After the plateau between 1 and 2 hours, a decrease was observed in the extracted amount. Although no further study to understand this behavior was conducted, this can be associated with the stability of the analyte in aqueous solution. Because the 2-hour extraction had lower standard deviation values for both analytes, it was chosen for further investigations.

2.3.7.3 Optimization of Desorption Time

Another investigated SPME parameter was the evaluation of desorption time. In this study, it was aimed to find the time when all analytes were desorbed quantitatively from the sampler in the shortest possible time. For this reason, a further detailed evaluation of desorption time was performed with tested desorption times of 5 min, 15 min, 30 min, 1 h, 2 h, and 6 h. The obtained desorption time profiles are shown in Figure 2.19.

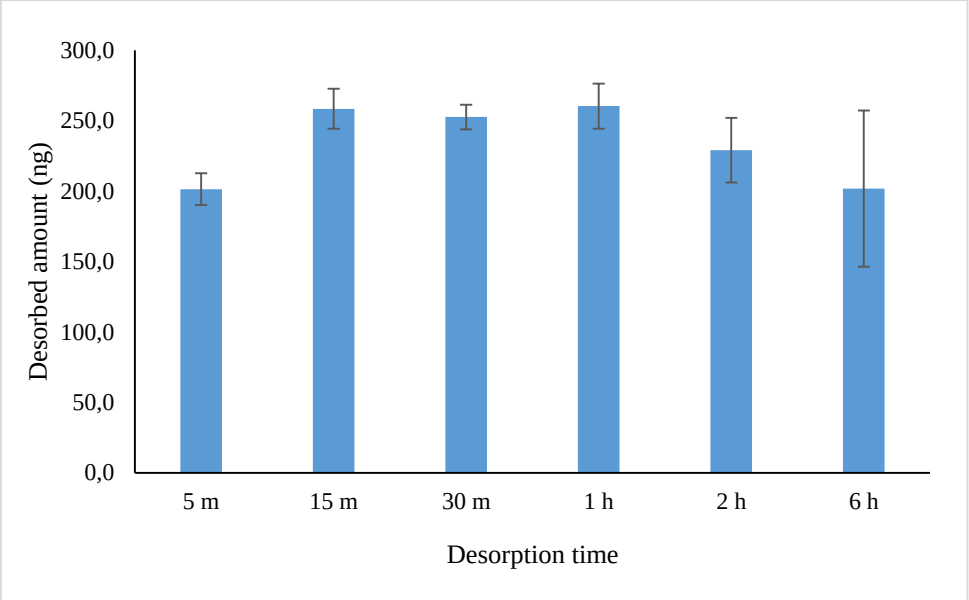

(a)

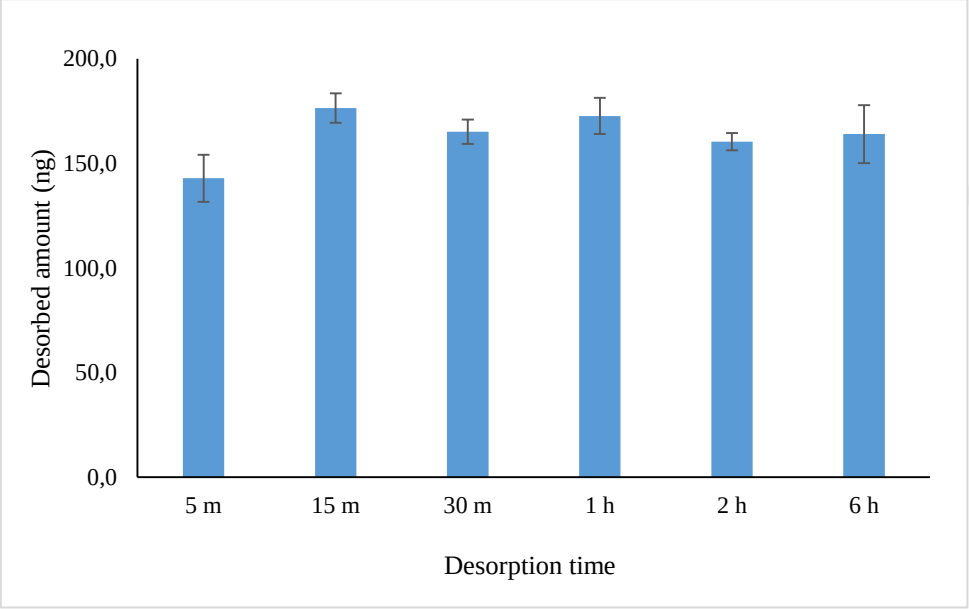

(b)

Figure 2.19. Effect of desorption time on the desorbed amount of a) trifluralin and b) carbaryl (Extraction conditions; sample matrix: UPW, analyte concentration: 500.0 ng/mL carbaryl and 200.0 ng/mL trifluralin, sample volume: 4.0 mL, extraction time: 120 min, agitation speed: 1000 rpm, desorption solvent: MeOH, desorption volume: 1.5 mL, agitation speed: 1000 rpm)

As given in the figures, there was a significant increase in desorption between 5 minutes and 15 minutes for either analyte. After the 15th minute, the desorbed amount of both trifluralin and carbaryl remained constant. As a result, it was determined that complete desorption had been reached after 15 minutes, which was accepted as the optimal desorption time.

2.3.8 Effect of Nanofibrous Surface of the Sampler

It is well accepted that as the surface area to volume ratio increases, more binding sites become available for interaction with analytes; therefore, for such materials enhanced sorption capacity can be expected. Moreover, with nanofibrous structures, it is also known that radial diffusion dominates, increasing analyte diffusion and extraction rate [154], [155]. Therefore, it can be said that the sorbent surface's morphology affects the extraction's overall efficiency. To examine the effect of nanofibrous sampler surface on extraction, NIP samplers were prepared using electrospinning (nanofibrous structure) and dip-coating (bulk polymer) methods, and extractions were conducted. In addition, electrospun PMIP (P5) samplers were also included in this test to examine the extraction enrichment of the samplers further. The optimized parameters were used for the SPME steps. The relative enrichment of analytes in NIP and PMIP samplers prepared by the electrospinning method compared to samplers prepared by the dip coating method are shown in Figure 2.20.

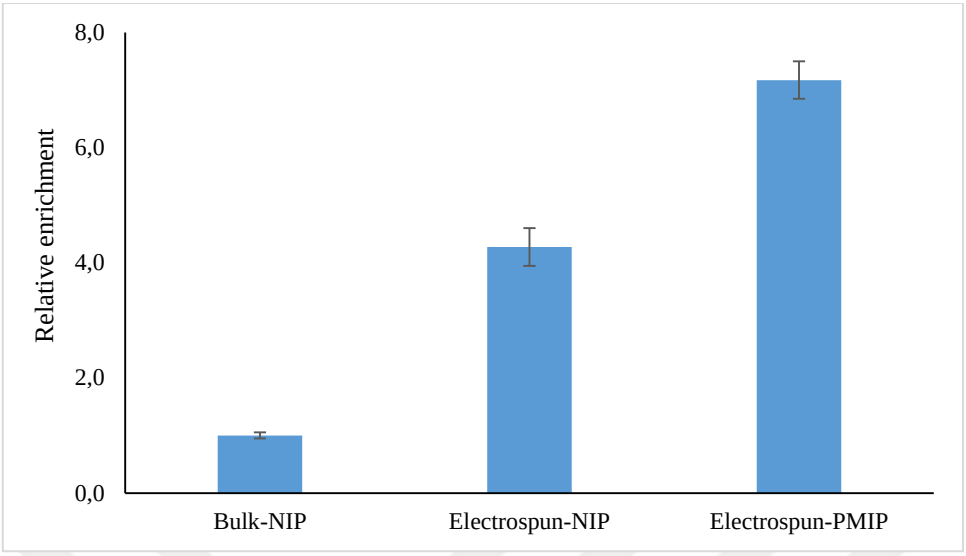

(a)

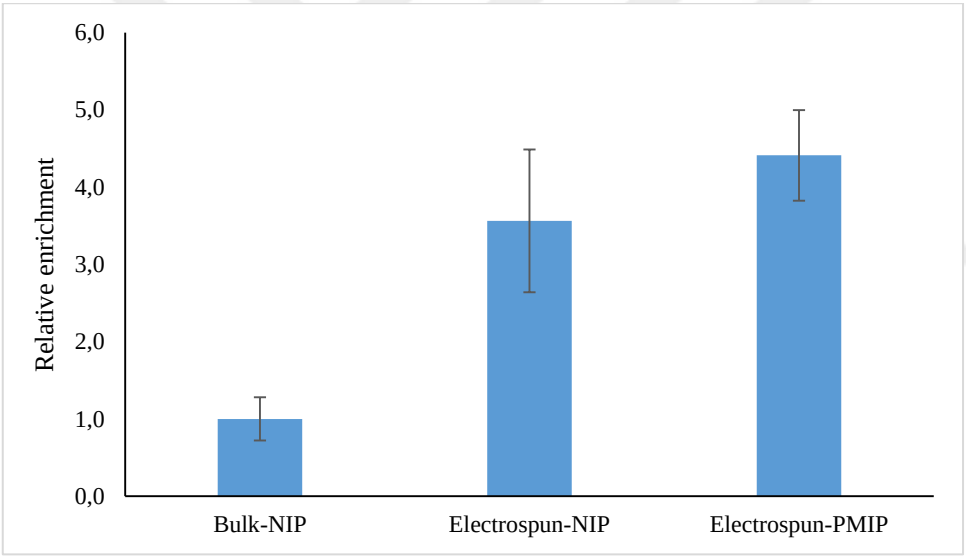

(b)

Figure 2.20. Evaluation of extraction enrichment for a) trifluralin and b) carbaryl with electrospun-NIP, and electrospun-PMIP (P5) relative to dip-coated bulk-NIP extractive phases (Extraction conditions; sample matrix: UPW, analyte concentration: 500.0 ng/mL carbaryl and 200.0 ng/mL trifluralin, sample volume: 4.0 mL, extraction time: 120 min, agitation speed: 1000 rpm, desorption solvent: MeOH, desorption volume: 1.5 mL, desorption time: 15 min, agitation speed: 1000 rpm)

As mentioned before, it is expected that the nanofibrous coatings produced via electrospinning should have a higher surface area-to-volume ratio and more surface-abundant adsorption sites, resulting in significantly greater extraction compared to the extractive phases made by dip coating which was observed clearly during this study (Figure 2.20). Additionally, it can be speculated that possible structural orientation in the nanofibrous PAN may be another factor that further enhances the extraction performance of electrospun materials compared to bulk material by increasing the availability of functional groups for interaction. Moreover, as described in Section 2.3.1.1, PAN nanofibers have an average fiber diameter of 343 ± 12 nm. According to Bard et al. devices smaller than 25 μm are expected to exhibit radial diffusion [156], which indicates that diffusion occurs radially throughout three-dimensional space in such devices, resulting in fast extraction kinetics. On this note, it is also important to mention that each electrospun fiber situated at the exterior part of the sampler can function as a singular microextraction device holding the advantage of radial diffusion.

Additionally, using the nanofibrous PMIP samplers instead of nanofibrous NIP further improved extraction efficiency, leading to a more than four times increase for carbaryl, and a seven times increase for trifluralin. This can be speculated as a better orientation of trifluralin in PAN during electrospinning due to the partial charges on the molecule. Due to this orientation, the template-specific interaction sites formed in the PMIP samplers are more favorable for trifluralin. Consequently, this phenomenon has a positive impact on the extraction performance.

2.3.9 Selectivity Investigations

As mentioned in the limitations of MIPs, since not all templates can be removed via washing, a certain amount of template leakage occurs each time MIP extractive phases are used, leading to quantification errors. To reduce the quantification errors

due to template leaks, several MIP studies employed dummy templates that were not the analytes but had similar functional groups [157], [158]. Due to the cross-reactivity of these similar functional groups in analytes, they can also be bound to template selective binding sites. However, since this cross-reactivity occurs with all molecules with template-like functional groups, it reduces the selectivity and analyte-specific performance of the extraction. As a result, the present investigation aimed to evaluate the cross-reactivity of newly prepared PMIP. This test investigated if the PMIP sampler increased the extraction of molecules other than the templates (malathion and diazinon) or if PMIP samplers only showed a template-specific extraction enhancement. Figure 2.21 shows the extracted amount of trifluralin, carbaryl, malathion, and diazinon using NIP and PMIP samplers.

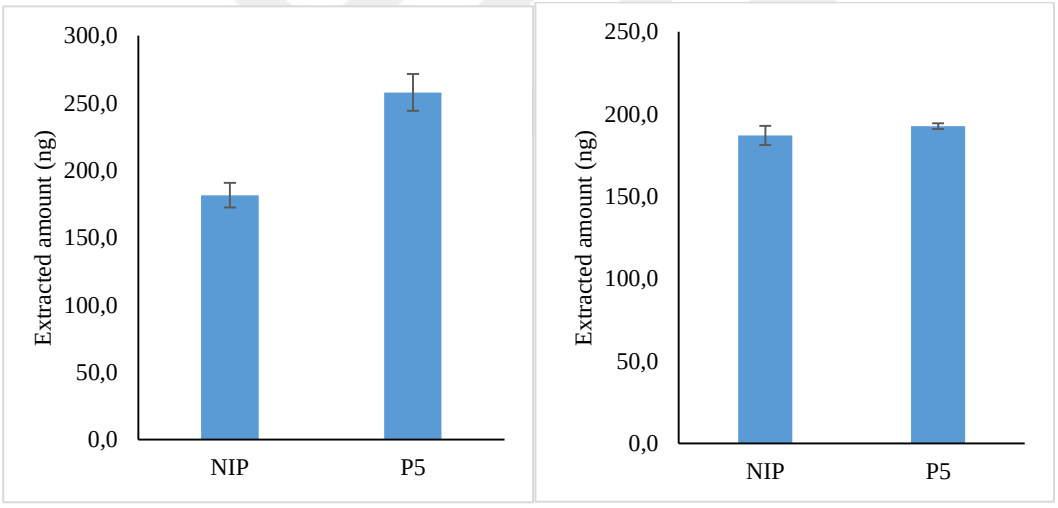

(a) (b)

Figure 2.21. The extracted amount of a) trifluralin, b) carbaryl, c) malathion, and d) diazinon with NIP and P5 sorbents (Extraction conditions; sample matrix: UPW, analyte concentration: 500.0 ng/mL carbaryl and 200.0 ng/mL trifluralin, sample volume: 4.0 mL, extraction time: 120 min, agitation speed: 1000 rpm, desorption solvent: MeOH, desorption volume: 1.5 mL, desorption time: 15 min, agitation speed: 1000 rpm)

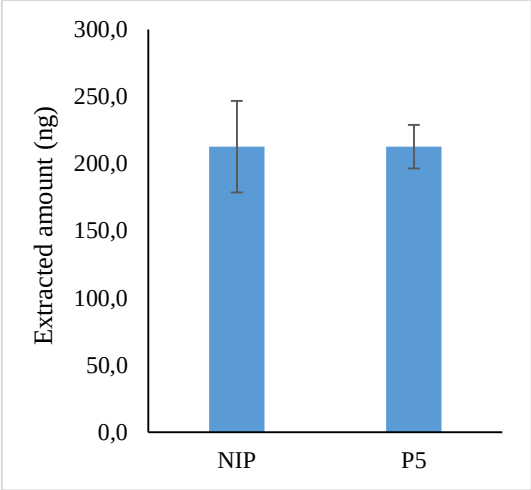

(c)

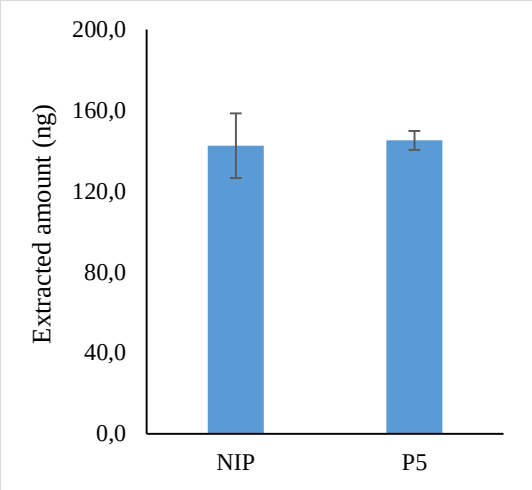

(d)

Figure 2.21. (cont'd) The extracted amount of a) trifluralin, b) carbaryl, c) malathion, and d) diazinon with NIP and P5 sorbents (Extraction conditions; sample matrix: UPW, analyte concentration: 500.0 ng/mL carbaryl and 200.0 ng/mL trifluralin, sample volume: 4.0 mL, extraction time: 120 min, agitation speed: 1000 rpm, desorption solvent: MeOH, desorption volume: 1.5 mL, desorption time: 15 min, agitation speed: 1000 rpm)

Similar to previous experiments, a significant increase in the extraction of trifluralin was observed with PMIP sorbents compared to NIP sorbents. Additionally, a relatively minor but observable increase in carbaryl extraction was found. On the other hand, as predicted, there was no significant increase in extractions of malathion and diazinon (at 95% CL). This indicates that the extraction enhancement obtained with PMIP is not specific to non-template analytes but rather to the analytes used as templates.

Furthermore, the imprinting factor (IF) (Equation 10) and relative selectivity (Srel) (Equation 11) values were calculated to examine the enhancement of the extraction of the analytes relative to others.

$$IF = \frac{Q_{MIP}}{Q_{NIP}} \quad \text{Equation 10}$$

$$S_{rel} = \frac{IF_{target}}{IF_{interferent}} \quad \text{Equation 11}$$

where Q_{MIP} and Q_{NIP} are the amount of analyte extracted by the MIP and NIP polymers, respectively. A greater relative selectivity value indicates enhanced selectivity by the MIP for the target analyte in comparison to competing species. Conversely, if S_{rel} is approximately equal to 1, it implies poor selectivity, suggesting that the MIP is unable to selectively extract the target from other compounds. Table 2.4 illustrates the imprinting factors of analytes and relative selectivity values of trifluralin and carbaryl in comparison to other analytes.

Table 2.5 Imprinting Factors of Analytes and Relative Selectivity Values of Trifluralin and Carbaryl

Analytes	**Q_{NIP} (ng)**	**Q_{MIP} (ng)**	**IF**	**$S_{rel,\ trifluralin}$**	**$S_{rel,\ carbaryl}$**
Trifluralin	121.0	171.9	1.42		0.72
Carbaryl	124.7	128.4	1.03	1.38	
Malathion	141.8	141.8	1.00	1.42	1.03
Diazinon	95.0	96.7	1.02	1.39	1.01

As given in Table 2.4, trifluralin exhibits a considerably higher imprinting factor and relative selection value in comparison to other analytes. Conversely, in a competitive matrix, the relative selectivity value of carbaryl is approximately equal to one. This indicates that the selectivity enhancement of PMIP for carbaryl extraction is less effective in more complex matrices compared to trifluralin. As discussed in section 2.3.8, the more pronounced enhancement of extraction performance in trifluralin

may be because partial charges on the molecule favor the formation of template-specific interaction sites by electrospinning.

2.4 Summary and Conclusion

Molecularly imprinted polymers (MIPs) have gained popularity as extractive phases in solid-phase microextraction (SPME). The popularity of MIPs may be due to several key advantages, such as analyte-specific binding sites, high surface-area-to-volume ratio, and their stabilities. On the other hand, MIPs also present significant challenges. While their binding sites are designed to target specific analytes, their specificity is significantly reduced in complex matrices containing structurally similar compounds or when analyte concentrations are very low. Furthermore, the synthesis of MIPs requires extensive optimization, and the issue of template leakage remains a significant challenge due to the difficulty of completely removing residual templates. Moreover, their dependence on hydrophobic interactions can impede the efficacy of extraction in aqueous environments.

In this study, a novel approach that does not require an extensive synthesis protocol for the preparation of MIP was proposed and used for the preparation of TFME samplers suitable for selective extraction of trifluralin and carbaryl, two commonly used pesticides. The novel MIP preparation approach was based on imprinting water-insoluble poly(acrylonitrile) with probe analytes during the production of an electrospun nanofibrous mat. Different from the traditional MIP production technique where the analyte-monomer couple first interacts in a pre-polymerization solution and then polymerization is conducted, in this new approach the analyte was first dissolved in a polymeric solution and then this solution was used to create analyte-specific regions by using electrospinning approach. Thus, the new extractive phase was named pseudo-molecularly imprinted polymer (PMIP).

In the course of the electrospinning process, a voltage of 20.0 kV was applied to the collector with a syringe, with a distance of 15.0 cm between them. The coating was performed on aluminum foil with a flow rate of 1.0 mL/h. The resulting polymer mat was cut to the appropriate size, peeled off the foil, and sandwiched between two stainless steel wire meshes. In the final step, the samplers were prepared for use by subjecting them to a washing process involving agitation in a mixture of 15% (v/v) acetic acid in methanol, followed by methanol washing with the Soxhlet extraction method.

The characterization studies for obtained electrospun materials were conducted using scanning electron microscopy (SEM), Fourier-transform infrared spectroscopy (FTIR), X-ray diffraction (XRD) spectroscopy, and Brunauer-Emmett-Teller (BET) surface characterization method. The SEM images obtained revealed a fine fibrous structure with an average diameter of 343 ± 12 nm (NIP) and 516 ± 196 nm (PMIP). In the subsequent characterization study, the FTIR spectra of NIP and PMIP nanofibers were obtained. Upon comparison of these spectra, both exhibited peaks that could be attributed to PAN. The PMIP spectrum exhibited additional peaks of trifluralin and carbaryl, suggesting successful immobilization of the templates within the polymer matrix. In the XRD characterization, the XRD patterns of pure PAN powder, electrospun NIP nanofibers, and electrospun PMIP nanofibers were investigated. It was observed that the 11% crystallinity of pure PAN powder increased with electrospinning, and the crystallinity of electrospun NIP and PMIP reached 48%. In the final characterization, the BET and Barrett-Joyner- Halenda (BJH) method calculations show an increase in pore volume and pore diameter for PMIP compared to NIP. By imprinting PAN with template molecules, pore volume increased from 1.1 cm^3/g to 1.5 cm^3/g and pore diameter from 1.3 nm to 4.0 nm.

Critical parameters for the fabrication of the sorbents and TFME samplers were optimized, including template-to-polymer ratio and sampler size. Among the tested polymer analyte ratios (0.5, 1.3, 2.5, and 5.0 mg of templates dissolved in 1.0 mL of PAN solution) the PMIP prepared by adding 5.0 mg each of trifluralin and carbaryl to 1.0 mL of PAN solution provided the highest extraction for both analytes.

Succeeding the selection of the optimum polymer analyte ratio, the effect of sampler size on the extracted amount was investigated using samplers with varying sizes (3x3, 7x3, 10x5, 15x5, and 20x5, in mm) for which the best recoveries were obtained with a 20x5 mm sampler. Moreover, a comparison of extraction amounts of NIP and PMIP samplers showed that the best selectivity is obtained for both analytes when a sampler with dimensions of 10x5 mm is used.

Following the selection of the samplers, parameters that affect extraction recoveries and desorption of analytes were evaluated. The sample pH was found to significantly affect the extraction of both analytes, with the highest value obtained under neutral pHs as under acidic conditions, reduced analyte adsorption occurs due to electrostatic repulsion between the positively charged analyte and PAN surface, and under basic conditions, analyte hydrolysis results in lower extractions. Evaluation of the extraction time profile revealed an increase in the amount of analyte extracted as interaction time increases and reaches a plateau at 1 hour of extraction suggesting that the equilibrium is established for the system. The evaluation of desorption time using methanol as solvent revealed that only 15 minutes of desorption is sufficient to achieve complete desorption.

Succeeding the above-described optimization parameters, an evaluation was conducted to examine the selectivity of the samplers in the presence of other pesticides. Cross-selectivity tests indicated improved selectivity for trifluralin ($S_{rel} \geq 1.3$), highlighting the potential of PMIP sorbents to minimize interference from structurally similar non-target analytes.

Finally, the effect of nanofibrous structure on the extraction performance of the new samplers was compared to TFME samplers prepared by the dip-coating method which deposited the same polymer in bulk on the surface of a support. The findings showed that electrospun nanofibers with enhanced surface area-to-volume ratio and radial diffusion, facilitate more efficient analyte adsorption compared to dip-coated bulk sorbents. Moreover, compared to TFME samplers containing dip-coated-bulk NIP sorbents, electrospun NIP sorbents showed significantly higher extraction

efficiencies (around four times increase for trifluralin and carbaryl). The extracted amount was further increased by using electrospun PMIP sorbents. In the extraction process of trifluralin, electrospun PMIP samplers demonstrated a seven-fold increase in recovery compared to bulk NIP samplers. For carbaryl, a four-fold increase was obtained in electrospun PMIP samplers compared to bulk NIP samplers.

These findings demonstrate that PMIP sorbents provide a versatile, efficient, and selective platform for extracting target analytes, with significant potential for applications in environmental, food, and pharmaceutical analyses. However, further evaluations of the new MIP preparation technique should be conducted to determine whether the preparation of PMIP can be extended to other electrospinnable polymers and analytes with different physicochemical properties.

CHAPTER 3

A NOVEL ELECTROSPINNING METHOD FOR SOLID-PHASE MICROEXTRACTION COATINGS: SINGLE-DROP STATIC BLADE ELECTROSPINNING

3.1 Introductory Summary

In this study, it has been proposed to develop samplers that have fast extraction kinetics which are possible by use of ultrathin coatings and nanofibrous materials. For this purpose, TFME samplers made by electrospinning approach were suggested. Although the electrospinning approach appears as one of the simpler ways to coat a surface with a nanofibrous structure (providing high surface area for interaction), reproducible preparation of electrospun coating is challenging. This is difficult as the electrospinning process is highly sensitive to environmental changes such as air humidity and temperature and small changes affecting the viscosity of the samples. Even under strict control of these parameters the syringe system used during the electrospinning process produces unevenly coated mats. Especially when very thin coatings are desired. Thus, the aim of this study was to develop a new electrospinning approach based on the electrospinning of a limited amount of solutions under static conditions, which allows having a controlled amount of mat with a thin layer of material. Using a flat surfaced stainless-steel blade as a source for electrospinning new samplers were produced.

3.2 Experimental

3.2.1 Chemicals and Supplies

The reagents for the synthesis of poly(divinylbenzene) (PDVB) nanoparticles; (divinyl benzene (DVB, 80% technical grade), aluminum oxide (activated, basic), sodium dodecyl sulfate (SDS, ACS reagent ≥99.0%), and hexadecane (HD, re-agent plus 99%) were purchased from Sigma-Aldrich (St. Louis, MO, USA). The initiator 2-2′-azobis(2-methyl-propionitrile) (AIBN, 98%) was acquired from Acros Organics (Geel, Antwerpen, Belgium). Polyacrylonitrile (PAN, Mw 150 KDa) used to prepare the electrospun mat was purchased from Sigma-Aldrich (St. Louis, MO, USA). N, N-Dimethylformamide (DMF), was acquired from Sigma-Aldrich (St. Louis, MO, USA) and used to dissolve PAN. Pesticides, trifluralin, parathion, malathion, and diazinon pesticides (≥98.0% purity), were obtained from Sigma-Aldrich (St. Louis, MO, USA) and used as model analytes for the study.

Pesticide stock solutions (1.0 mg/mL) were prepared by dissolving solid pesticides in LC-grade methanol (MeOH, ISOLAB Chemicals, Eschau, Bavaria, Germany). The prepared solutions were kept in the fridge at 4°C. Working solutions were prepared before each analysis in water, and calibration solutions were prepared by diluting the stock solution with LC-grade MeOH. High-purity (99.999%) helium used in gas chromatography was purchased from Koyuncu (Ümraniye, İstanbul, Turkey).

3.2.2 Instrumentation

SONICS VibraCell VCX500/VCX750 ultrasonic processor was employed during PDVB synthesis to mix and homogenize solutions (Sonics & Materials, Inc., Newtown, CT, USA). A benchtop centrifuge (NüveNf200, Akyurt, Ankara) was

used to separate synthesized PDVB nanoparticles from their reaction mixture. Nanofiber coatings were prepared using a nanoWEB Electro-spin110 electrospinning instrument coupled with an NE-1000 syringe pump (New Era Pump Systems, New York, USA). During the SPME procedure, the samples were agitated using a CAT AEK-SH10 plate shaker. The ultrapure water (18.2 MΩ.cm at 25°C) was obtained using the Millipore Milli Q Plus (Massachusetts, USA).

Analytes were separated and quantified using an Agilent 6890A gas chromatograph coupled with an Agilent 5973 quadrupole mass selective detector (California, USA) equipped with a 30-meter ultra-inert (5%-phenyl)-methylpolysiloxane capillary column with a 0.25 mm inner diameter and a 0.25 μm film thickness (Agilent Technologies, HP-5MS).

The surface of the electrospun nanofibers and the morphology of the synthesized PDVB nanoparticles were analyzed using a QUANTA 400F Field Emission Scanning Electron Microscope (SEM, Oregon, USA).

3.2.3 Preparation of TFME Samplers

A series of precise optimizations are required to achieve the targeted coating with low thickness and high homogeneity, high reproducibility, and low material consumption. In addition to the optimization of the electrospinning parameters (applied voltage, the distance between the collector and blade, etc.), the properties of the polymer solution that will form the coating are also taken into account to achieve thin, homogeneous, and reproducible coating. The following sections detail the synthesis of the poly(divinylbenzene) (PDVB) nanoparticles, polyacrylonitrile (PAN) solution preparation, and nanoparticle integration by electrospinning and coating optimization processes.

3.2.3.1 Synthesis of Poly(divinylbenzene) Nanoparticles

A modified mini-emulsion polymerization based on the procedure described by Migenda et al. was used to synthesize self-crosslinked PDVB nanoparticles [159]. The DVB monomer was passed through activated basic alumina to eliminate the inhibitor p-tert-butylcatechol before polymerization. Prior to the polymerization reaction, 0.90 g of SDS was dissolved in 12.0 mL distilled water in a 20 mL vial. In another 20 mL vial, a mixture of 0.162 mL of HD, 3.0 mL of the inhibitor-free DVB, and 0.050 g of AIBN was mixed. After combining the two solutions in the vials and stirring the resulting mixture for 30 minutes at 990 rpm, a milky emulsion was obtained. After cooling in an ice bath, this emulsion was homogenized for three minutes using an ultrasonic probe. The polymerization was then carried out in an oil bath with continuous stirring at 990 rpm overnight at 70 °C. After the reaction, the resulting milky mixture (containing the particles and reaction media) was mixed with methanol and centrifuged to collect the resultant PDVB nanoparticles. This step was followed by washing the particles with methanol and drying overnight them at 70 °C. Figure 3.1 shows the schematic representation of the synthesis of PDVB nanoparticles. The crosslinked PDVB structure is shown in Figure 3.2.

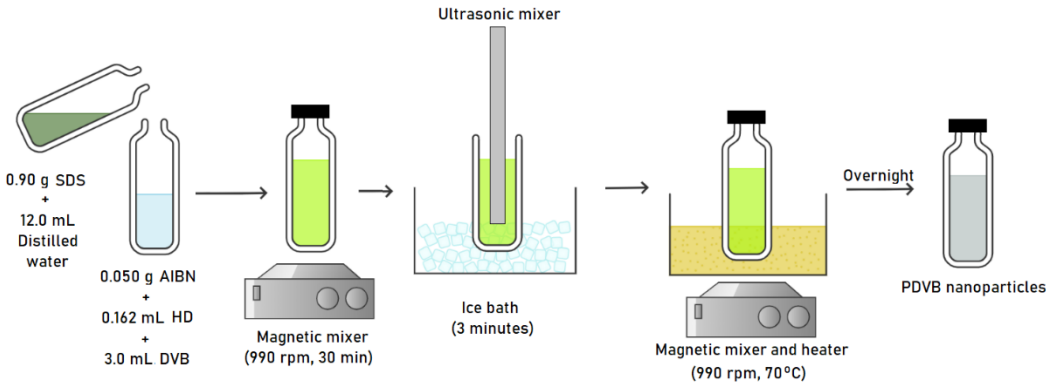

Figure 3.1. The schematic representation of the synthesis of PDVB nanoparticles

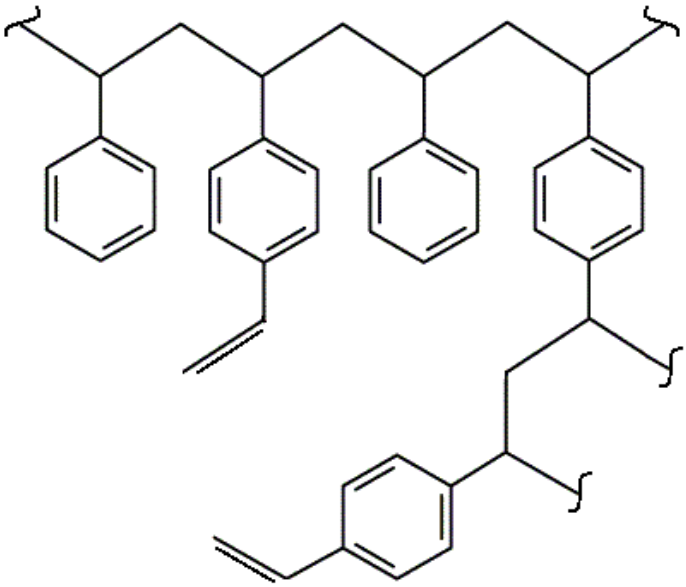

Figure 3.2. The structure of crosslinked PDVB

3.2.3.2 Immobilization of PDVB Nanoparticles into PAN by a Novel Electrospinning Approach: Single-Drop Static Blade Electrospinning

In this study, PAN nanofibers were used as a carrier phase for PDVB nanoparticles. To obtain PAN nano/micro-fibers in which PDVB particles are embedded, a 10% PAN (w/w) solution was first prepared. For this, 1.0 g PAN was added into 9.6 mL (9.0 g) DMF. The mixture was stirred at 600 rpm for 24 hours.

Different amounts of synthesized PDVB nanoparticles were added to the prepared PAN solution to obtain a slurry that provides the best coating morphology. Three new slurries were prepared with PDVB: PAN ratios of 1:4, 1:2, and 1:1. For this, 0.050, 0.10, and 0.20 g of PDVB nanoparticles were added into 2.0 g of PAN solution and stirred at 600 rpm for 2 hours. These slurries were coded as M05, M1, and M2, respectively.

The optimization of electrospinning parameters (applied voltage and the distance between the blade tip and collector) was performed using all the mixtures described above. The coatings were obtained on 0.2 mm thick aluminum sheets placed on a collector surface with a horizontal electrospinning setup (Figure 3.3). Static electrospinning was used in this setup. Instead of conventional electrospinning which utilizes a syringe and continuous infusion of polymer solution, a blade was used, and the polymer solution was added as a drop onto the blade surface. The circuit was completed between the voltage supply with alligator clips connected to the blade and collector (Figure 3.4). The following steps were performed during the coating: attaching circuit clips to a properly fixed blade and collector plate, dropping a drop of polymer solution on the blade with the help of a Pasteur pipette, turning on the voltage supply, and continuing the coating for 40 seconds, waiting 1 minute for the coating to dry and performing a second coating layer for 40 seconds. This was repeated for different voltages and distances. The applied voltages of 5.0, 10.0, and 15.0 kV were fluxed between ± 0.5 kV to determine the optimum values for coating. The tested distances between the blade tip and the collector were 8.0, 10.0, and 15.0 cm.

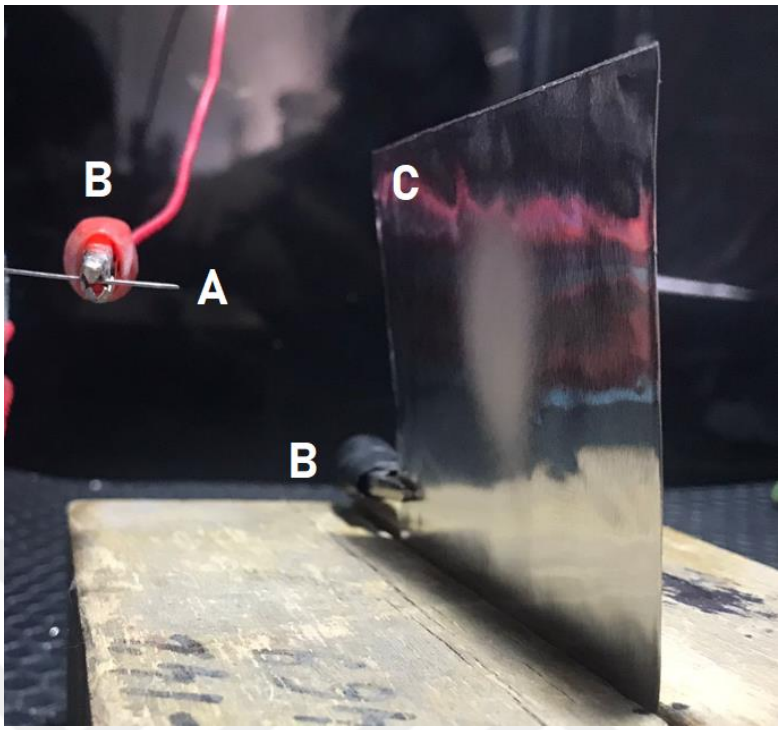

Figure 3.3. Horizontal electrospinning setup with a) blade, b) alligator clips connected to the voltage supply, and c) collector plate.

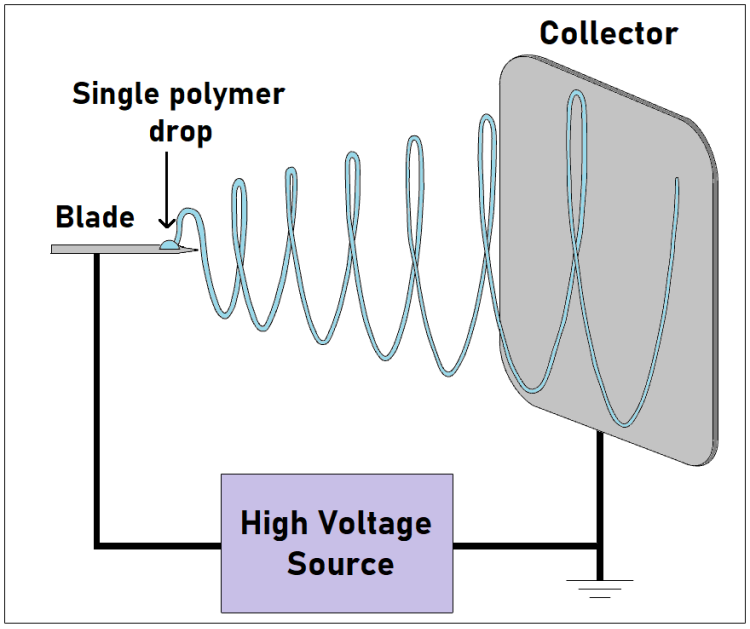

Figure 3.4. Schematic diagram of single-drop static blade electrospinning

3.2.3.3 Optimization of the Electrospinnability of PAN/PDVB Slurry

Once the electrospinning parameters were optimized for the coating slurry, the mixtures were diluted and tested to further enhance the coating performance. For this, 0.44 g (300 μL) each of the M05, M1, and M2 mixtures were diluted with 100, 300, and 500 μL DMF and mixed at 600 rpm for 1 hour. These dilutions were coded as D1, D3, and D5, respectively (e.g. the M2 mixture diluted with 500 μL was coded as M2-D5).

With the above-mentioned diluted solutions, coating optimization was performed with the setup described in Section 3.2.3.2. SEM images of the coatings were taken and coatings containing the most uniform nanofiber and PDVB nanoparticle distribution were selected. TFME samplers were produced by cutting 7.0x15.0 mm pieces from these coatings and folding them along the short edges to pass through the neck of the vial.

Finally, extractions were performed to test the performance of the prepared TFME samplers. For the conditioning step, the samplers were soaked in LC-Grade MeOH for 30 minutes and then dried with a tissue. Each sampler was placed in 20.0 mL of UPW which was spiked to contain 200.0 ng/mL trifluralin and 500.0 ng/mL of malathion, parathion, and diazinon and agitated at 1000 rpm for 2 hours. At the end of the extraction, the samplers were dried again with a tissue. Finally, desorption into 0.50 mL LC-Grade MeOH at 1000 rpm for 1 h was performed. Desorption solutions were analyzed by the method described in Section "2.2.5 GC-MS Method".

3.2.4 Reproducibility of the TFME Samplers

The objective of this study was to investigate the reproducibility of the prepared TFME samplers. To this end, fifteen new M2-D3 samplers with optimized coating parameters were prepared. In conditioning, samplers were placed in 1.5 mL of LC-

grade methanol for 30 minutes and dried with a clean tissue. The SPME procedure was mainly carried out as follows: each sampler was placed in 20.0 mL of UPW which was spiked to contain 200.0 ng/mL trifluralin and 500.0 ng/mL of malathion, parathion, and diazinon and agitated at 1000 rpm for 2 hours. At the end of the extraction, the samplers were dried again with a tissue. Finally, desorption into 0.50 mL LC-Grade MeOH at 1000 rpm for 1 h was performed. After injection of the extracts into GC-MS, the coherence of the extraction results between samplers was investigated. Furthermore, following the completion of the aforementioned test, the reusability of these coatings was examined according to the peeling of their coatings.

3.2.5 Optimization of the Desorption Time

Optimization of the desorption time is an important step in SPME to ensure the best analyte transfer from the extraction phase to the desorption solvent. In this study, the desorption time profile was investigated to find the shortest time to achieve complete analyte desorption.

Before use for extraction, the samplers were conditioned in 1.5 mL of LC-grade methanol for 30 minutes and then dried with a clean tissue. For extraction, M2-D3 samplers were immersed into 20.0 mL UPW which was spiked to contain 200.0 ng/mL trifluralin and 500.0 ng/mL of malathion, parathion, and diazinon and agitated at 1000 rpm for 2 hours. At the end of the extraction, the samplers were dried again with a tissue. Following the drying step, desorption to 0.50 mL LC-Grade MeOH was performed at 1000 rpm for 5 min, 10 min, 15 min, 20 min, and 30 min. M2-D3 samplers (N=3) were used in this test.

3.2.6 Effect of Nanofibrous Surface of the Samplers on Extraction Kinetics

TFME samplers with electrospun-coated nanofibrous and dip-coated bulk polymer extractive phases were compared in terms of their extraction kinetics. Since the slurry prepared for the electrospinning process was not suitable for dip coating, a new slurry was prepared. For this purpose, the PAN solution that can be used for dip coating was prepared as described in Section 2.2.9. This PAN solution was then used for the preparation of the M2-D3 slurry (as described in Sections 3.2.3.2 and 3.2.3.3). During the dip coating, the blades were immersed in the slurry by 18.0 mm to have the same area and volume of extractive phase as the nanofibrous sorbents. The blades were kept for 1 minute in the slurry, withdrawn at a constant speed of 1.3 mm/s, the solvent was evaporated in a 90^{o}C oven for 1 minute, and the same steps were repeated for the second layer of coating.

In addition, nanofibrous M2-D3 sorbents were also re-prepared for this test. Then, the extraction kinetics study was performed by placing the bulk-M2-D3, and nanofibrous-M2-D3 samplers in 20.0 mL of UPW which was spiked to contain 200.0 ng/mL trifluralin and 500.0 ng/mL of malathion, parathion, and diazinon. The extraction times tested were 30, 60, 120, 180, 300, 600 seconds. The optimized parameters described in Section 3.2.5 were utilized in the SPME procedure.

3.2.7 Comparison of Extraction Kinetics Under Static and Stirring Conditions

The effect of agitation conditions on extraction kinetics was evaluated to see if the kinetic of extraction differs significantly from static extraction to extraction with agitation. In kinetic studies, extractions of 30, 60, 120, 180, 300, and 600 seconds were applied. Three nanofibrous M2-D3 samplers were used for this test. Extraction

kinetics were studied with the parameters given above and desorption was performed under optimized conditions.

3.3 Results and Discussion

3.3.1 Characterization Studies

Scanning electron microscope (SEM) images of the coatings were taken to observe the morphology and measure the diameter of electrospun fibers containing PDVB nanoparticles immobilized in continuous PAN fibers. The SEM images of M05-D3, M05-D5, M1-D1, M1-D3, M1-D5, M2-D1, M2-D3, and M2-D5 coatings (their preparation is explained in Sections 3.2.3.2 and 3.2.3.3) are shown in Figure 3.5. SEM images of M05-D1 were not taken because a coating could not be obtained with this solution.

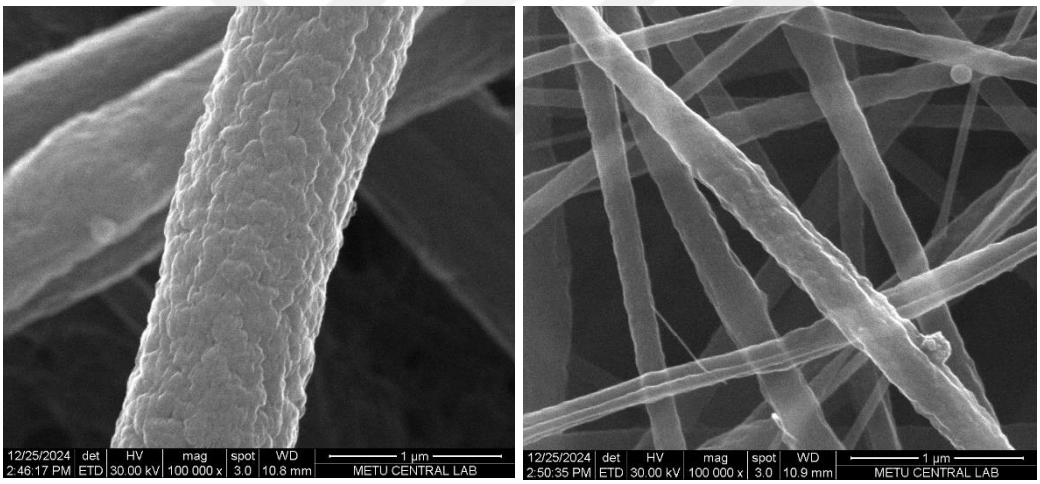

(a) (b)

Figure 3.5. SEM images of the electrospun coatings prepared using a) M05-D3 b) M05-D5, c) M1-D1, d) M1-D3, e) M1-D5, f) M2-D1, g) M2-D3, and h) M2-D5 polymer solutions.

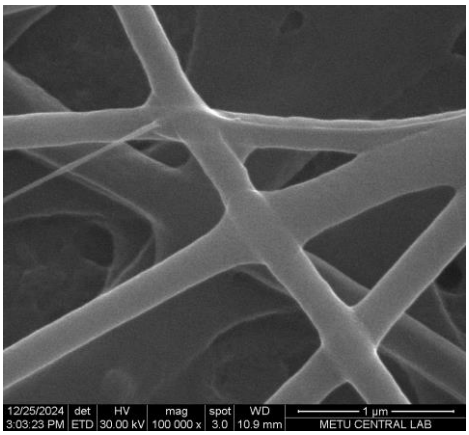

(c)

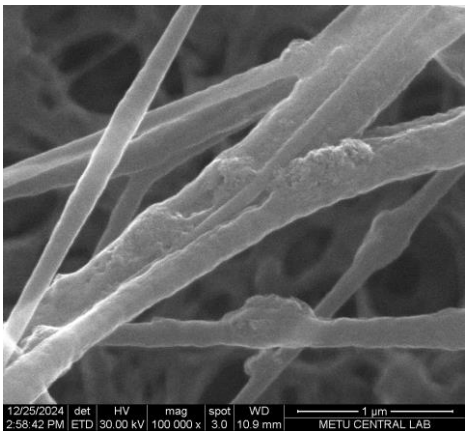

(d)

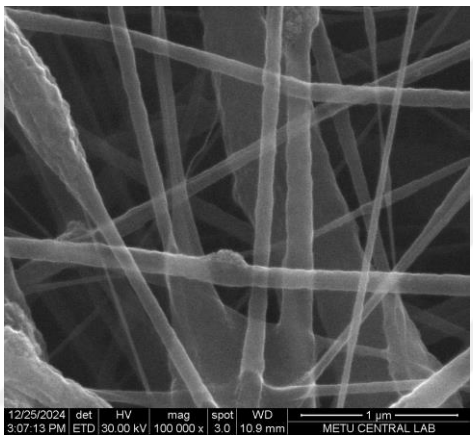

(e)

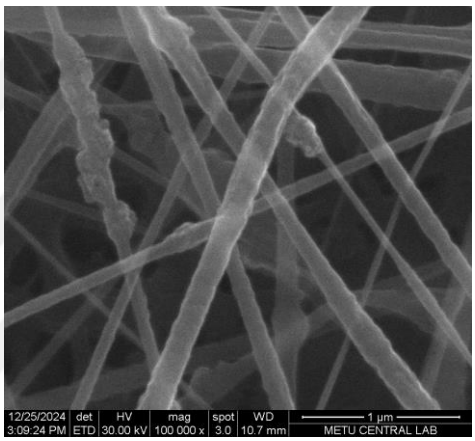

(f)

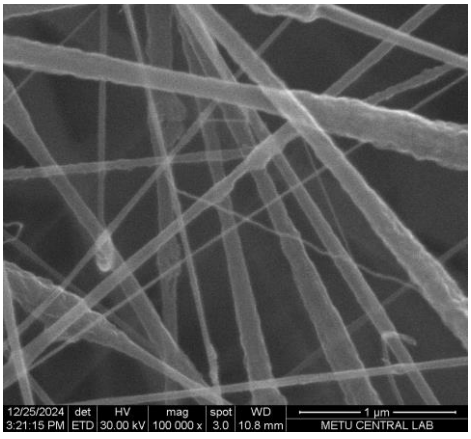

(g)

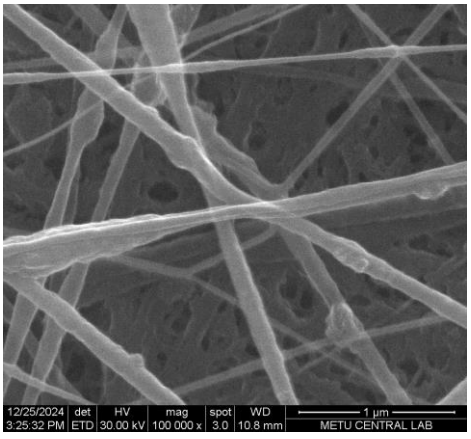

(h)

Figure 3.5. (cont'd) SEM images of the electrospun coatings prepared using a) M05-D3 b) M05-D5, c) M1-D1, d) M1-D3, e) M1-D5, f) M2-D1, g) M2-D3, and h) M2-D5 polymer solutions.

The diameters of 20 randomly selected microfiber sections were measured using ImageJ software (N=20). The mean diameters of M05-D3, M05-D5, M1-D1, M1-D3, M1-D5, M2-D1, M2-D3, and M2-D5 nanofibers were 809 ± 273 nm, 250 ± 99 nm, 293 ± 71 nm, 198 ± 74 nm, 99 ± 26 nm, 166 ± 84 nm, 112 ± 52 nm, 77 ± 21 nm, respectively. As observed in the images, thinner fibers were obtained as the dilution amount increased. In addition, the surface roughness of the fibers is increased by the embedding of PDVB into PAN fibers. Furthermore, it was observed that the immobilization of PDVB did not result in any negative impact on the fiber formation and electrospinning capability of the polymer mixture, including the slurry with the highest PDVB concentration. These SEM images, together with the results of the extraction tests given in Section 3.2.3.3, were used to select the most suitable coating solution for further studies.

3.3.2 Preparation of TFME Samplers

3.3.2.1 Immobilization of PDVB Nanoparticles into PAN by a Novel Electrospinning Approach: Single-Drop Static Blade Electrospinning

PDVB/PAN slurries with different ratios of PDVB nanoparticles to PAN were investigated for their ease of electrospinning. The slurries prepared with PDVB: PAN ratios of 1:4, 1:2, and 1:1 were coded as M05, M1, and M2 respectively and electrospinning was performed with different parameters using these mixtures. The images of the obtained coatings and the applied electrospinning parameters (applied voltage and the distance between the blade and the collector) are shown in Table 3.1.

Table 3.1 The Pictures of Electrospun Coatings Using M05, M1, and M2 Slurries and the Applied Electrospinning Parameters

Sampler	**Image**	**Electrospinning Parameters**
M05		9.9 kV 5.0 cm
M05		10.4 kV 8.0 cm
M05	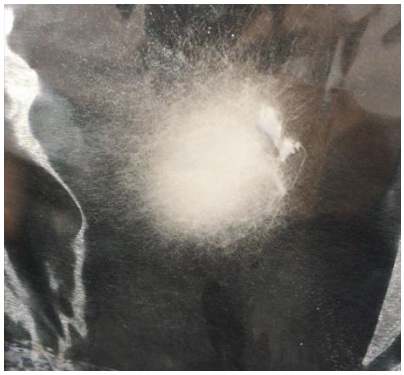	15.0 kV 10.0 cm

Table 3.1. (cont'd) The Pictures of Electrospun Coatings Using M05, M1, and M2 Slurries and the Applied Electrospinning Parameters

M1		10.4 kV 8.0 cm
M1		15.0 kV 10.0 cm
M2		10.4 kV 8.0 cm
M2		15.0 kV 10.0 cm

The appropriate voltage-distance pair from which the nanofibrous coatings shown in Table 3.1 were obtained was in a sensitive correlation. If more voltage or a closer distance than this pair was used, the polymer was pulled into the collector so violently that it sprayed out polymer beads in the form of a spray. On the other hand, at a greater distance or when less voltage was applied, the Taylor cone failed to form, and no coating was formed. Only the M05-D1 slurry yielded a coating with the applied parameters of 9.9 kV and 5.0 cm distance. However, this structure was not homogeneous and was not fully coated, causing agglomeration at one point. Furthermore, electrospinning at 15.0 kV and a distance of 10 cm resulted in the accumulation of unwanted droplets in the collector for all the prepared solutions. For these reasons, the parameters of 10.4 kV applied voltage and 8.0 cm distance, which provided the most homogeneous coating for all slurries, were preferred for further electrospinning.

3.3.2.2 Optimization of the Electrospinnability of PAN/PDVB Slurry

To further improve the coating homogeneity and electrospinnability performance, the prepared polymer solutions were diluted with DMF. The diluted solutions were coated on a 0.2 mm thick aluminum sheet by electrospinning with optimized electrospinning parameters (10.4 kV voltage and 8.0 cm distance) and the coating morphologies were examined. The images of the obtained coatings are shown in Table 3.2

Table 3.2 Images of Electrospun Coatings Obtained with Diluted Solutions

	Dilutions		
	D1	**D3**	**D5**
M05	-	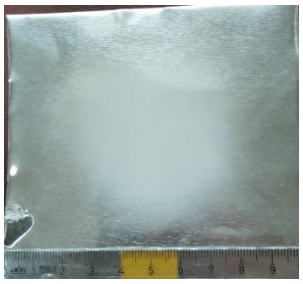	
M1	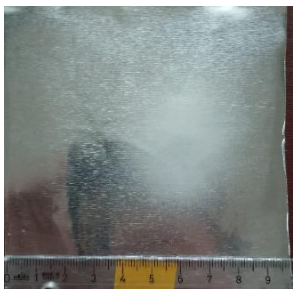	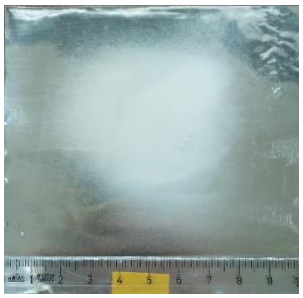	
M2	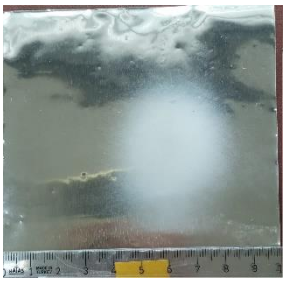	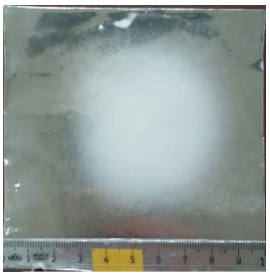	

It was observed that the diameter of the coated area increased with increasing the slurry dilution. Accordingly, the mats formed by M05-D5, M1-D5, and M2-D5 slurries had the largest coated surface areas. However, as the surface area increases, the reproducibility of the coatings decreases because it is difficult to obtain coatings with the same circular shape. In addition, homogeneous coating thickness could not be obtained because the thickness of the coating decreased from the center to the outside.

As the dilution amount decreased, the viscosities of the slurries increased, and the formation of Taylor cone and nanofibers became difficult. As a result, a very small

amount of coating could be obtained and the nanofibers formed clustered in the center, resulting in a heterogeneous coating. In addition, as a result of this coating challenge, no coating could be obtained from the M05-D1 slurry. Considering these results, it was decided that the optimal dilution amount was D3 (300 µL of PDVB: PAN slurry diluted with 300 µL of DMF).

SEM images (shown in Section 3.3.1) and extraction analysis were examined to determine the best coating and extraction performance among M05-D1, M1-D1, and M2-D2 solutions. For this, extractions were performed with TFME samplers prepared with M1-D1 and M2-D2 coatings.

In addition to the physical observations, an evaluation of the extraction performance of these coatings was performed to support the final extractive phase choice. The extractions were performed as described in Section 3.2.3.3. Extracted amounts are shown in Figure 3.6 and Figure 3.7. For easier visualization, the extractions of diazinon are shown in Figure 3.7.

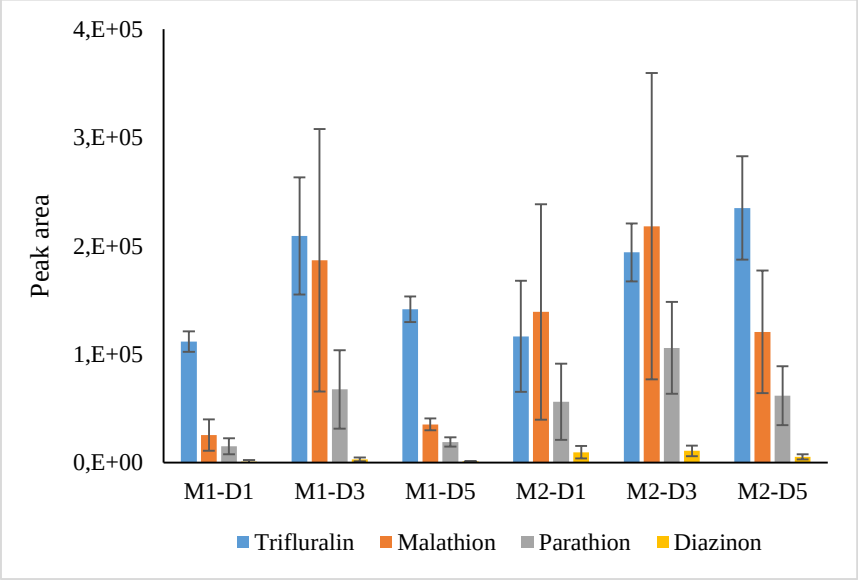

Figure 3.6. Performance of each prepared sampler for extraction of trifluralin, malathion, parathion, and diazinon (Extraction conditions; sample matrix: UPW, analyte concentration: 500.0 ng/mL malathion, parathion, and diazinon and 200.0

ng/mL trifluralin, sample volume: 20.0 mL, extraction time: 120 min, agitation speed: 1000 rpm, desorption solvent: MeOH, desorption volume: 0.5 mL, desorption time: 60 min, agitation speed: 1000 rpm)

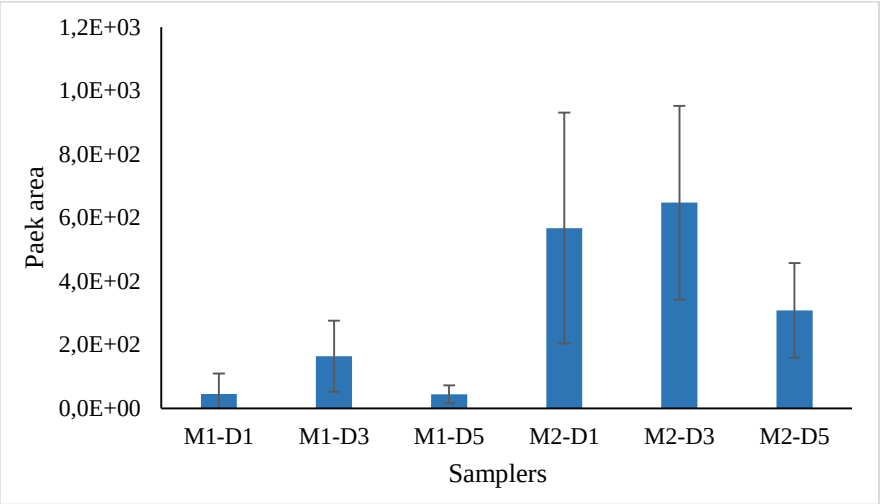

Figure 3.7. Performance of each prepared sampler for extraction of diazinon (Extraction conditions; sample matrix: UPW, analyte concentration: 500.0 ng/mL malathion, parathion, and diazinon and 200.0 ng/mL trifluralin, sample volume: 20.0 mL, extraction time: 120 min, agitation speed: 1000 rpm, desorption solvent: MeOH, desorption volume: 0.5 mL, desorption time: 60 min, agitation speed: 1000 rpm)

In general, the samplers prepared with D3-diluted slurries gave the highest extractions. In addition, considering their overall performance, M2 coatings were observed to show a higher extraction trend than the coatings corresponding to M1 solutions. However, high standard deviations were obtained because the reproducibility of the prepared samplers was not known and the SPME parameters were not optimized. Albeit M2-D3 samplers provided high standard deviations, as the highest extraction was obtained with these samplers they were selected for further evaluations.

3.3.3 Reproducibility of the TFME Samplers

In this study, fifteen new M2-D3 samplers were prepared and their reproducibility was investigated using the extraction parameters described in Section 3.2.4. This study was critical because, in the previous experiment, it was observed that the coatings of the samplers peeled off easily during the preparation of samplers and extraction steps in which the samplers were reused. The damage resulted in large variations in extractions obtained in former studies. Therefore, here the samplers were handled with the utmost care, and damaged samplers were not used in extraction tests. Figure 3.8 shows the extraction results for a single use of each prepared sampler.

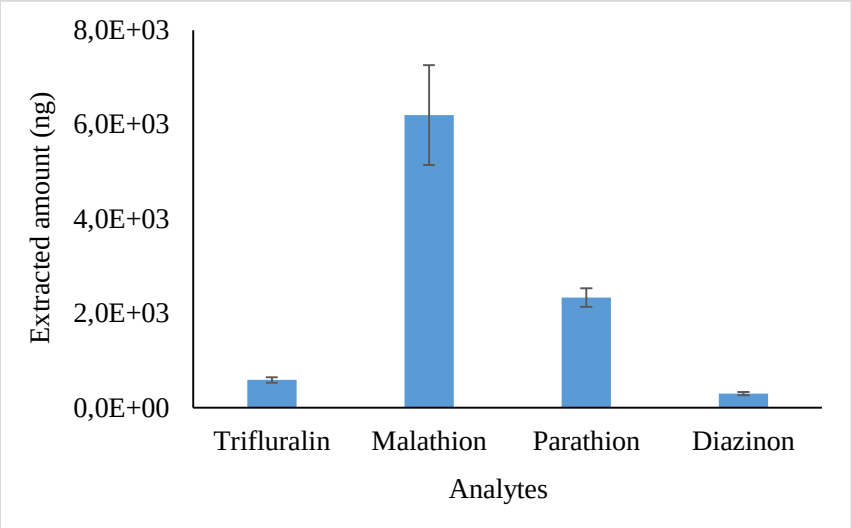

Figure 3.8. Evaluation of extraction reproducibility for trifluralin, malathion, parathion, and diazinon using fifteen samplers used for the first time (Extraction conditions; sample matrix: UPW, analyte concentration: 500.0 ng/mL malathion, parathion, and diazinon and 200.0 ng/mL trifluralin, sample volume: 20.0 mL, extraction time: 120 min, agitation speed: 1000 rpm, desorption solvent: MeOH, desorption volume: 0.5 mL, desorption time: 60 min, agitation speed: 1000 rpm)

From Figure 3.8 it is clear that careful use of the samplers can significantly reduce the standard deviation of the extraction results. Accordingly, the relative standard deviation of the analytes trifluralin, malathion, parathion, and diazinon was 9%, 17%, 8%, and 11%, respectively. However, due to the ease of damage, for future studies, it was decided to consider these samplers as single-use devices.

3.3.4 Optimization of the Desorption Time

Desorption time was investigated to find the shortest time that provides complete desorption of analytes as described in Section 3.2.5. Obtained results of the study are shown in Figure 3.9.

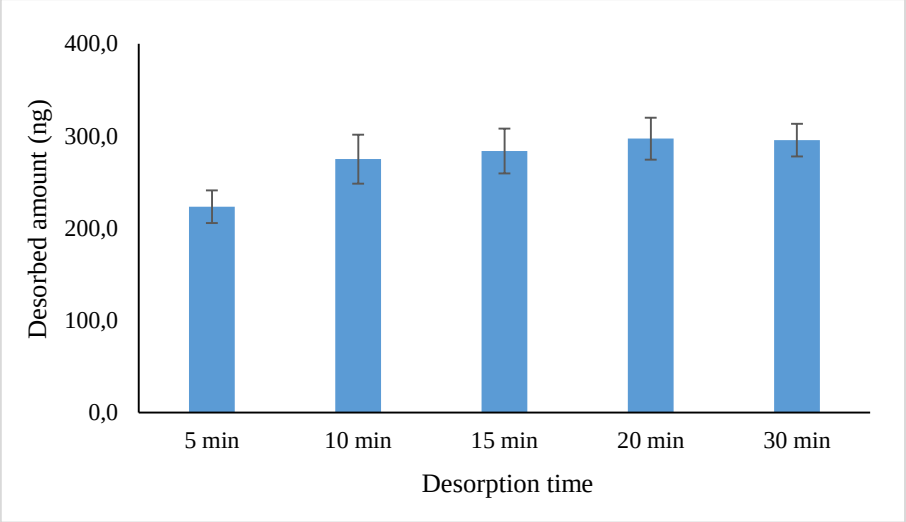

(a)

Figure 3.9. Effect of desorption time on the desorbed amount of a) trifluralin, b) malathion, c) parathion, and d) diazinon (Extraction conditions; sample matrix: UPW, analyte concentration: 500.0 ng/mL malathion, parathion, and diazinon and 200.0 ng/mL trifluralin, sample volume: 20.0 mL, extraction time: 120 min, agitation speed: 1000 rpm, desorption solvent: MeOH, desorption volume: 0.5 mL, agitation speed: 1000 rpm)

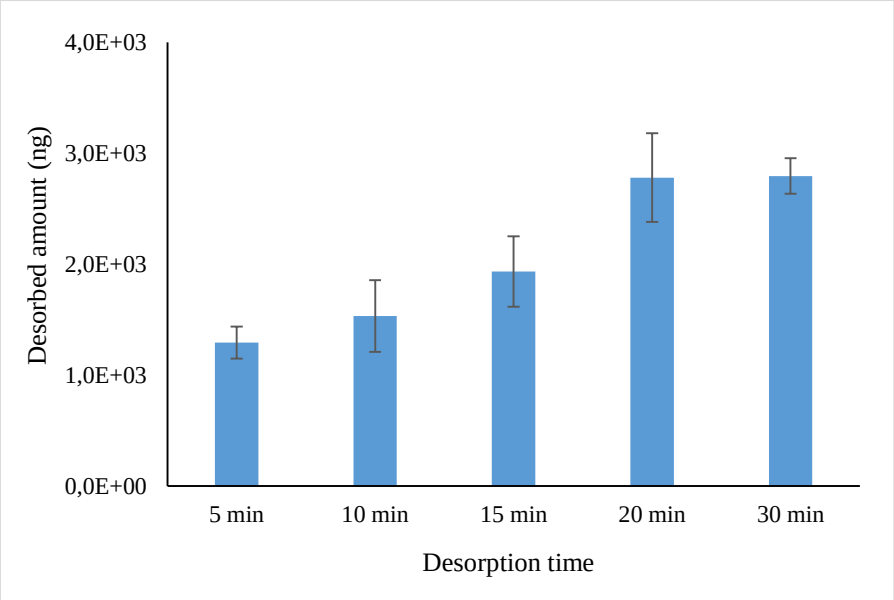

(b)

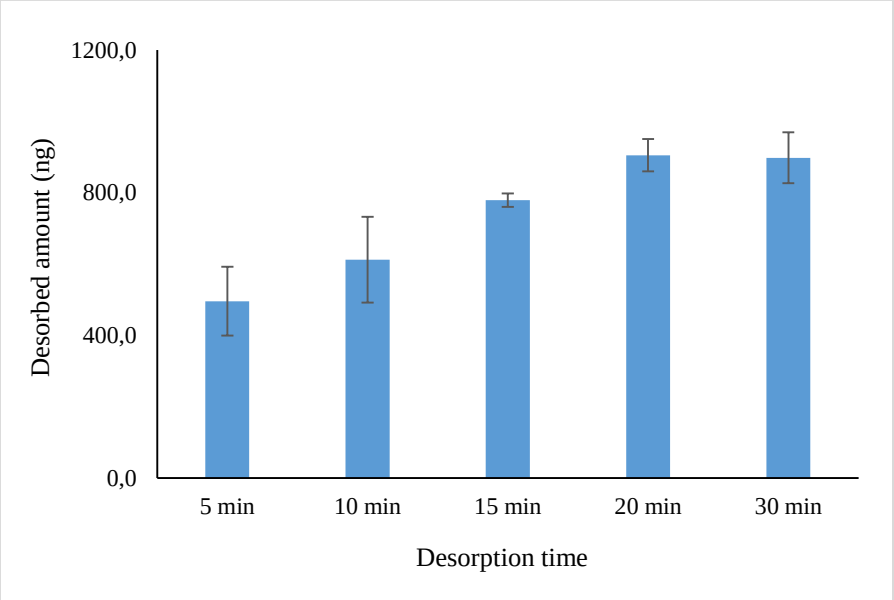

(c)

Figure 3.9. (cont'd) Effect of desorption time on the desorbed amount of a) trifluralin, b) malathion, c) parathion, and d) diazinon (Extraction conditions; sample matrix: UPW, analyte concentration: 500.0 ng/mL malathion, parathion, and diazinon and 200.0 ng/mL trifluralin, sample volume: 20.0 mL, extraction time: 120 min, agitation speed: 1000 rpm, desorption solvent: MeOH, desorption volume: 0.5 mL, agitation speed: 1000 rpm)

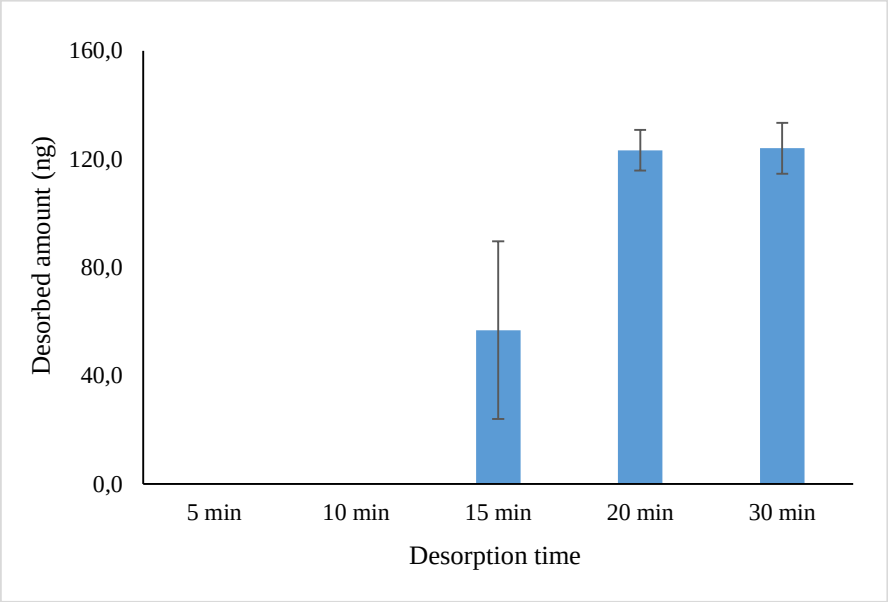

(d)

Figure 3.9. (cont'd) Effect of desorption time on the desorbed amount of a) trifluralin, b) malathion, c) parathion, and d) diazinon (Extraction conditions; sample matrix: UPW, analyte concentration: 500.0 ng/mL malathion, parathion, and diazinon and 200.0 ng/mL trifluralin, sample volume: 20.0 mL, extraction time: 120 min, agitation speed: 1000 rpm, desorption solvent: MeOH, desorption volume: 0.5 mL, agitation speed: 1000 rpm)

As given in Figure 3.9, the nanofibrous structure of samplers provided fast desorption kinetics reaching a plateau between 10 to 20 minutes. For instance, there is a statistically significant difference (95% CL) in desorbed amounts between 15 and 20 minutes for malathion, parathion, and diazinon but not for comparison of 20- and 30-minute desorption. In the case of trifluralin, maximum desorption was achieved in a shorter time (10 minutes) compared to the other compounds, as no significant differences were observed between 10 and 15 minutes of desorption. In the case of diazinon, the first two desorption points did not show any peaks, which

may indicate insufficient instrumental sensitivity or slower desorption compared to other analytes. Considering all compounds together, the maximum desorption with the shortest time was obtained at 20 minutes of desorption time, which was considered the optimum desorption time for further tests.

3.3.5 Effect of Nanofibrous Surface of the Samplers on Extraction Kinetics

The extraction kinetics of new samplers were investigated by evaluation of initial extraction kinetics for the selected analytes using 30 s, 1 min, 2 min, 3 min, 5 min, and 10 min as extraction time in the extraction method described in Section 3.2.6. The extraction time profiles obtained with optimized parameters are shown in Figure 3.10.

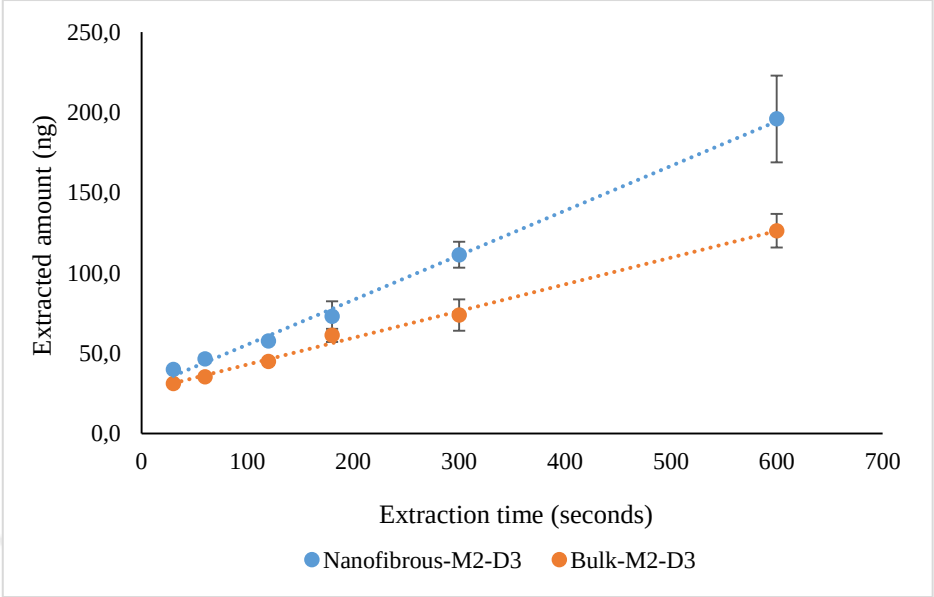

(a)

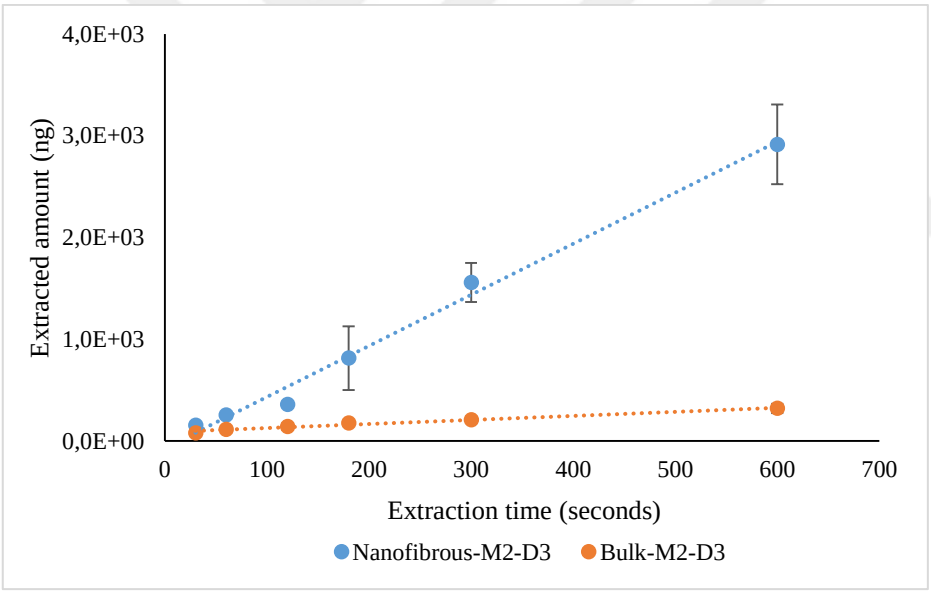

(b)

Figure 3.10. Evaluation of extraction kinetics for a) trifluralin, b) malathion, c) parathion, and d) diazinon using nanofibrous-M2-D3 and bulk-M2-D3 (Extraction conditions; sample matrix: UPW, analyte concentration: 500.0 ng/mL malathion, parathion, and diazinon and 200.0 ng/mL trifluralin, sample volume: 20.0 mL, extraction time: 120 min, agitation speed: 1000 rpm, desorption solvent: MeOH, desorption volume: 0.5 mL, desorption time: 20 min, agitation speed: 1000 rpm)

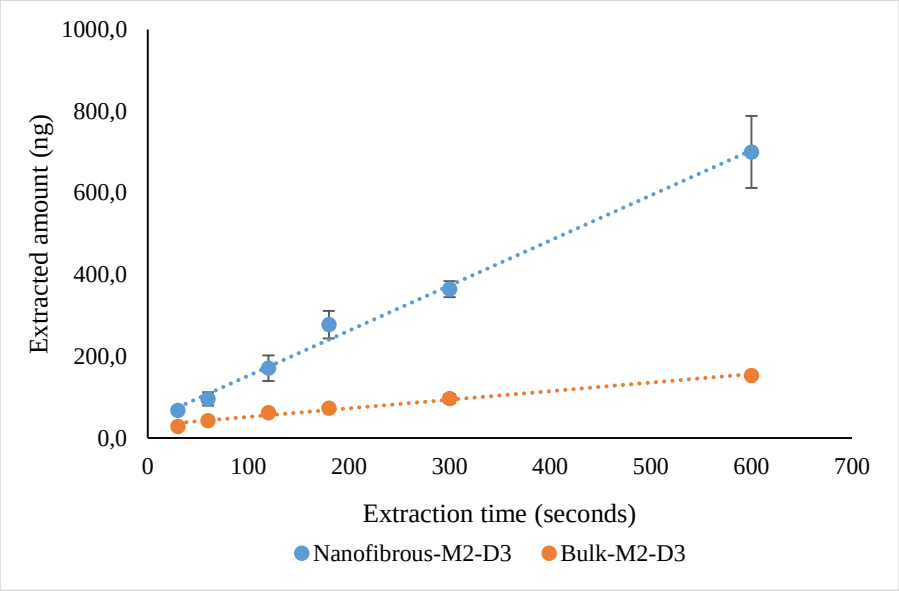

(c)

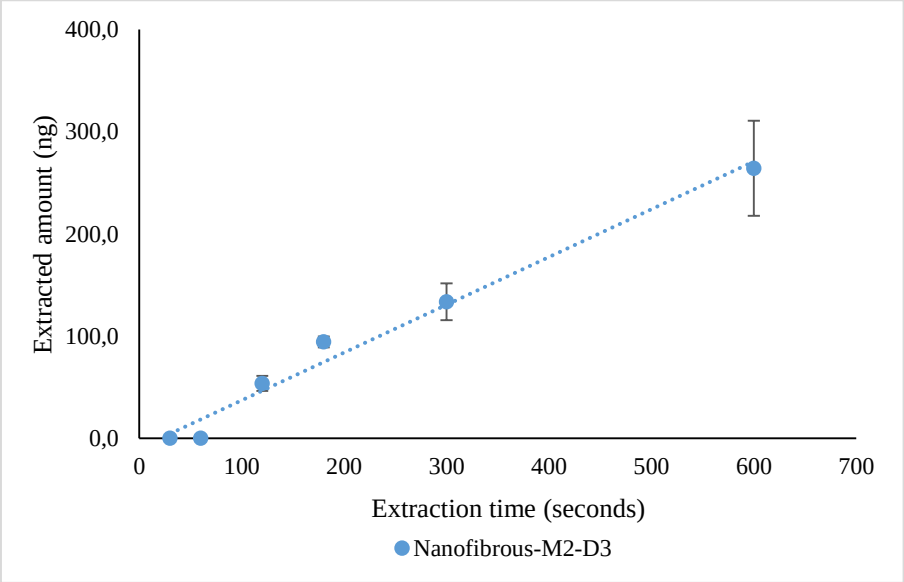

(d)

Figure 3.10. (cont'd) Evaluation of extraction kinetics for a) trifluralin, b) malathion, c) parathion, and d) diazinon using nanofibrous-M2-D3 and bulk-M2-D3 (Extraction conditions; sample matrix: UPW, analyte concentration: 500.0 ng/mL malathion, parathion, and diazinon and 200.0 ng/mL trifluralin, sample volume: 20.0 mL, extraction time: 120 min, agitation speed: 1000 rpm, desorption solvent: MeOH, desorption volume: 0.5 mL, desorption time: 20 min, agitation speed: 1000 rpm)

As given in Figure 3.10, the extractions showed a linear increase for all analytes when electrospun-coated (nanofibrous) samplers were used. Figure 3.10 clearly shows that all the nanofibrous samplers achieved faster extraction kinetics than the samplers containing bulk polymer extractive phases. Moreover, this kinetic enhancement of extraction was less pronounced for trifluralin while the difference was dramatic for the rest of the analytes. In the case of diazinon, no analyte peaks were observed with bulk-coated samplers at the tested time interval. This can be associated with low instrumental sensitivity, low analyte affinity for the extractive phase, or low extraction kinetics.

One reason for the faster extraction kinetics observed with nanofibrous samplers may be attributed to the fact that electrospun coatings have a much higher surface area/volume ratio and correspondingly larger number of adsorption sites. Another reason is radial diffusion which happens in samplers with a diameter smaller than 25 μm (Bard et al. [156]). This unique property, absent in bulk materials, means that each electrospun nanofiber acts as an independent nanoscale sampler. As a result, it was concluded that the amount of analytes obtained with Bulk-M2-D3 samplers could be obtained in much shorter times with Nanofibrous-M2-D3 samplers, clearly indicating the advantage of the new samplers.

3.3.6 Comparison of Extraction Kinetics Under Static and Stirring Conditions

In addition to kinetic studies performed in the previous part, the extraction kinetics were evaluated under static extraction conditions to see if the kinetic advantage of the nanofibrous structure is also valid under the static conditions as many cases require the use of static extraction/sampling. The extraction results of the study are shown in Figure 3.11.

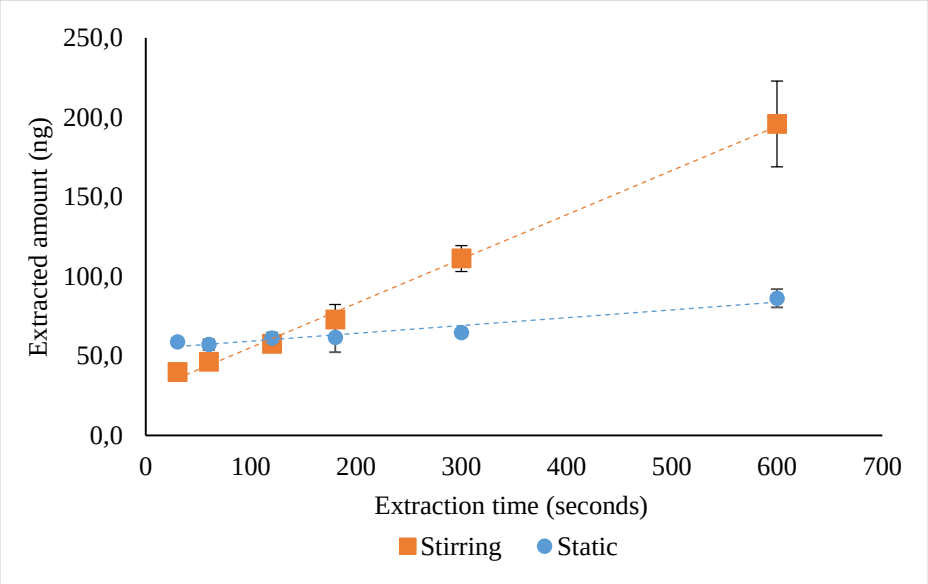

(a)

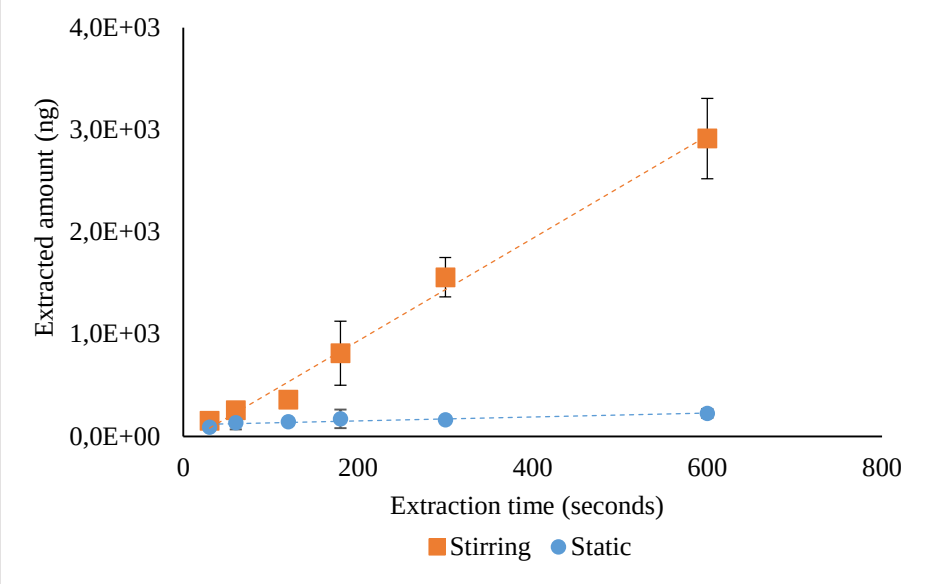

(b)

Figure 3.11. Evaluation of extraction kinetics for a) trifluralin, b) malathion, c) parathion, and d) diazinon with static and stirring conditions (Extraction conditions; sample matrix: UPW, analyte concentration: 500.0 ng/mL malathion, parathion, and diazinon and 200.0 ng/mL trifluralin, sample volume: 20.0 mL, extraction time: 120 min, agitation speed: 1000 rpm, desorption solvent: MeOH, desorption volume: 0.5 mL, desorption time: 20 min, agitation speed: 1000 rpm)

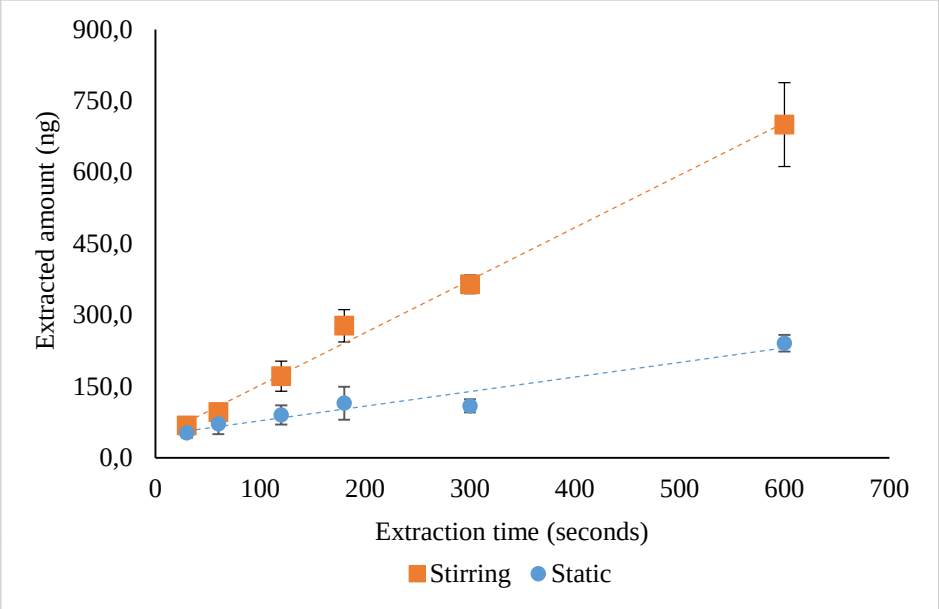

(c)

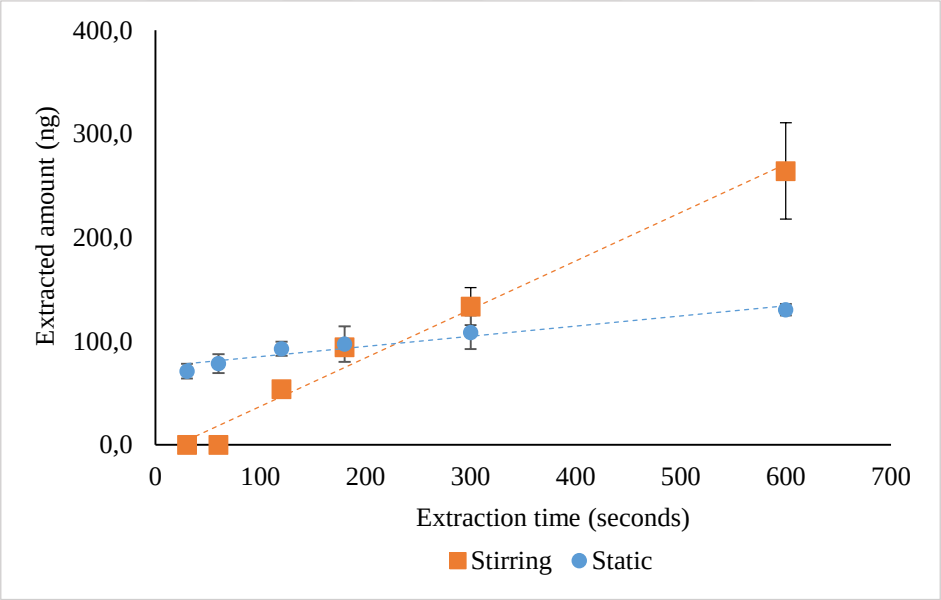

(d)

Figure 3.11. Evaluation of extraction kinetics for a) trifluralin, b) malathion, c) parathion, and d) diazinon with static and stirring conditions (Extraction conditions; sample matrix: UPW, analyte concentration: 500.0 ng/mL malathion, parathion, and diazinon and 200.0 ng/mL trifluralin, sample volume: 20.0 mL, extraction time: 120 min, agitation speed: 1000 rpm, desorption solvent: MeOH, desorption volume: 0.5 mL, desorption time: 20 min, agitation speed: 1000 rpm)

As depicted in Figure 3.11, all extraction kinetic profiles show linear trends. In addition, stirring extractions can extract larger amounts of analytes as the extraction time increases. Exceptionally, in trifluralin and diazinon, more analytes were extracted in static conditions in extractions lasting less than approximately 100 and 250 seconds, respectively. In addition, analyte recoveries were also achieved under static conditions, albeit with less extraction than under agitation. This shows that satisfactory results can be obtained with fast extraction kinetics in both stirring and static conditions.

3.4 Summary and Conclusion

Among coating methods, electrospinning is one of the most promising due to its unique characteristics. Coatings with desired fiber diameters can be produced via controllable parameters of electrospinning such as applied voltage, distance between the syringe and the collector, flow rate, and viscosity of the polymer. When an extractive polymer that is insoluble in water and other common solvents acquired in chromatography is used for electrospinning it is possible to convert the resulting mat to an extractive sampler. Moreover, various functional materials can be immobilized within the polymeric fibrous structure. Furthermore, the nanofibrous structure of the coatings obtained using electrospinning enables to obtain rapid extraction kinetics which is critical to complete the analytical process in the shortest time possible. However, a significant limitation of this technique is its sensitivity to even minor alterations in environmental conditions, which can significantly impact the electrospinning process. This complicates the reproducibility of the coating fabrication, particularly for the thinner coatings and microextraction applications where the volume of extractive phase is one of the most significant parameters to control the extracted amount of analytes.

In this study, a novel electrospinning method was proposed for producing thinner coatings with fast extraction and desorption kinetics without sacrificing the reproducibility of extraction. The novel method provides a simpler and highly effective alternative to conventional syringe electrospinning. In this technique, in contrast to conventional electrospinning which utilizes electrospinning from a polymer-filled syringe by continuous feeding, a blade that has only a drop of polymer solution is used for electrospinning. The proposed method enables more precise coating on a smaller surface area while evading the sensitivity of conventional electrospinning to environmental factors. Consequently, the method facilitates the reproducible and consistent production of homogeneous and ultrathin fibrous coatings with fast extraction and desorption kinetics.

In this study, novel TFME samplers were fabricated by immobilization of PDVB nanoparticles within PAN matrix using single-drop static blade electrospinning. The synthesis of PDVB nanoparticles was conducted via a modified mini-emulsion polymerization process based on the procedure described by Migenda et al. [159]. Afterwards, coating solutions were prepared for electrospinning, with the PDVB: PAN concentrations of 1:4, 1:2, and 1:1 (w/w). Subsequently, 0.44 g of these solutions were diluted by the addition of 100, 300, and 500 µL of DMF to 300 µL of coating solutions, thereby enhancing their electrospinnability. Following the electrospinning process, the most homogeneous coatings were obtained with the 300 µL DMF-diluted polymer solution. Electrospinning parameters were optimized by testing applied voltages of 5.0, 10.0, and 15.0 kV (and fine-tuning was applied around these values) and distances of 8.0, 10.0, and 15.0 cm between the blade tip and collector to determine optimum values for coating. Consequently, 8.0 kV and 10.4 cm were determined to be the optimum parameters.

The evaluation of the samplers in TFME format was conducted with a selection of four pesticides that are commonly used in agricultural production, including trifluralin, malathion, parathion, and diazinon. As a first evaluation, the reproducibility of the coating method and the reusability of the samplers were evaluated. When the samplers were reused, high relative standard deviations were

observed indicating their sensitive structural integrity. The relative standard deviations (N=15) obtained for extraction of trifluralin, malathion, parathion, and diazinon with single-use devices were 9%, 17%, 8%, and 11%, respectively, indicating sufficient intra-device repeatability which can be further improved using internal standards during the sampling.

The final part of the study focused on examining the extraction kinetics of prepared new samplers by comparing them to the extraction kinetics of bulk-coated samplers made with the same PDVB-PAN slurry. The use of fibrous samplers produced by single-drop static blade electrospinning demonstrated superior extraction performance compared to samplers made by the dip-coating approach. Further comparison of extraction kinetics for both samplers under static and stirring conditions revealed that stirring conditions facilitated faster extraction kinetics at shorter extraction times. Moreover, although lower recoveries were obtained in static conditions compared to stirring, all analytes could be detected, indicating that the samplers subject to the study can be used in matrices where stirring cannot be applied.

Overall, these results indicated that the electrospinning process is crucial to obtain significant enhancement in the extracted amount of analytes. Moreover, when fast analysis of a sample must be conducted, these samplers and the developed analytical method can be the method of choice as provide high sensitivity under pre-equilibrium extraction.

CHAPTER 4

CONCLUSION

Solid phase microextraction (SPME) is a widely preferred technique due to its several advantages. These advantages are the ability to combine sampling and sample preparation, suitability for in-vivo applications, geometric flexibility, and the capacity to determine free and total concentration in the sample. The versatility of SPME is associated to the wide range of options available for the elements that comprise an SPME sampler, including the extractive phase, sampler geometry, and coating method. Currently, a variety of sampler geometries have been developed, such as fiber, thin-film, and in-tube SPME spanning its applicability in diverse research areas.

Advanced materials such as molecularly imprinted polymers (MIPs) are frequently employed as extractive phases due to their advantageous characteristics, including analyte-specific binding sites, high surface area to volume ratio, and high stability. However, MIPs also exhibit significant limitations, including insufficient specific extraction, a challenging preparation and optimization process.

In the first study of this thesis, a novel method for preparing MIP that eliminates the need for a complex synthesis process was proposed. Further, the method was applied to produce TFME samplers that could be used to selectively extract two widely used pesticides, trifluralin and carbaryl. The new MIP preparation method involved creating an electrospun nanofibrous mat by imprinting template analytes to PAN.

A four-step preparation of the SPME samplers included preparation of NIP and PMIP solutions, obtaining nanofibrous polymer mats using electrospinning technique, sandwiching polymer mats between meshes, and removing the templates from the resulting samplers. When compared to pure PAN powder, the electrospun nanofibers' enhanced crystallinity and effective template immobilization have been

confirmed. According to the optimization of sampler fabrication parameters, employment of a polymer-template ratio of 5.0 mg analyte /mL for electrospinning and the use of a sampler size with 20x5 mm dimensions achieved optimum extraction recoveries, while 10x5 mm samplers demonstrated the best selectivity. The optimized SPME parameters and obtained optimum values were a sample of pH 7.0, extraction time of 2 hours, and desorption time of 15 minutes. When compared to bulk PAN sorbent made by dip-coating approach, electrospun PMIP nanofibers demonstrated better extraction performance, by increasing trifluralin and carbaryl recoveries approximately seven and four times, respectively. Cross-selectivity experiments verified enhanced selectivity for trifluralin, while the high surface area-to-volume ratio and radial diffusion of the nanofibrous structure enabled effective analyte adsorption. These results highlight the potential for improved analyte-specific extraction using samplers based on electrospun nanofibers.

As stated in several parts of this thesis, the electrospinning method has many advantages in preparing SPME samplers. To name some of these advantages, many polymers can be electrospun, functional particles can be embedded in the continuous fibrous structure, and polymer groups can be modified to obtain functional groups with enhanced/selective analyte interactions. However, one notable disadvantage of this approach is its sensitivity to changes in ambient conditions, which can significantly limit the reproducible coating fabrication process, especially for thinner coatings.

The second study of the thesis was focused on a potential solution to this problem by introducing a novel single-drop static blade electrospinning method for fabricating ultrathin, homogeneous nanofibrous coatings for TFME applications. This approach minimizes sensitivity to ambient conditions while enabling more precise, reproducible coatings on smaller surfaces by applying a high voltage to a spray blade containing a polymer drop, in contrast to traditional syringe electrospinning in which polymer solution is continuously fed through a needle. In this study, the single-drop static blade electrospinning was used to immobilize homemade produced PDVB nanoparticles within a PAN nanofiber matrix to create

novel TFME samplers and evaluate their performances in proof-of-the concept study for extraction of pesticides from water. The most homogeneous coatings with the best extraction performance were obtained by using 0.44 g of PDVB:PAN solution (1:1, w/w) diluted with 300 μL of DMF. The optimal electrospinning parameters were determined as 8.0 kV and a blade-to-collector distance of 10.4 cm. The samplers' modest relative standard deviations (8–17%) suggested structural integrity and reproducibility of the disposable samplers. Because of their large surface area and radial diffusion, nanofibrous samplers demonstrated greater recoveries and quicker extraction kinetics than bulk polymer coatings at short extraction times. Static extraction confirmed their adaptability in different sampling scenarios by enabling sufficient analyte recovery under no stirring conditions, whereas stirring conditions substantially improved extraction efficiency.

REFERENCES

[1] H. Kataoka and K. Saito, 'Recent advances in SPME techniques in biomedical analysis', *J Pharm Biomed Anal*, vol. 54, no. 5, pp. 926–950, 2011, doi: https://doi.org/10.1016/j.jpba.2010.12.010.

[2] W. Filipiak and B. Bojko, 'SPME in clinical, pharmaceutical, and biotechnological research – How far are we from daily practice?', *TrAC Trends in Analytical Chemistry*, vol. 115, pp. 203–213, 2019, doi: https://doi.org/10.1016/j.trac.2019.02.029.

[3] G. Ouyang and J. Pawliszyn, 'SPME in environmental analysis', *Anal Bioanal Chem*, vol. 386, no. 4, pp. 1059–1073, 2006, doi: 10.1007/s00216-006-0460-z.

[4] M. Llompart, M. Celeiro, C. García-Jares, and T. Dagnac, 'Environmental applications of solid-phase microextraction', *TrAC Trends in Analytical Chemistry*, vol. 112, pp. 1–12, 2019, doi: https://doi.org/10.1016/j.trac.2018.12.020.

[5] H. Kataoka, H. L. Lord, and J. Pawliszyn, 'Applications of solid-phase microextraction in food analysis', *J Chromatogr A*, vol. 880, no. 1, pp. 35–62, 2000, doi: https://doi.org/10.1016/S0021-9673(00)00309-5.

[6] S. Balasubramanian and S. Panigrahi, 'Solid-Phase Microextraction (SPME) Techniques for Quality Characterization of Food Products: A Review', *Food Bioproc Tech*, vol. 4, no. 1, pp. 1–26, 2011, doi: 10.1007/s11947-009-0299-3.

[7] A. Menezes Filho, F. N. dos Santos, and P. A. de Paula Pereira, 'Development, validation and application of a methodology based on solid-phase micro extraction followed by gas chromatography coupled to mass spectrometry (SPME/GC–MS) for the determination of pesticide residues in mangoes',

Talanta, vol. 81, no. 1, pp. 346–354, 2010, doi: https://doi.org/10.1016/j.talanta.2009.12.008.

[8] J. Beltran, A. Peruga, E. Pitarch, F. J. López, and F. Hernández, 'Application of solid-phase microextraction for the determination of pyrethroid residues in vegetable samples by GC-MS', *Anal Bioanal Chem*, vol. 376, no. 4, pp. 502–511, 2003, doi: 10.1007/s00216-003-1916-z.

[9] J. Zheng *et al.*, 'Detection of bile acids in small volume human bile samples via an amino metal-organic framework composite based solid-phase microextraction probe', *J Chromatogr A*, vol. 1685, p. 463634, 2022, doi: https://doi.org/10.1016/j.chroma.2022.463634.

[10] M. Ghorbani, M. Keshavarzi, M. Pakseresht, P. Mohammadi, M. Ojaghzadeh Khalil Abad, and A. Mehraban, 'Advancements, Applications, and prospects of Metal-Organic frameworks and their derivatives as distinct sorbents in exhaustive and non-exhaustive extraction strategies', *Microchemical Journal*, vol. 198, p. 110158, 2024, doi: https://doi.org/10.1016/j.microc.2024.110158.

[11] W. Guo, H. Tao, H. Tao, Q. Shuai, and L. Huang, 'Recent progress of covalent organic frameworks as attractive materials for solid-phase microextraction: A review', *Anal Chim Acta*, vol. 1287, p. 341953, 2024, doi: https://doi.org/10.1016/j.aca.2023.341953.

[12] J. Yuan *et al.*, 'In-situ growth of covalent organic framework on stainless steel needles as solid-phase microextraction probe coupled with electrospray ionization mass spectrometry for rapid and sensitive determination of tricyclic antidepressants in biosamples', *J Chromatogr A*, vol. 1695, p. 463955, 2023, doi: https://doi.org/10.1016/j.chroma.2023.463955.

[13] T. D. Ho, A. J. Canestraro, and J. L. Anderson, 'Ionic liquids in solid-phase microextraction: A review', *Anal Chim Acta*, vol. 695, no. 1, pp. 18–43, 2011, doi: https://doi.org/10.1016/j.aca.2011.03.034.

[14] Z. Liu, W. Zhou, C. Wang, W. Hu, and Z. Chen, ‘Cotton thread modified with ionic liquid copolymerized polymer for online in-tube solid-phase microextraction and HPLC analysis of nonsteroidal anti-inflammatory drugs’, *J Sep Sci*, vol. 43, no. 14, pp. 2827–2833, Jul. 2020, doi: https://doi.org/10.1002/jssc.202000212.

[15] F. Shahhoseini, A. Azizi, and C. S. Bottaro, ‘A critical evaluation of molecularly imprinted polymer (MIP) coatings in solid phase microextraction devices’, *TrAC Trends in Analytical Chemistry*, vol. 156, p. 116695, 2022, doi: https://doi.org/10.1016/j.trac.2022.116695.

[16] M. Rahimi and S. Bahar, ‘Preparation of a New Solid-Phase Microextraction Fiber Based on Molecularly Imprinted Polymers for Monitoring of Phenobarbital in Urine Samples’, *J Chromatogr Sci*, vol. 61, no. 1, pp. 87–95, Jan. 2023, doi: 10.1093/chromsci/bmac001.

[17] G. Vasapollo *et al.*, ‘Molecularly imprinted polymers: Present and future prospective’, Sep. 2011. doi: 10.3390/ijms12095908.

[18] Y. Chen, Z. Guo, X. Wang, and C. Qiu, ‘Sample preparation’, Mar. 14, 2008. doi: 10.1016/j.chroma.2007.10.026.

[19] J. Pawliszyn, ‘Theory of Extraction’, in *Handbook of Sample Preparation*, John Wiley and Sons, 2011, pp. 1–24. doi: 10.1002/9780813823621.ch1.

[20] P. L. Buldini, L. Ricci, and J. L. Sharma, ‘R ecent applications of sample preparation techniques in food analysis’, 2002. [Online]. Available: www.elsevier.com/locate/chroma

[21] M. Ibourki, O. Hallouch, K. Devkota, D. Guillaume, A. Hirich, and S. Gharby, ‘Elemental analysis in food: An overview’, Jul. 01, 2023, *Academic Press Inc.* doi: 10.1016/j.jfca.2023.105330.

[22] M. Fairulnizal, R. D. N. Gunasegavan, N. M. Khalid, V. Balasubramaniam, S. Mustar, and A. A. Rashed, ‘Recent techniques in nutrient analysis for food

composition database', Oct. 01, 2020, *MDPI AG*. doi: 10.3390/molecules25194567.

[23] V. Lopez-Avila, 'Sample preparation for environmental analysis', 1999, *CRC Press Inc*. doi: 10.1080/10408349891199392.

[24] C. Ribeiro, A. R. Ribeiro, A. S. Maia, V. M. F. Gonçalves, and M. E. Tiritan, 'New Trends in Sample Preparation Techniques for Environmental Analysis', *Crit Rev Anal Chem*, vol. 44, no. 2, pp. 142–185, 2014, doi: 10.1080/10408347.2013.833850.

[25] M. Nasiri, H. Ahmadzadeh, and A. Amiri, 'Sample preparation and extraction methods for pesticides in aquatic environments: A review', Feb. 01, 2020, *Elsevier B.V.* doi: 10.1016/j.trac.2019.115772.

[26] L. Wu, R. Sun, Y. Li, and C. Sun, 'Sample preparation and analytical methods for polycyclic aromatic hydrocarbons in sediment', Oct. 01, 2019, *Elsevier B.V.* doi: 10.1016/j.teac.2019.e00074.

[27] C. Devos, M. Vliegen, B. Willaert, F. David, L. Moens, and P. Sandra, 'Automated headspace-solid-phase micro extraction-retention time locked-isotope dilution gas chromatography-mass spectrometry for the analysis of organotin compounds in water and sediment samples', *J Chromatogr A*, vol. 1079, no. 1-2 SPEC. ISS., pp. 408–414, Jun. 2005, doi: 10.1016/j.chroma.2004.12.020.

[28] Á. I. López-Lorente, F. Pena-Pereira, S. Pedersen-Bjergaard, V. G. Zuin, S. A. Ozkan, and E. Psillakis, 'The ten principles of green sample preparation', Mar. 01, 2022, *Elsevier B.V.* doi: 10.1016/j.trac.2022.116530.

[29] H. Kataoka and H. L. Lord, 'Sampling and sample preparation for clinical and pharmaceutical analysis', 2002.

[30] S. Yıldırım, C. Erkmen, and B. Uslu, 'Novel Trends in Analytical Methods for β-Blockers: An Overview of Applications in the Last Decade', 2020, *Taylor and Francis Ltd.* doi: 10.1080/10408347.2020.1791043.

[31] J. L. Luque-Garcia and T. A. Neubert, 'Sample preparation for serum/plasma profiling and biomarker identification by mass spectrometry', Jun. 15, 2007. doi: 10.1016/j.chroma.2006.11.054.

[32] X. Chen, X. Wu, T. Luan, R. Jiang, and G. Ouyang, 'Sample preparation and instrumental methods for illicit drugs in environmental and biological samples: A review', *J Chromatogr A*, vol. 1640, Mar. 2021, doi: 10.1016/j.chroma.2021.461961.

[33] A. Kabir, H. Holness, K. G. Furton, and J. R. Almirall, 'Recent advances in micro-sample preparation with forensic applications', 2013, *Elsevier B.V.* doi: 10.1016/j.trac.2012.11.013.

[34] B. J. Pollo, G. L. Alexandrino, F. Augusto, and L. W. Hantao, 'The impact of comprehensive two-dimensional gas chromatography on oil & gas analysis: Recent advances and applications in petroleum industry', Aug. 01, 2018, *Elsevier B.V.* doi: 10.1016/j.trac.2018.05.007.

[35] S. Linnarsson, 'Recent advances in DNA sequencing methods - general principles of sample preparation', 2010, *Academic Press Inc.* doi: 10.1016/j.yexcr.2010.02.036.

[36] D. Vuckovic, 'Current trends and challenges in sample preparation for global metabolomics using liquid chromatography-mass spectrometry', Jun. 2012. doi: 10.1007/s00216-012-6039-y.

[37] P. J. Schoenmakers, 'Editorial on "Critical overview of selected contemporary sample preparation techniques" by L. Ramos', Jan. 20, 2012. doi: 10.1016/j.chroma.2011.12.026.

[38] Luigi. Mondello, Janusz. Pawliszyn, and Paola. Dugo, *Comprehensive sampling and sample preparation : analytical techniques for scientists. Vol. 4, Extraction techniques and applications : food and beverage*. Elsevier, 2012.

[39] H. Kurosaki, S. M. L. Asbury, J. D. Navatril, and S. B. Clark, 'Flow-through sequential extraction approach developed from a batch extraction method', *Environ Sci Technol*, vol. 36, no. 22, pp. 4880–4885, Nov. 2002, doi: 10.1021/es020653a.

[40] R. D. McDowall, 'SAMPLE HANDLING | Automated Sample Preparation', in *Encyclopedia of Analytical Science (Second Edition)*, P. Worsfold, A. Townshend, and C. Poole, Eds., Oxford: Elsevier, 2005, pp. 177–183. doi: https://doi.org/10.1016/B0-12-369397-7/00542-2.

[41] G. Ouyang and J. Pawliszyn, 'A critical review in calibration methods for solid-phase microextraction', Oct. 10, 2008. doi: 10.1016/j.aca.2008.08.015.

[42] Y. Di Feng, Z. Q. Tan, and J. F. Liu, 'Development of a static and exhaustive extraction procedure for field passive preconcentration of chlorophenols in environmental waters with hollow fiber-supported liquid membrane', *J Sep Sci*, vol. 34, no. 8, pp. 965–970, Apr. 2011, doi: 10.1002/jssc.201000775.

[43] R. E. Majors, 'Solid-Phase Extraction', in *Handbook of Sample Preparation*, John Wiley and Sons, 2011, pp. 53–79. doi: 10.1002/9780813823621.ch4.

[44] C. F. Poole, 'New trends in solid-phase extraction', Jun. 01, 2003, *Elsevier*. doi: 10.1016/S0165-9936(03)00605-8.

[45] 'Solid Phase Extraction Technique - Trends, Opportunities and Applications', *Pol J Environ Stud*, vol. 15, no. 5, pp. 677–690, 2006, [Online]. Available: https://www.pjoes.com/Solid-Phase-Extraction-Technique-Trends-Opportunities-and-Applications,87920,0,2.html

[46] W. B. Jensen and J. Andraos, ‘The Origin of the Soxhlet Extractor Question What is the origin of the Soxhlet extractor?’, 2007. [Online]. Available: www.JCE.DivCHED.org

[47] M. D. Luque de Castro and F. Priego-Capote, ‘Soxhlet extraction: Past and present panacea’, Apr. 2010. doi: 10.1016/j.chroma.2009.11.027.

[48] M. A. López-Bascón-Bascon and M. D. Luque de Castro, ‘Soxhlet extraction’, in *Liquid-Phase Extraction*, Elsevier, 2019, pp. 327–354. doi: 10.1016/B978-0-12-816911-7.00011-6.

[49] J. L. Luque-García and M. D. Luque De Castro, ‘Ultrasound-assisted Soxhlet extraction: An expeditive approach for solid sample treatment - Application to the extraction of total fat from oleaginous seeds’, *J Chromatogr A*, vol. 1034, no. 1–2, pp. 237–242, Apr. 2004, doi: 10.1016/j.chroma.2004.02.020.

[50] L. E. García-Ayuso and M. D. Luque de Castro, ‘A multivariate study of the performance of a microwave-assisted Soxhlet extractor for olive seeds’, *Anal Chim Acta*, vol. 382, no. 3, pp. 309–316, 1999, doi: https://doi.org/10.1016/S0003-2670(98)00795-8.

[51] C. L. Arthur and Janusz. Pawliszyn, ‘Solid phase microextraction with thermal desorption using fused silica optical fibers’, *Anal Chem*, vol. 62, no. 19, pp. 2145–2148, Oct. 1990, doi: 10.1021/ac00218a019.

[52] S. Risticevic, D. Vuckovic, and J. Pawliszyn, ‘Solid-Phase Microextraction’, in *Handbook of Sample Preparation*, 2010, pp. 81–101. doi: https://doi.org/10.1002/9780813823621.ch5.

[53] H. Lord and J. Pawliszyn, ‘Microextraction of drugs’, *J Chromatogr A*, vol. 902, no. 1, pp. 17–63, 2000, doi: https://doi.org/10.1016/S0021-9673(00)00836-0.

[54] K. Walsh, E. Vidal, and B. Mishra, ‘Thermodynamics of Extraction’, 2009, pp. 55–64. doi: 10.31399/asm.tb.bcp.t52230055.

[55] J. Pawliszyn and L. Müller, ‘Field analysis by SPME’, in *Applications of Solid Phase Microextraction*, J. Pawliszyn, Ed., The Royal Society of Chemistry, 1999, p. 0. doi: 10.1039/9781847550149-00269.

[56] L. Kudlejova, S. Risticevic, and D. Vuckovic, ‘7 - Solid-Phase Microextraction Method Development’, in *Handbook of Solid Phase Microextraction*, J. Pawliszyn, Ed., Oxford: Elsevier, 2012, pp. 201–249. doi: https://doi.org/10.1016/B978-0-12-416017-0.00007-3.

[57] D. Fiorini, D. Pacetti, R. Gabbianelli, S. Gabrielli, and R. Ballini, ‘A salting out system for improving the efficiency of the headspace solid-phase microextraction of short and medium chain free fatty acids’, *J Chromatogr A*, vol. 1409, pp. 282–287, 2015, doi: https://doi.org/10.1016/j.chroma.2015.07.051.

[58] S. Risticevic, D. Vuckovic, H. L. Lord, and J. Pawliszyn, ‘2.21 - Solid-Phase Microextraction’, in *Comprehensive Sampling and Sample Preparation*, J. Pawliszyn, Ed., Oxford: Academic Press, 2012, pp. 419–460. doi: https://doi.org/10.1016/B978-0-12-381373-2.00055-7.

[59] A. B. Deger, T. J. Gremm, F. H. Frimmel, and L. Mendez, ‘Optimization and application of SPME for the gas chromatographic determination of endosulfan and its major metabolites in the ng L−1 range in aqueous solutions’, *Anal Bioanal Chem*, vol. 376, no. 1, pp. 61–68, 2003, doi: 10.1007/s00216-003-1855-8.

[60] N. Manousi, E. Rosenberg, and G. A. Zachariadis, ‘Solid-phase microextraction arrow for the sampling of volatile organic compounds in milk samples’, *Separations*, vol. 7, no. 4, pp. 1–12, Dec. 2020, doi: 10.3390/separations7040075.

[61] L. Kudlejova, S. Risticevic, and D. Vuckovic, ‘7 - Solid-Phase Microextraction Method Development’, in *Handbook of Solid Phase*

Microextraction, J. Pawliszyn, Ed., Oxford: Elsevier, 2012, pp. 201–249. doi: https://doi.org/10.1016/B978-0-12-416017-0.00007-3.

[62] G. Ouyang and J. Pawliszyn, 'A critical review in calibration methods for solid-phase microextraction', *Anal Chim Acta*, vol. 627, no. 2, pp. 184–197, 2008, doi: https://doi.org/10.1016/j.aca.2008.08.015.

[63] H. Piri-Moghadam, Md. N. Alam, and J. Pawliszyn, 'Review of geometries and coating materials in solid phase microextraction: Opportunities, limitations, and future perspectives', *Anal Chim Acta*, vol. 984, pp. 42–65, 2017, doi: https://doi.org/10.1016/j.aca.2017.05.035.

[64] H. Kataoka, 'Chapter 1 - Sample preparation for liquid chromatography', in *Liquid Chromatography (Second Edition)*, S. Fanali, P. R. Haddad, C. F. Poole, and M.-L. Riekkola, Eds., Elsevier, 2017, pp. 1–37. doi: https://doi.org/10.1016/B978-0-12-805392-8.00001-3.

[65] H. Lord and J. Pawliszyn, 'Evolution of solid-phase microextraction technology', *J Chromatogr A*, vol. 885, no. 1, pp. 153–193, 2000, doi: https://doi.org/10.1016/S0021-9673(00)00535-5.

[66] Y. A. Olcer, M. Tascon, A. E. Eroglu, and E. Boyacı, 'Thin film microextraction: Towards faster and more sensitive microextraction', *TrAC Trends in Analytical Chemistry*, vol. 113, pp. 93–101, 2019, doi: https://doi.org/10.1016/j.trac.2019.01.022.

[67] F. S. Mirnaghi and J. Pawliszyn, 'Development of coatings for automated 96-blade solid phase microextraction-liquid chromatography–tandem mass spectrometry system, capable of extracting a wide polarity range of analytes from biological fluids', *J Chromatogr A*, vol. 1261, pp. 91–98, 2012, doi: https://doi.org/10.1016/j.chroma.2012.07.012.

[68] J. Ríos-Gómez, R. Lucena, and S. Cárdenas, 'Paper supported polystyrene membranes for thin film microextraction', *Microchemical Journal*, vol. 133, pp. 90–95, 2017, doi: https://doi.org/10.1016/j.microc.2017.03.026.

[69] J. J. Grandy, E. Boyacı, and J. Pawliszyn, ‘Development of a Carbon Mesh Supported Thin Film Microextraction Membrane As a Means to Lower the Detection Limits of Benchtop and Portable GC/MS Instrumentation’, *Anal Chem*, vol. 88, no. 3, pp. 1760–1767, Feb. 2016, doi: 10.1021/acs.analchem.5b04008.

[70] H. Kataoka, ‘Spme Techniques for Biomedical Analysis’, *Bioanalysis*, vol. 7, no. 17, pp. 2135–2144, Sep. 2015, doi: 10.4155/bio.15.145.

[71] B. J. G. Silva, F. M. Lanças, and M. E. C. Queiroz, ‘In-tube solid-phase microextraction coupled to liquid chromatography (in-tube SPME/LC) analysis of nontricyclic antidepressants in human plasma’, *Journal of Chromatography B*, vol. 862, no. 1, pp. 181–188, 2008, doi: https://doi.org/10.1016/j.jchromb.2007.12.006.

[72] Y. Moliner-Martinez, R. Herráez-Hernández, J. Verdú-Andrés, C. Molins-Legua, and P. Campíns-Falcó, ‘Recent advances of in-tube solid-phase microextraction’, *TrAC Trends in Analytical Chemistry*, vol. 71, pp. 205–213, 2015, doi: https://doi.org/10.1016/j.trac.2015.02.020.

[73] R. E. Shirey, ‘4 - SPME Commercial Devices and Fibre Coatings’, in *Handbook of Solid Phase Microextraction*, J. Pawliszyn, Ed., Oxford: Elsevier, 2012, pp. 99–133. doi: https://doi.org/10.1016/B978-0-12-416017-0.00004-8.

[74] R. P. Belardi and J. B. Pawliszyn, ‘The Application of Chemically Modified Fused Silica Fibers in the Extraction of Organics from Water Matrix Samples and their Rapid Transfer to Capillary Columns’, *Water Quality Research Journal*, vol. 24, no. 1, pp. 179–191, Feb. 1989, doi: 10.2166/wqrj.1989.010.

[75] Jiaqi. Wu and Janusz. Pawliszyn, ‘Dual Detection for Capillary Isoelectric Focusing with Refractive Index Gradient and Absorption Imaging Detectors’, *Anal Chem*, vol. 66, no. 6, pp. 867–873, Mar. 1994, doi: 10.1021/ac00078a018.

[76] C. L. Arthur, L. M. Killam, K. D. Buchholz, J. Pawliszyn, and J. R. Berg, ‘Automation and Optimization of Solid-Phase Microextraction’, *Anal Chem*, vol. 64, no. 17, pp. 1960–1966, 1992, doi: 10.1021/AC00041A034.

[77] N. Reyes-Garcés *et al.*, ‘Advances in Solid Phase Microextraction and Perspective on Future Directions’, *Anal Chem*, vol. 90, no. 1, pp. 302–360, Jan. 2018, doi: 10.1021/acs.analchem.7b04502.

[78] M. D. Gallidabino, K. Bylenga, S. Elliott, R. C. Irlam, and C. Weyermann, ‘Comparison of four commercial solid-phase micro-extraction (SPME) fibres for the headspace characterisation and profiling of gunshot exhausts in spent cartridge casings’, *Anal Bioanal Chem*, vol. 414, no. 17, pp. 4987–4998, 2022, doi: 10.1007/s00216-022-04129-w.

[79] L. Tuduri, V. Desauziers, and J. L. Fanlo, ‘Potential of Solid-Phase Microextraction Fibers for the Analysis of Volatile Organic Compounds in Air’, *J Chromatogr Sci*, vol. 39, no. 12, pp. 521–529, Dec. 2001, doi: 10.1093/chromsci/39.12.521.

[80] O. J. Portillo-Castillo *et al.*, ‘Developments of solid-phase microextraction fiber coatings for environmental pharmaceutical and personal care products analysis’, vol. 37, no. 2, 2018, doi: doi:10.1515/revac-2017-0018.

[81] W. M. Mullett, P. Martin, and J. Pawliszyn, ‘In-Tube Molecularly Imprinted Polymer Solid-Phase Microextraction for the Selective Determination of Propranolol’, *Anal Chem*, vol. 73, no. 11, pp. 2383–2389, Jun. 2001, doi: 10.1021/ac0100502.

[82] A. Azizi and C. S. Bottaro, ‘A critical review of molecularly imprinted polymers for the analysis of organic pollutants in environmental water samples’, *J Chromatogr A*, vol. 1614, p. 460603, 2020, doi: https://doi.org/10.1016/j.chroma.2019.460603.

[83] Z. Terzopoulou, M. Papageorgiou, G. Z. Kyzas, D. N. Bikiaris, and D. A. Lambropoulou, ‘Preparation of molecularly imprinted solid-phase

microextraction fiber for the selective removal and extraction of the antiviral drug abacavir in environmental and biological matrices', *Anal Chim Acta*, vol. 913, pp. 63–75, 2016, doi: https://doi.org/10.1016/j.aca.2016.01.059.

[84] M. M. Sanagi *et al.*, 'Molecularly imprinted polymer solid-phase extraction for the analysis of organophosphorus pesticides in fruit samples', *Journal of Food Composition and Analysis*, vol. 32, no. 2, pp. 155–161, 2013, doi: https://doi.org/10.1016/j.jfca.2013.09.001.

[85] R. Mirzajani, Z. Ramezani, and F. Kardani, 'Selective determination of thidiazuron herbicide in fruit and vegetable samples using molecularly imprinted polymer fiber solid phase microextraction with ion mobility spectrometry detection (MIPF-SPME-IMS)', *Microchemical Journal*, vol. 130, pp. 93–101, 2017, doi: https://doi.org/10.1016/j.microc.2016.08.009.

[86] Y. Lei, G. Xu, F. Wei, J. Yang, and Q. Hu, 'Preparation of a stir bar coated with molecularly imprinted polymer and its application in analysis of dopamine in urine', *J Pharm Biomed Anal*, vol. 94, pp. 118–124, 2014, doi: https://doi.org/10.1016/j.jpba.2014.01.041.

[87] C. Lancioni, C. Castells, R. Candal, and M. Tascon, 'Headspace solid-phase microextraction: Fundamentals and recent advances', *Advances in Sample Preparation*, vol. 3, p. 100035, 2022, doi: https://doi.org/10.1016/j.sampre.2022.100035.

[88] A. Martín-Esteban and B. Sellergren, '2.17 - Molecularly Imprinted Polymers', in *Comprehensive Sampling and Sample Preparation*, J. Pawliszyn, Ed., Oxford: Academic Press, 2012, pp. 331–344. doi: https://doi.org/10.1016/B978-0-12-381373-2.00046-6.

[89] A. N. Hasanah, N. Safitri, A. Zulfa, N. Neli, and D. Rahayu, 'Factors affecting preparation of molecularly imprinted polymer and methods on finding template-monomer interaction as the key of selective properties of the materials', Sep. 02, 2021, *MDPI*. doi: 10.3390/molecules26185612.

[90] E. Turiel and A. Martín-Esteban, 'Molecularly imprinted polymers for solid-phase microextraction', *J Sep Sci*, vol. 32, no. 19, pp. 3278–3284, Oct. 2009, doi: https://doi.org/10.1002/jssc.200900218.

[91] X. Hu, Y. Hu, and G. Li, 'Preparation and Characterization of Prometryn Molecularly Imprinted Solid- Phase Microextraction Fibers', *Anal Lett*, vol. 40, no. 4, pp. 645–660, Mar. 2007, doi: 10.1080/00032710600966127.

[92] X. Hu, Y. Hu, and G. Li, 'Development of novel molecularly imprinted solid-phase microextraction fiber and its application for the determination of triazines in complicated samples coupled with high-performance liquid chromatography', *J Chromatogr A*, vol. 1147, no. 1, pp. 1–9, 2007, doi: https://doi.org/10.1016/j.chroma.2007.02.037.

[93] X. Hu, J. Pan, Y. Hu, Y. Huo, and G. Li, 'Preparation and evaluation of solid-phase microextraction fiber based on molecularly imprinted polymers for trace analysis of tetracyclines in complicated samples', *J Chromatogr A*, vol. 1188, no. 2, pp. 97–107, 2008, doi: https://doi.org/10.1016/j.chroma.2008.02.062.

[94] X. Hu, J. Pan, Y. Hu, and G. Li, 'Preparation and evaluation of propranolol molecularly imprinted solid-phase microextraction fiber for trace analysis of β-blockers in urine and plasma samples', *J Chromatogr A*, vol. 1216, no. 2, pp. 190–197, 2009, doi: https://doi.org/10.1016/j.chroma.2008.11.064.

[95] B. B. Prasad, K. Tiwari, M. Singh, P. S. Sharma, A. K. Patel, and S. Srivastava, 'Molecularly imprinted polymer-based solid-phase microextraction fiber coupled with molecularly imprinted polymer-based sensor for ultratrace analysis of ascorbic acid', *J Chromatogr A*, vol. 1198–1199, pp. 59–66, 2008, doi: https://doi.org/10.1016/j.chroma.2008.05.059.

[96] E. Turiel, J. L. Tadeo, and A. Martin-Esteban, 'Molecularly Imprinted Polymeric Fibers for Solid-Phase Microextraction', *Anal Chem*, vol. 79, no. 8, pp. 3099–3104, Apr. 2007, doi: 10.1021/ac062387f.

[97] D. Djozan and T. Baheri, ‘Preparation and evaluation of solid-phase microextraction fibers based on monolithic molecularly imprinted polymers for selective extraction of diacetylmorphine and analogous compounds’, *J Chromatogr A*, vol. 1166, no. 1, pp. 16–23, 2007, doi: https://doi.org/10.1016/j.chroma.2007.08.003.

[98] D. Djozan and B. Ebrahimi, ‘Preparation of new solid phase micro extraction fiber on the basis of atrazine-molecular imprinted polymer: Application for GC and GC/MS screening of triazine herbicides in water, rice and onion’, *Anal Chim Acta*, vol. 616, no. 2, pp. 152–159, 2008, doi: https://doi.org/10.1016/j.aca.2008.04.037.

[99] D. Djozan, M. Mahkam, and B. Ebrahimi, ‘Preparation and binding study of solid-phase microextraction fiber on the basis of ametryn-imprinted polymer: Application to the selective extraction of persistent triazine herbicides in tap water, rice, maize and onion’, *J Chromatogr A*, vol. 1216, no. 12, pp. 2211–2219, 2009, doi: https://doi.org/10.1016/j.chroma.2008.12.101.

[100] S. Ansari and M. Karimi, ‘Recent progress, challenges and trends in trace determination of drug analysis using molecularly imprinted solid-phase microextraction technology’, *Talanta*, vol. 164, pp. 612–625, 2017, doi: https://doi.org/10.1016/j.talanta.2016.11.007.

[101] E. Turiel and A. Martín-Esteban, ‘Molecularly imprinted polymers for sample preparation: A review’, *Anal Chim Acta*, vol. 668, no. 2, pp. 87–99, 2010, doi: https://doi.org/10.1016/j.aca.2010.04.019.

[102] A. Sarafraz-Yazdi and N. Razavi, ‘Application of molecularly-imprinted polymers in solid-phase microextraction techniques’, *TrAC Trends in Analytical Chemistry*, vol. 73, pp. 81–90, 2015, doi: https://doi.org/10.1016/j.trac.2015.05.004.

[103] M. D. Ariani, A. Zuhrotun, P. Manesiotis, and A. N. Hasanah, ‘Dummy template molecularly imprinted polymers as potential sorbents in the

separation and purification of active compounds in natural products', *Polym Adv Technol*, vol. 35, no. 1, p. e6201, Jan. 2024, doi: https://doi.org/10.1002/pat.6201.

[104] K. Delińska, G. Machowski, and A. Kloskowski, 'Development of SPME fiber coatings with tunable porosity for physical confinement of ionic liquids as an extraction media', *Microchemical Journal*, vol. 178, p. 107392, 2022, doi: https://doi.org/10.1016/j.microc.2022.107392.

[105] J. Nawała, B. Dawidziuk, D. Dziedzic, D. Gordon, and S. Popiel, 'Applications of ionic liquids in analytical chemistry with a particular emphasis on their use in solid-phase microextraction', *TrAC Trends in Analytical Chemistry*, vol. 105, pp. 18–36, 2018, doi: https://doi.org/10.1016/j.trac.2018.04.010.

[106] M. Liu *et al.*, 'Innovative chemically bonded ionic liquids-based sol–gel coatings as highly porous, stable and selective stationary phases for solid phase microextraction', *Anal Chim Acta*, vol. 683, no. 1, pp. 96–106, 2010, doi: https://doi.org/10.1016/j.aca.2010.10.004.

[107] Y. Fan and S. Zhang, 'Ionic liquid-based microextraction: A sample pretreatment technique for chromatographic analysis', *European Journal of Chemistry*, vol. 2, no. 2, pp. 282–288, Jun. 2011, doi: 10.5155/eurjchem.2.2.282-288.393.

[108] N. Reyes-Garcés, B. Bojko, and J. Pawliszyn, 'High throughput quantification of prohibited substances in plasma using thin film solid phase microextraction', *J Chromatogr A*, vol. 1374, pp. 40–49, 2014, doi: https://doi.org/10.1016/j.chroma.2014.11.047.

[109] J. J. Grandy, V. Singh, M. Lashgari, M. Gauthier, and J. Pawliszyn, 'Development of a Hydrophilic Lipophilic Balanced Thin Film Solid Phase Microextraction Device for Balanced Determination of Volatile Organic

Compounds', *Anal Chem*, vol. 90, no. 23, pp. 14072–14080, Dec. 2018, doi: 10.1021/acs.analchem.8b04544.

[110] N. Reyes-Garcés *et al.*, 'Advances in Solid Phase Microextraction and Perspective on Future Directions', Jan. 02, 2018, *American Chemical Society*. doi: 10.1021/acs.analchem.7b04502.

[111] C. F. Poole and S. K. Poole, '2.14 - Principles and Practice of Solid-Phase Extraction', in *Comprehensive Sampling and Sample Preparation*, J. Pawliszyn, Ed., Oxford: Academic Press, 2012, pp. 273–297. doi: https://doi.org/10.1016/B978-0-12-381373-2.00041-7.

[112] C. J. Brinker, 'Dip Coating', in *Chemical Solution Deposition of Functional Oxide Thin Films*, T. Schneller, R. Waser, M. Kosec, and D. Payne, Eds., Vienna: Springer Vienna, 2013, pp. 233–261. doi: 10.1007/978-3-211-99311-8_10.

[113] R. G. Larson and T. J. Rehg, 'Spin Coating', in *Liquid Film Coating: Scientific principles and their technological implications*, S. F. Kistler and P. M. Schweizer, Eds., Dordrecht: Springer Netherlands, 1997, pp. 709–734. doi: 10.1007/978-94-011-5342-3_20.

[114] F. Riazi Kermani and J. Pawliszyn, 'Sorbent Coated Glass Wool Fabric as a Thin Film Microextraction Device', *Anal Chem*, vol. 84, no. 21, pp. 8990–8995, Nov. 2012, doi: 10.1021/ac301861z.

[115] M. D. Tyona, 'A theoritical study on spin coating technique', *Advances in materials Research*, vol. 2, no. 4, pp. 195–208, Dec. 2013, doi: 10.12989/amr.2013.2.4.195.

[116] U. G. Lee, W. B. Kim, D. H. Han, and H. S. Chung, 'A modified equation for thickness of the film fabricated by spin coating', *Symmetry (Basel)*, vol. 11, no. 9, pp. 1–20, Sep. 2019, doi: 10.3390/sym11091183.

[117] M. A. Butt, ‘Thin-Film Coating Methods: A Successful Marriage of High-Quality and Cost-Effectiveness—A Brief Exploration’, Aug. 01, 2022, *MDPI*. doi: 10.3390/coatings12081115.

[118] R. Dewi, N. I. Baa’yah, and I. A. Talib, ‘The effect of spin coating rate on the microstructure, grain size, surface roughness and thickness of Ba 0.6 Sr 0.4 TiO 3 thin film prepared by the sol-gel process’, 2007.

[119] N. Tucker, J. J. Stanger, M. P. Staiger, H. Razzaq, and K. Hofman, ‘The History of the Science and Technology of Electrospinning from 1600 to 1995’, *J Eng Fiber Fabr*, vol. 7, no. 2_suppl, p. 155892501200702S10, Jun. 2012, doi: 10.1177/155892501200702S10.

[120] A. Keirouz *et al.*, ‘The History of Electrospinning: Past, Present, and Future Developments’, *Adv Mater Technol*, vol. 8, no. 11, p. 2201723, Jun. 2023, doi: https://doi.org/10.1002/admt.202201723.

[121] J. W. Zewe, J. K. Steach, and S. V Olesik, ‘Electrospun Fibers for Solid-Phase Microextraction’, *Anal Chem*, vol. 82, no. 12, pp. 5341–5348, Jun. 2010, doi: 10.1021/ac100891t.

[122] M. Ahmadi Bonakdar and D. Rodrigue, ‘Electrospinning: Processes, Structures, and Materials’, Mar. 01, 2024, *Multidisciplinary Digital Publishing Institute (MDPI)*. doi: 10.3390/macromol4010004.

[123] H. Piri-Moghadam, Md. N. Alam, and J. Pawliszyn, ‘Review of geometries and coating materials in solid phase microextraction: Opportunities, limitations, and future perspectives’, *Anal Chim Acta*, vol. 984, pp. 42–65, 2017, doi: https://doi.org/10.1016/j.aca.2017.05.035.

[124] D. Hussain, S. T. Raza Naqvi, M. N. Ashiq, and M. Najam-ul-Haq, ‘Analytical sample preparation by electrospun solid phase microextraction sorbents’, *Talanta*, vol. 208, p. 120413, 2020, doi: https://doi.org/10.1016/j.talanta.2019.120413.

[125] G. Ajith *et al.*, 'Recent Developments in Electrospun Nanofibers as Delivery of Phytoconstituents for Wound Healing', *Drugs and Drug Candidates*, vol. 2, no. 1, pp. 148–171, Mar. 2023, doi: 10.3390/ddc2010010.

[126] J. Macossay, A. Marruffo, R. Rincon, T. Eubanks, and A. Kuang, 'Effect of needle diameter on nanofiber diameter and thermal properties of electrospun poly(methyl methacrylate)', *Polym Adv Technol*, vol. 18, no. 3, pp. 180–183, Mar. 2007, doi: https://doi.org/10.1002/pat.844.

[127] S. V Fridrikh, J. H. Yu, M. P. Brenner, and G. C. Rutledge, 'Controlling the Fiber Diameter during Electrospinning', *Phys Rev Lett*, vol. 90, no. 14, p. 144502, Apr. 2003, doi: 10.1103/PhysRevLett.90.144502.

[128] A. H. Hekmati, A. Rashidi, R. Ghazisaeidi, and J.-Y. Drean, 'Effect of needle length, electrospinning distance, and solution concentration on morphological properties of polyamide-6 electrospun nanowebs', *Textile Research Journal*, vol. 83, no. 14, pp. 1452–1466, Jan. 2013, doi: 10.1177/0040517512471746.

[129] D. Zhang, P. Davoodi, X. Li, Y. Liu, W. Wang, and Y. Y. S. Huang, 'An empirical model to evaluate the effects of environmental humidity on the formation of wrinkled, creased and porous fibre morphology from electrospinning', *Sci Rep*, vol. 10, no. 1, p. 18783, 2020, doi: 10.1038/s41598-020-74542-7.

[130] S. Ramazani and M. Karimi, 'Investigating the influence of temperature on electrospinning of polycaprolactone solutions', vol. 14, no. 5, pp. 323–333, 2014, doi: doi:10.1515/epoly-2014-0110.

[131] A. Mollahosseini, M. Rastegari, and N. Hatefi, 'Electrospun Polyacrylonitrile as a New Coating for Mechanical Stir Bar Sorptive Extraction of Polycyclic Aromatic Hydrocarbons from Water Samples', *Chromatographia*, vol. 83, no. 4, pp. 549–558, 2020, doi: 10.1007/s10337-020-03874-3.

[132] I. Minet, L. Hevesi, M. Azenha, J. Delhalle, and Z. Mekhalif, 'Preparation of a polyacrylonitrile/multi-walled carbon nanotubes composite by surface-

initiated atom transfer radical polymerization on a stainless steel wire for solid-phase microextraction', *J Chromatogr A*, vol. 1217, no. 17, pp. 2758–2767, 2010, doi: https://doi.org/10.1016/j.chroma.2010.02.030.

[133] 'National Center for Biotechnology Information (2025). PubChem Compound Summary for CID 7855, Acrylonitrile. Retrieved January 19, 2025 from https://pubchem.ncbi.nlm.nih.gov/compound/Acrylonitrile.'

[134] 'National Center for Biotechnology Information (2025). PubChem Compound Summary for CID 4004, Malathion. Retrieved January 19, 2025 from https://pubchem.ncbi.nlm.nih.gov/compound/Malathion.'

[135] 'National Center for Biotechnology Information (2025). PubChem Compound Summary for CID 3017, Diazinon. Retrieved January 19, 2025 from https://pubchem.ncbi.nlm.nih.gov/compound/Diazinon.'.

[136] 'National Center for Biotechnology Information (2025). PubChem Compound Summary for CID 6129, Carbaryl. Retrieved January 19, 2025 from https://pubchem.ncbi.nlm.nih.gov/compound/Carbaryl.'

[137] 'National Center for Biotechnology Information (2025). PubChem Compound Summary for CID 5569, Trifluralin. Retrieved January 19, 2025 from https://pubchem.ncbi.nlm.nih.gov/compound/Trifluralin.'

[138] O. Eren, N. Ucar, A. Onen, N. Kizildag, and I. Karacan, 'Synergistic effect of polyaniline, nanosilver, and carbon nanotube mixtures on the structure and properties of polyacrylonitrile composite nanofiber', *J Compos Mater*, vol. 50, no. 15, pp. 2073–2086, Aug. 2015, doi: 10.1177/0021998315601891.

[139] J. Gao, X. Wang, J. Zhang, and R. Guo, 'Preparation of heat-treated PAN/SiO2 hybrid hollow fiber membrane contactor for acetylene absorption', *Sep Purif Technol*, vol. 159, pp. 116–123, 2016, doi: https://doi.org/10.1016/j.seppur.2016.01.005.

[140] M. Gallignani, S. Garrigues, A. Martínez-Vado, and M. de la Guardia, ‘Determination of carbaryl in pesticide formulations by Fourier transform infrared spectrometry with flow analysis’, *Analyst*, vol. 118, no. 8, pp. 1043–1048, 1993, doi: 10.1039/AN9931801043.

[141] G. Daneshvari *et al.*, ‘Controlled-release formulations of trifluralin herbicide by interfacial polymerization as a tool for environmental hazards’, *Biointerface Res Appl Chem*, vol. 11, no. 6, pp. 13866–13877, 2021, doi: 10.33263/BRIAC116.1386613877.

[142] M. A. A. Beg and H. C. Clark, ‘CHEMISTRY OF THE TRIFLUOROMETHYL GROUP: PART IV. DIPHENYLTRIFLUOROMETHYLPHOSPHINE AND COMPLEX FORMATION BY PHENYLTRIFLUOROMETHYLPHOSPHINES’, *Can J Chem*, vol. 40, no. 2, pp. 283–288, Feb. 1962, doi: 10.1139/v62-046.

[143] D. Sawai, M. Miyamoto, T. Kanamoto, and M. Ito, ‘Lamellar thickening in nascent poly(acrylonitrile) upon annealing’, *J Polym Sci B Polym Phys*, vol. 38, no. 19, pp. 2571–2579, Oct. 2000, doi: https://doi.org/10.1002/1099-0488(20001001)38:19<2571::AID-POLB90>3.0.CO;2-4.

[144] W. Pan and H. Zou, ‘Characterization of PAN/ATO nanocomposites prepared by solution blending’, *Bulletin of Materials Science*, vol. 31, no. 5, pp. 807–811, 2008, doi: 10.1007/s12034-008-0128-8.

[145] E. Zussman *et al.*, ‘Mechanical and structural characterization of electrospun PAN-derived carbon nanofibers’, *Carbon N Y*, vol. 43, no. 10, pp. 2175–2185, 2005, doi: https://doi.org/10.1016/j.carbon.2005.03.031.

[146] S. S. S. Bakar, K. C. Fong, A. Eleyas, and M. F. M. Nazeri, ‘Effect of Voltage and Flow Rate Electrospinning Parameters on Polyacrylonitrile Electrospun Fibers’, *IOP Conf Ser Mater Sci Eng*, vol. 318, no. 1, p. 012076, 2018, doi: 10.1088/1757-899X/318/1/012076.

[147] P. Ryšánek, O. Benada, J. Tokarský, M. Syrový, P. Čapková, and J. Pavlík, ‘Specific structure, morphology, and properties of polyacrylonitrile (PAN) membranes prepared by needleless electrospinning; Forming hollow fibers’, *Materials Science and Engineering: C*, vol. 105, p. 110151, 2019, doi: https://doi.org/10.1016/j.msec.2019.110151.

[148] J. Meléndez-Marmolejo *et al.*, ‘Design and application of molecularly imprinted polymers for adsorption and environmental assessment of anti-inflammatory drugs in wastewater samples’, *Environmental Science and Pollution Research*, vol. 29, no. 30, pp. 45885–45902, 2022, doi: 10.1007/s11356-022-19130-0.

[149] R. Tabaraki and N. Sadeghinejad, ‘Preparation and application of magnetic molecularly imprinted polymers for rutin determination in green tea’, *Chemical Papers*, vol. 74, no. 6, pp. 1937–1944, 2020, doi: 10.1007/s11696-019-01039-7.

[150] O. A. A.-Q. Mahmood and B. I. Waisi, ‘Synthesis and characterization of polyacrylonitrile based precursor beads for the removal of the dye malachite green from its aqueous solutions’, *Desalination Water Treat*, vol. 216, pp. 445–455, 2021, doi: https://doi.org/10.5004/dwt.2021.26906.

[151] X. Wen, J. Fei, X. Chen, L. Yi, F. Ge, and M. Huang, ‘Electrochemical analysis of trifluralin using a nanostructuring electrode with multi-walled carbon nanotubes’, *Environmental Pollution*, vol. 156, no. 3, pp. 1015–1020, 2008, doi: https://doi.org/10.1016/j.envpol.2008.05.002.

[152] A. Ramesh and M. Balasubramanian, ‘Kinetics and Hydrolysis of Fenamiphos, Fipronil, and Trifluralin in Aqueous Buffer Solutions’, *J Agric Food Chem*, vol. 47, no. 8, pp. 3367–3371, Aug. 1999, doi: 10.1021/jf980885m.

[153] W. Wesela, ‘Final Human Health and Ecological Risk Assessment for Carbaryl Rangeland Grasshopper and Mormon Cricket Suppression

Applications', 2019. [Online]. Available: http://www.ascr.usda.gov/complaint_filing_file.html.

[154] M. Háková, L. Chocholoušová Havlíková, P. Solich, F. Švec, and D. Šatínský, 'Electrospun nanofiber polymers as extraction phases in analytical chemistry – The advances of the last decade', *TrAC Trends in Analytical Chemistry*, vol. 110, pp. 81–96, 2019, doi: https://doi.org/10.1016/j.trac.2018.10.030.

[155] P. Khodayari, N. Jalilian, H. Ebrahimzadeh, and S. Amini, 'Electrospun cellulose acetate /polyacrylonitrile /thymol /Mg-metal organic framework nanofibers as efficient sorbent for pipette-tip micro-solid phase extraction of anti-cancer drugs', *React Funct Polym*, vol. 173, p. 105217, 2022, doi: https://doi.org/10.1016/j.reactfunctpolym.2022.105217.

[156] Bard A. J. and Faulkner L. R., *Electrochemical methods: fundamentals and applications*, 2nd Edition. Hoboken: John Wiley & Sons, 2007.

[157] C. Marchioni, T. M. Vieira, A. E. Miller Crotti, J. A. Crippa, and M. E. Costa Queiroz, 'In-tube solid-phase microextraction with a dummy molecularly imprinted monolithic capillary coupled to ultra-performance liquid chromatography-tandem mass spectrometry to determine cannabinoids in plasma samples', *Anal Chim Acta*, vol. 1099, pp. 145–154, 2020, doi: https://doi.org/10.1016/j.aca.2019.11.017.

[158] J. Zhu, D. Chen, Y. Ai, X. Dang, J. Huang, and H. Chen, 'A dummy molecularly imprinted monolith for selective solid-phase microextraction of vanillin and methyl vanillin prior to their determination by HPLC', *Microchimica Acta*, vol. 184, no. 4, pp. 1161–1167, 2017, doi: 10.1007/s00604-017-2107-5.

[159] J. Migenda, S. Werner, R. Ellinghaus, and B. M. Smarsly, 'Mesoporous Poly(divinylbenzene) Fibers Based On Crosslinked Nanoparticles', *Macromol Chem Phys*, vol. 219, no. 5, p. 1700471, Mar. 2018, doi: https://doi.org/10.1002/macp.201700471.

APPENDICES

A. GC-MS chromatograms of pesticides used in the study

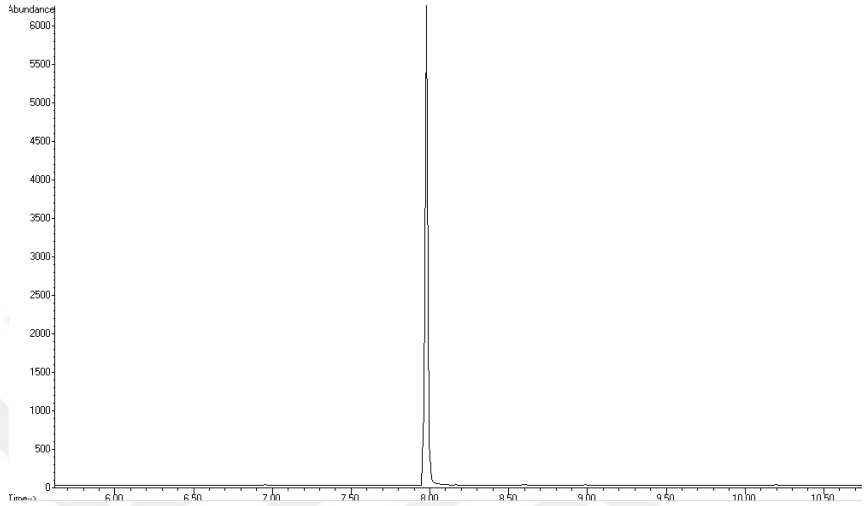

Figure A.1. GC-MS chromatogram of trifluralin (m/z=306)

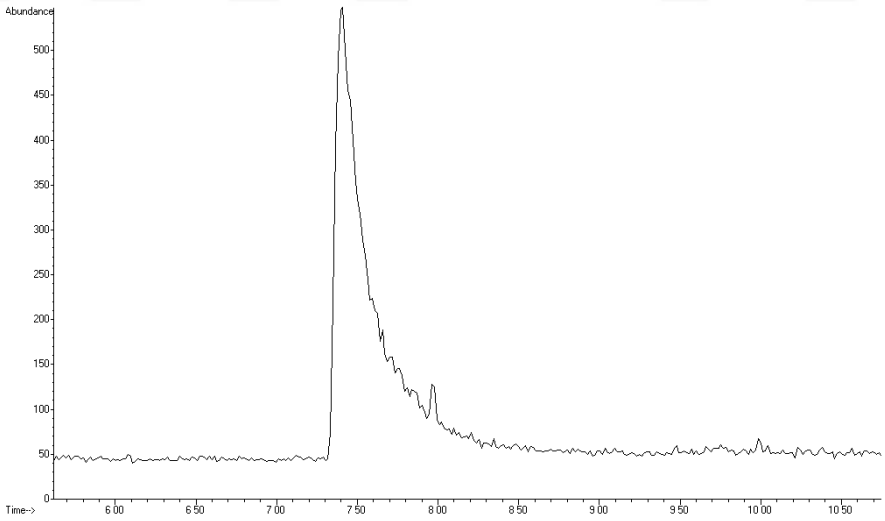

Figure A.2. GC-MS chromatogram of carbaryl (m/z=144)

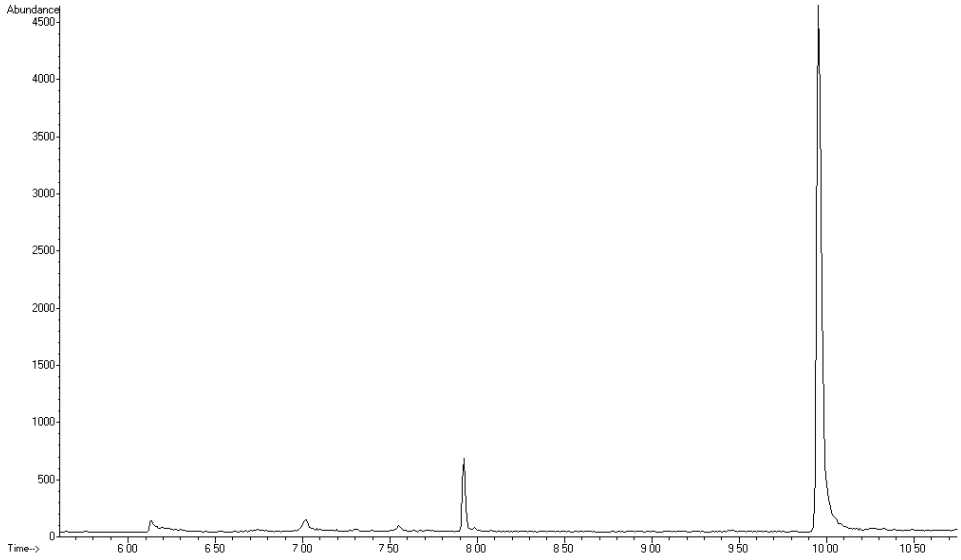

Figure A.3. GC-MS chromatogram of malathion (m/z=173)

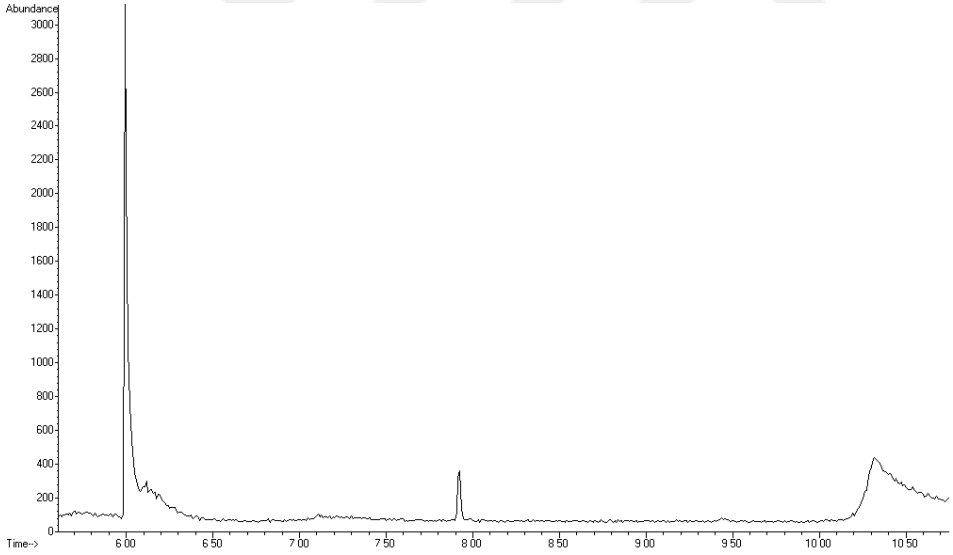

Figure A.4. GC-MS chromatogram of diazinon (m/z=152)

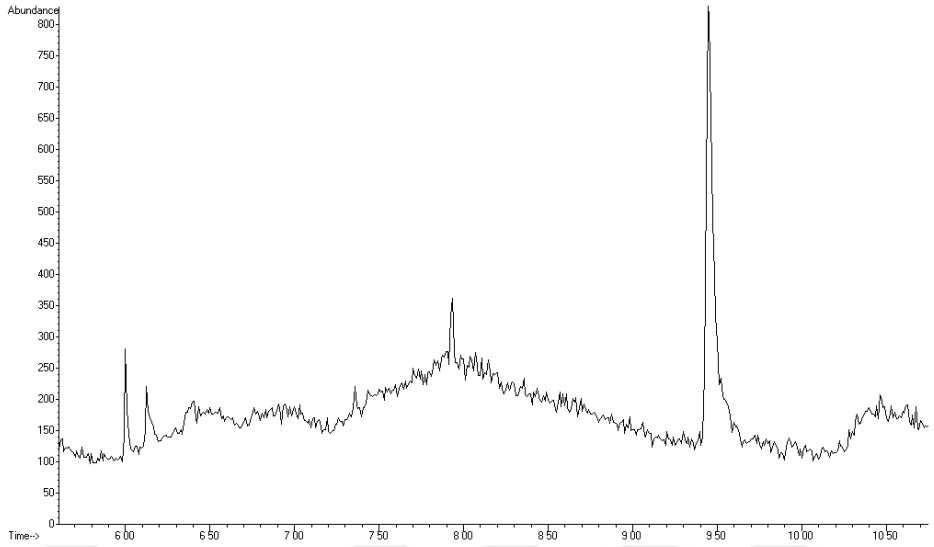

Figure A.5. GC-MS chromatogram of parathion (m/z=109)

B. Mass spectra of pesticides (electron impact ionization)

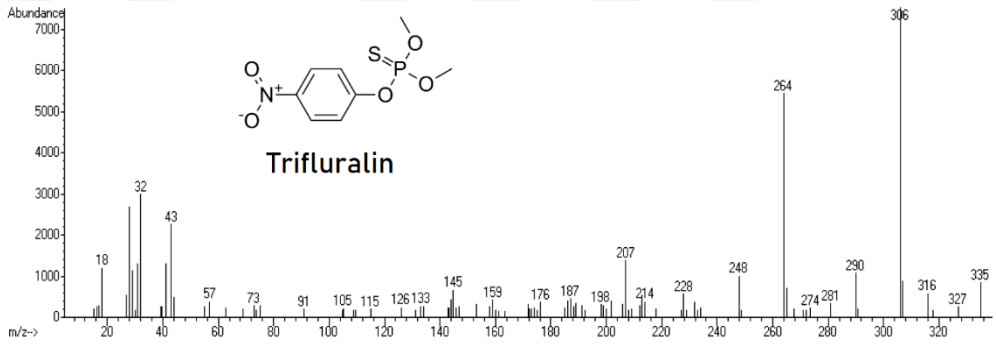

Figure B. 1. Mass spectrum of trifluralin obtained in GC-MS full scan mode

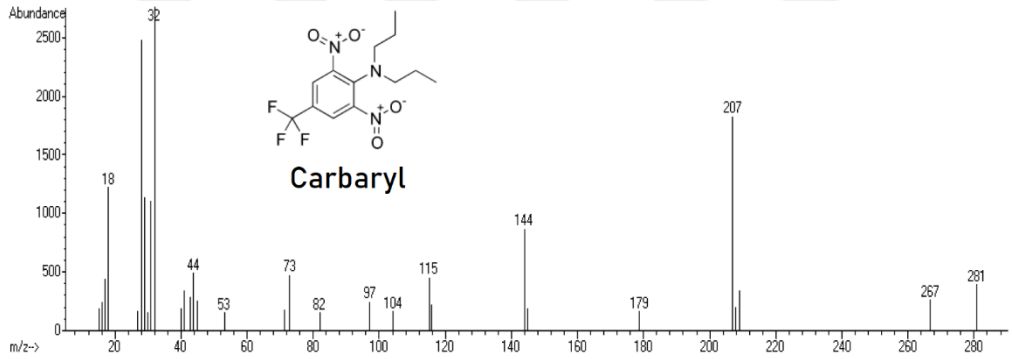

Figure B. 2. Mass spectrum of carbaryl obtained in GC-MS full scan mode

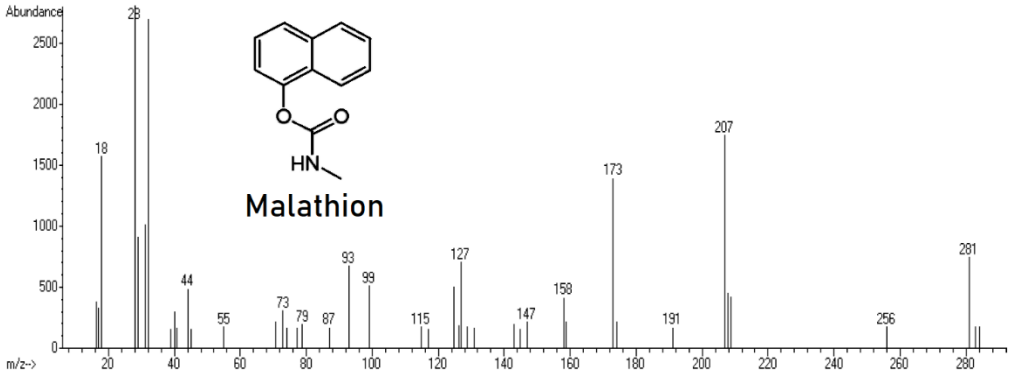

Figure B. 3. Mass spectrum of malathion obtained in GC-MS full scan mode

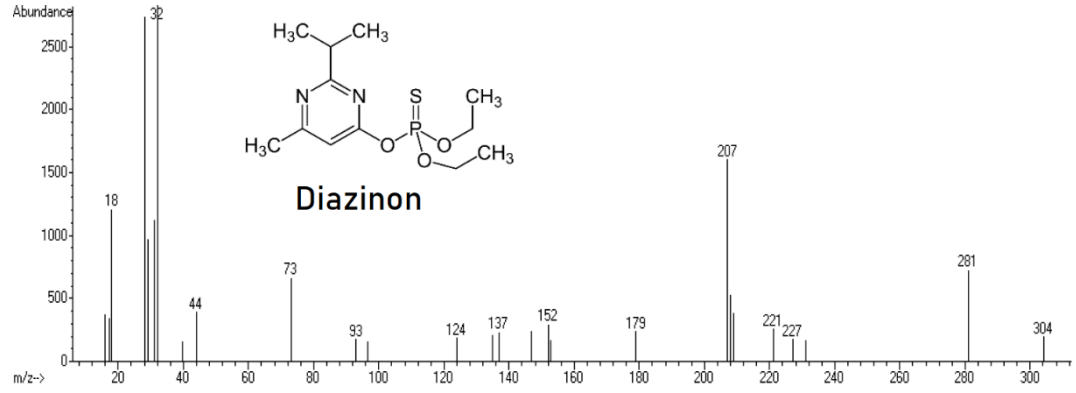

Figure B. 4. Mass spectrum of diazinon obtained in GC-MS full scan mode

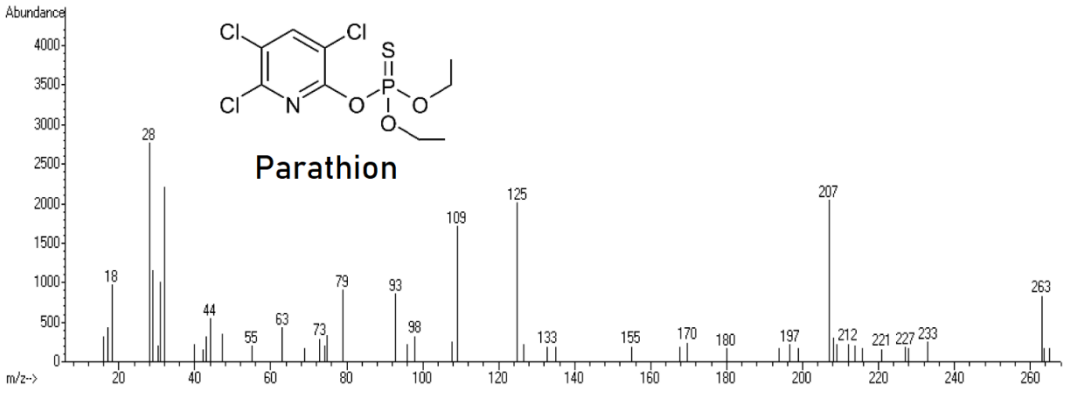

Figure B. 5. Mass spectrum of parathion obtained in GC-MS full scan mode